Le rôle de l'activation microgliale via le récepteur TLR2 suite à une ischémie cérébrale.

Thèse

Pierre Jr Cordeau

Doctorat en neurobiologie
Philosophiae doctor (Ph.D)

Québec, Canada

Résumé

Suite à un traumatisme cérébral, les microglies sont impliquées dans la réponse cellulaire inflammatoire. Le passage de la forme quiescente à la forme activée des microglies est associé à l'augmentation marquée du récepteur membranaire TLR2 (Toll-like receptor). Le rôle de ce récepteur sur la récupération fonctionnelle à court et à longs termes demeure incertain. C'est pourquoi cette thèse a pour but de clarifier la dynamique et le rôle de l'activation des microglies en utilisant le récepteur TLR2 comme marqueur suite à une ischémie cérébrale transitoire. Pour ce faire, nous avons entre autre utilisé un modèle murin généré dans le laboratoire, la souris TLR2-luc-GFP, pour étudier de façon longitudinale la réponse inflammatoire *in-vivo*. En premier lieu, l'activation microgliale, suite à la lésion, a été analysée chez une souris n'exprimant pas le récepteur TLR2. Les résultats de cette étude démontrent que l'absence du récepteur TLR2 retarde la réponse immunitaire et cause à long terme une augmentation du volume ischémique. De plus, la perte des récepteurs TLR2 corrèle avec la baisse des niveaux de IGF-1, un facteur anti-apoptotique et neurotrophique exprimé par les microglies dans la région ischémique. En deuxième lieu, nous avons évalué l'effet de l'environnement sur la réponse microgliale suite à une ischémie cérébrale induite par photothrombose. Une baisse d'activation microgliale fut mesurée chez les souris en milieu enrichi et cette diminution est accompagnée d'une meilleure récupération fonctionnelle. En troisième lieu, l'activation microgliale, en absence d'estrogène a été analysée chez une souris ErαKO à la suite d'une ischémie cérébrale transitoire. Les résultats de cette étude démontrent que l'absence du récepteur Erα diminue l'activation microgliale. De plus, la voie signalétique JAK/STAT, via la cytokine IL-6, serait préférentiellement utilisée chez ces souris au cours de la réponse inflammatoire. Finalement, cette thèse démontre l'importance de la microglie dans l'établissement de la réponse immunitaire ainsi que dans la récupération fonctionnelle suite à une ischémie cérébrale dans différents modèles. Grâce à une compréhension plus approfondie des mécanismes inflammatoires, la mise en place de stratégies thérapeutiques ne sera que plus efficace.

Abstract

Cerebral ischemia is associated with a strong inflammatory response. Glial activation that ensues contributes to neuronal damage and/or provides trophic support to injured neurons. Activated microglia is one of the key components of the cellular response to CNS injuries and the passage from the quiescent to reactive microglia is associated with an upregulation of a membrane receptor called the toll-like receptor 2 (TLR2). Although upregulation of TLR2 his known to play a major role in the innate immune response, the functional significance and the dynamics of this response in a model of focal cerebral ischemia is still unclear. Therefore, to further clarify the role of TLR2 after a cerebral ischemia, we developed a model system for *in vivo*, non-invasive analysis of the TLR2 activation in the brain. This thesis is divided in three distinct chapters. In the first chapter the role of the TLR2 signaling and microglial activation in a TLR2KO mouse was investigated beyond 72 hours. This work clearly demonstrates that the lack of TLR2 affects the neuroinflammatory response causing a delayed exacerbation of the ischemic lesion. Furthermore, TLR2 deficient mice reduced levels of IGF-1, a neurotrophic and antiapoptotic factor express by microglial cells. In the second chapter, we evaluated the effect of environmental enrichement on the inflammatory response after phototrombotic stroke in our TLR2-luc-gfp mice. Study of microglial activation showed that multisensory stimulation attenuated TLR2-induced microglial activation, thus leading to a greater neurological outcome. In the third chapter, we crossed TLR2-luc-gfp mice with ErαKO mice to study the effect of a major oestrogen signalling pathway on microglial activation after cerebral ischemia. The lack of Erα receptor reduced microglial activation in normal female mice as well as oestrogen-deprived mice. Likewise a shift toward the JAK/STAT pathway was observed suggesting its implication in the inflammatory process. Finally this thesis illustrates the significant impact of the microglia on the immune response and the recovery after a cerebral ischemia in different mouse models. With this newly acquired knowledge on inflammatory process the establishment of better therapeutic strategy could only benefit from it.

Table des matières

Liste des figures

Liste des abréviations

AD : maladie d'Alzheimer
AIF : facteur induisant l'apoptose
ATP : adénosine-5'-triphosphate
AVC : accident vasculaire cérébral
BDNF : facteur neurotrophique issu du cerveau
DAMPs : motifs moléculaires associés aux dégâts
DISC : complexe de signalisation de la mort induite
E2 : estrogène, 17β-estradiol
Erα/ Erβ : récepteurs des oestrogènes alpha/beta
ERE : élément de réponse des estrogènes
GFAP : protéine acide fibrillaire gliale
HIF : facteurs induits par l'hypoxie
HSP : protéine de choc thermique
IGF1 : facteur de croissance apparenté à l'insuline
IL-1β : interleukine 1 beta
IL-10 : interleukine 10
IRF : facteur de régulation de l'interféron
JNK : Jun-N-terminal kinase
MCP-1 : chimiokine attirant les monocytes
MMPs : métalloprotéinases de la matrice
NF-κB : facteur nucléaire kappa B (nuclear factor kappa-light-chain-enhancer of activated B cells)
NLRs : récepteur de type NOD
NO : oxyde nitrique
PAMPs : motifs moléculaires associés aux pathogénes
RLRs : récepteur de type RIG
ROS : espèces oxygénées réactives
SOD : superoxyde dismutase
tBID : BID tronqué
TGFβ : facteur de croissance de transformation beta
TLRs : récepteur de type toll
TNF-α : facteur de nécrose tumorale
TNFR : récepteur du facteur de nécrose tumorale

À Suki

Remerciements

Je tiens tout d'abord à remercier vivement Jasna Kriz de m'avoir accueilli dans son équipe et d'avoir cru en mes capacités à mener à terme un projet de recherche qui touchait peu mon domaine d'étude. De plus, ce laboratoire m'a donné l'opportunité de participer à des congrès d'ampleur nationale et internationale. Lors de mon doctorat, j'ai acquis de nouvelles techniques de laboratoire, j'ai pu y affûter mon esprit critique et parfaire mes connaissances dans le domaine des neurosciences tout en continuant les projets débutés lors de ma maîtrise.

J'aimerais aussi remercier tous mes collègues de travail, en particulier Mélanie Lalancette-Hébert, qui a pris le temps de m'enseigner et de m'expliquer ce que je connaissais qu'en partie ou très peu. J'aimerais aussi noter le support moral et financier de ma famille ainsi que l'amour inconditionnel de Karine.

De plus, il ne faut pas passer sous silence le dévouement des souris pour l'avancement de la science, sans elles tout ceci ne serait possible.

Avant-propos

Contributions des auteurs dans l'article: Real time imaging after cerebral ischemia: model systems for visualization of inflammation and neuronal repair. Publié dans Methods in Enzymology, 2012. Pierre Cordeau et Jasna Kriz ont coécrit le résumé.

Contributions des auteurs dans l'article: Toll-like receptor 2 deficiency leads to delayed exacerbation of ischemic injury publié dans le Journal of Neuroinflammation, 2012. Ivan Bohacek a effectué les immunohistochimies, a utilisé la trousse de cytokines ainsi qu'effectué les FACS. Il a aussi désigné l'expérience et écrit le manuscrit. Pierre Cordeau a utilisé la trousse de cytokines, fait et analysé les FACS en plus d'aider au design de l'expérience. Mélanie Hébert-Lalancette a effectué et analysé les hybridations in-situ. Dunja Gorup a effectué des analyses statistiques. Yuan-Cheng Weng a effectué les chirurgies. Srecko Gajovic a participé à la mise en place et la coordination de l'étude. Jasna Kriz a conçu et coordonné l'étude en plus d'écrire le manuscrit.

Contributions des auteurs dans l'article: Enriched housing down-regulates the Toll-like receptor 2 response in the mouse brain after experimental stroke publié dans Neurobiology of Disease, 2014. Mirianna Jlenia Quattromani a effectué les immunohistochimies, les comptes cellulaires, l'acquisition des images en bioluminescence ainsi qu'effectué l'évaluation comportementale. Elle a aussi écrit le manuscrit. Pierre Cordeau a participé à la mise en place du protocole d'imagerie en plus de diriger les sessions d'imagerie ainsi que l'analyse. Il a aussi apporté une aide technique lors de la chirurgie par photothrombose. Karsten Ruscher a effectué les chirurgies par photothrombose en plus d'assister lors des sessions d'imagerie. Jasna Kriz et Tadeusz Wieloch ont coordonné et conçu l'étude en plus d'apporter des correctifs au manuscrit.

Contributions des auteurs dans l'article: Estrogen receptors alpha mediates post-ischemic inflammation in chronically oestrogen- deprived mice. Pierre Cordeau a conçu, effectuer les expériences et écrit le manuscrit. Mélanie Hébert-Lalancette a écrit le manuscrit. Yuan-Cheng Weng a effectué les chirurgies. Jasna Kriz a coordonné et conçu l'étude en plus d'apporter des correctifs au manuscrit.

Chapitre 1. Introduction

1.1 L'ischémie cérébrale

1.1.1 Incidence et statistiques.

À toutes les dix minutes, une personne subie un accident vasculaire cérébrale (AVC) et une personne sur six en subira au moins un durant sa vie (Heart and Stroke Foundation, 2012). Dans les pays industrialisés, les décès engendrés par les accidents vasculaires cérébraux se classent au troisième rang derrière les problèmes cardiaques et toutes les formes de cancers confondus (Nedergaard, 2005). Au Canada, chaque année, plus de 14 000 personnes vont mourir des suites d'une ischémie cérébrale (Heart and Stroke Foundation, 2012). Parce que l'âge est l'un des principaux facteurs de risque et que l'espérance de vie de la population augmente, les accidents vasculaires cérébraux vont inévitablement augmenter, tout comme les conséquences négatives qui s'y rattachent. À partir de 55 ans les risques d'ischémie cérébrale double à tous les 10 ans. De plus, après avoir subie une ischémie cérébrale, seulement 10 % des gens vont se rétablir complètement. Toujours selon la Heart and Stroke Foundation, la majorité des gens atteints resteront handicapés, engendrant des coûts sociaux tant économiques que familiaux énormes. C'est pourquoi la recherche doit trouver rapidement des traitements efficaces. Selon une étude parue en 2006, pour chaque minute de délai entre l'accident vasculaire cérébral et le traitement, le patient va perdre en moyenne 1.9 millions de neurones, 13.8 milliards de synapses et 12 km de fibres axonales. Cela veut dire qu'une heure suffit pour que cette personne, en absence de traitement, perde autant de neurones qu'une personne en 3.6 années de vieillissement normal (Saver, 2006).

1.2 Étiologie

1.2.1 Causes

L'ischémie cérébrale survient lorsque l'apport de sang allant au cerveau n'est plus suffisant pour subvenir aux demandes métaboliques. L'arrêt d'afflux sanguin va faire chuter l'apport en oxygène, causant rapidement la mort des cellules cérébrales. Deux catégories d'AVC existent : l'AVC ischémique et l'AVC hémorragique. L'AVC ischémique est le plus fréquent (80 %) et est causé par l'interruption de l'afflux sanguin par un caillot. L'AVC ischémique se divise en deux sous-types : l'AVC thrombotique et l'AVC embolique (Heart and Stroke Foundation, 2012). L'AVC thrombotique survient lorsque le caillot se forme dans une artère à l'intérieur du cerveau. L'AVC embolique est caractérisé aussi par le blocage d'une artère, mais cette fois-ci l'embole, ou caillot, vient d'une région avoisinante du cerveau. Le caillot peut se former, par exemple, dans le cœur, entrer dans la circulation sanguine et se loger dans une artère cérébrale. La source la plus commune d'obstruction est l'accumulation de plaques athérosclérotiques composées de cholestérol, de calcium et de déchets de cellules. Avec le temps, les artères se bouchent ou libèrent dans la circulation des débris causant ainsi ces deux types d'AVC.

L'AVC hémorragique est moins fréquent (20%) et se caractérise par la rupture d'un vaisseau sanguin à l'intérieur du cerveau (hémorragie intracérébrale) ou entre la boite crânienne et le cerveau (hémorragie subarachnoïde) (Heart and Stroke Foundation, 2012). L'artère peut rompre à cause de l'hypertension ou à cause de la rupture d'un anévrisme. L'hémorragie ainsi créée peut très rapidement augmenter la pression intracrânienne causant la perte de conscience ou même la mort.

1.2.2 Facteurs de risques

Les facteurs de risques causant un AVC sont multiples, certains sont évitables ou contrôlables, d'autres pas. L'ischémie cérébrale est un problème qui affecte le

système circulatoire. C'est pourquoi certains facteurs de risques sont les mêmes que pour les maladies cardiovasculaires. Selon une étude récente, 90 % des AVC pourraient être attribués à 10 facteurs de risques associés à un comportement modifiable (O'Donnel, 2010). Une réduction de la pression artérielle, l'arrêt du tabagisme, faire de l'exercice et avoir des habitudes alimentaires saines pourraient réduire significativement les chances de subir un AVC. Pour ce qui est des facteurs non-modifiables, on dénote l'âge, le sexe, l'ethnicité ainsi que l'historique familial. En effet, il est intéressant de noter que les personnes afro-américaines ainsi que les autochtones ont des taux de mortalité suite à un AVC plus élevés que les caucasiens (Heart and Stroke Foundation, 2012).

Les AVC peuvent survenir à tout âge, par contre 75 % des accidents surviennent chez les gens de plus de 65 ans. Avec l'âge, des changements importants aux vaisseaux sanguins cérébraux se produisent. On dénote d'ailleurs la diminution de la densité des vaisseaux sanguins, un nombre réduit de mitochondries dans les cellules endothéliales ainsi qu'une dégénérescence des péricytes (Denes, 2010). Tous ces changements ont comme conséquence d'augmenter les probabilités d'avoir un AVC avec l'âge. Toutefois, le risque de subir une ischémie cérébrale est moindre chez les femmes comparativement aux hommes de même âge. Ce n'est qu'après la ménopause que les risques de subir un accident vasculaire cérébral, tout comme la sévérité ainsi que le taux de mortalité, augmentent (Stollough, 2011). Les hormones semblent donc avoir un effet préventif et protecteur chez la femme.

1.3 Réponse du cerveau suite à une ischémie cérébrale

Les mécanismes pathologiques et les zones affectées vont varier selon que l'occlusion soit transitoire ou permanente. La zone lésée se nomme 'foyer'. Elle est entourée par une région secondaire nommée 'pénombre' (Stoll, 1998). Avec les années, l'hypothèse de la mort des cellules du foyer et un rétablissement potentiel de la zone de pénombre c'est raffinée. Au niveau du foyer, la mort cellulaire est plus importante que dans la pénombre. Par contre, on ne voit plus la région

touchée comme un gros foyer lésé, mais bien comme de mini foyers entourés de mini pénombres (Dirnagl, 1999 et Zoppo, 2011). Les lésions vont varier en grosseur et en nombre en fonction de la microvasculature et du débit sanguin de celle-ci.

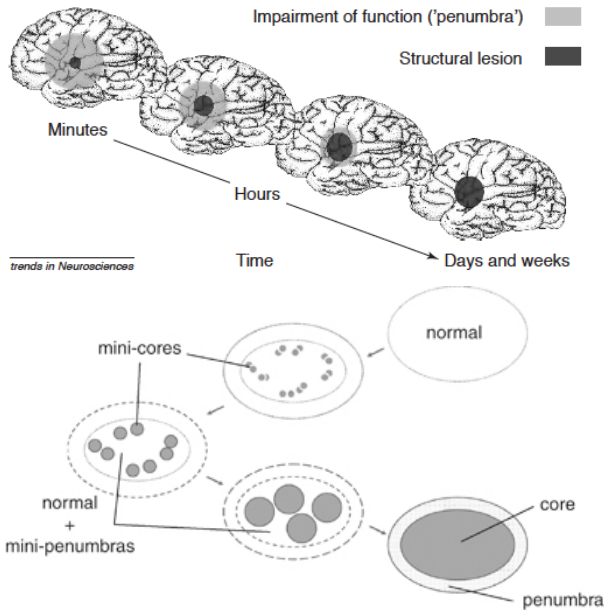

Figure 1. Deux modèles théoriques de la représentation de la pénombre et de son évolution dans le temps (Dirnagl, 1999 et Zoppo, 2011).

Avec le temps, les minifoyers ischémiques vont prendre de l'expansion suite à la mort des cellules dans les minipénombres et vont s'ajouter à la zone lésionnelle (Figure 1). Il s'en suit alors une chaîne d'évènements pathophysiologiques qui vont évoluer dans le temps et l'espace. Les mécanismes principaux qui font partie de cette chaîne d'évènements sont: l'excitotoxicité, une vague de dépolarisation, la génération de radicaux libres, la perturbation de l'intégrité de la barrière hémato-encéphalique, l'inflammation ainsi que la mort cellulaire (Dirnagl, 1999). Certains de ces phénomènes vont débuter dans les minutes suivant l'AVC (précoces) alors que d'autres vont prendre des semaines à se mettre en place (tardifs) (Figure 2).

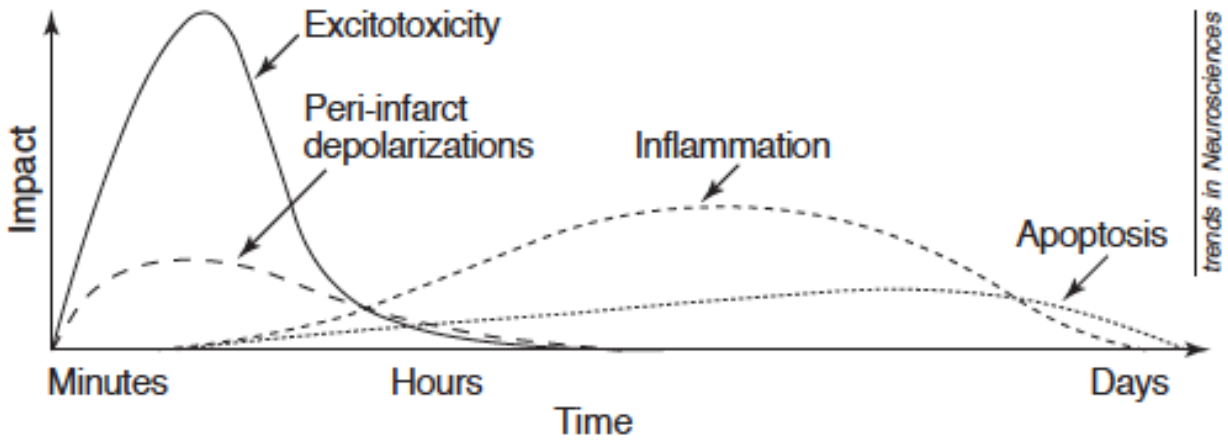

Figure 2. Cascade des évènements dommageables à la suite d'une ischémie cérébrale (Dirnagl, 1999).

1.4 Évènements précoces

1.4.1 L'excitotoxicité

Pour fonctionner, le cerveau consomme beaucoup de glucose et d'oxygène. Cependant ses réserves énergétiques sont très limitées (Brown, 2007). C'est pourquoi l'arrêt en apport énergétique se fait sentir aussi tôt que quelques minutes après l'accident et va engendrer plusieurs évènements pathophysiologiques. L'un des premiers éléments à se déréguler est le gradient ionique maintenu par les cellules (neurones et glies) avec le milieu extracellulaire (figure 3). Le cerveau consomme 20 % de toute l'énergie vouée au métabolisme de base de l'organisme. De ce 20 %, la moitié sert à maintenir le gradient ionique des pompes sodium (Dreier, 2011).

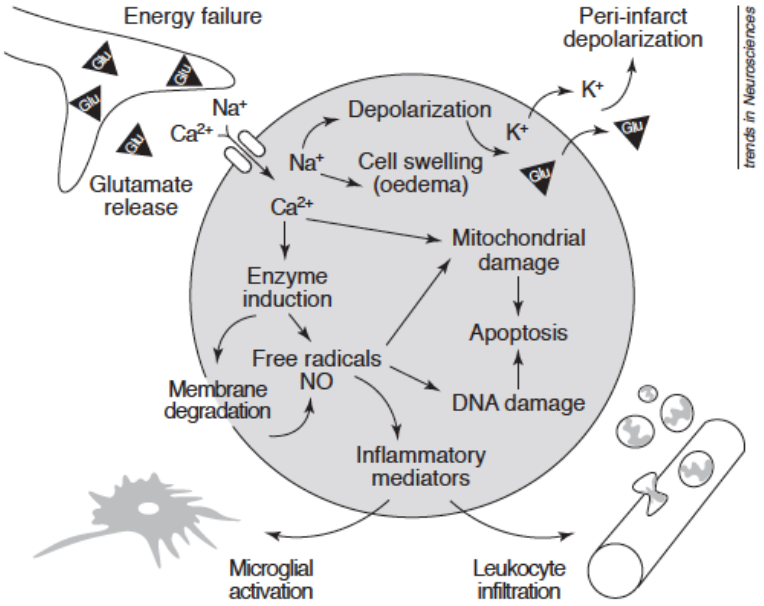

Figure 3. Vue simplifiée des évènements ayant lieu lors d'une ischémie cérébrale (Dirnagl, 1999).

Le calcium est aussi un ion important dans plusieurs fonctions cellulaires (différenciation, croissance, excitabilité de la membrane, activité synaptique) et le maintien de sa faible concentration intra neuronale est fortement régulé (Arundine, 2003). À la suite d'un AVC, les pompes ioniques ATP-dépendantes de type Na^+/K^+ et Ca^{2+}/H, sans apport d'énergie, vont arrêter de fonctionner causant l'accumulation intracellulaire du Ca^{2+}, du Na^+ et du Cl^-. Ce dérèglement des canaux va générer des anomalies métaboliques et la dépolarisation de la membrane cellulaire qui va à son tour déclencher l'activation des canaux calciques voltage-dépendants présynaptiques et ainsi libérer dans l'espace extracellulaire un acide aminé excitateur, le glutamate (Dreier, 2011). Le mécanisme de recapture des neurotransmetteurs étant stoppé, la concentration en glutamate dans les fentes synaptiques et dans le milieu extracellulaire va augmenter. Une concentration élevée en glutamate est toxique pour les neurones (Nishizawa, 2001). De plus, toujours dans le milieu extracellulaire, le glutamate va induire une entrée de sodium (Na^+) et de chlore (Cl^-) dans les neurones via les canaux perméables aux ions monovalents, notamment le récepteur-canal AMPA, un récepteur activé par le glutamate (Dirnagl, 1999). Finalement, les organelles

lésées comme le réticulum endoplasmique, les mitochondries et les vésicules synaptiques de la cellule libèrent à leur tour dans le milieu du Ca^{2+} (Durukan, 2007). Cette entrée massive d'ions à l'intérieur des neurones crée un appel d'eau par osmose, induisant l'œdème cérébral. L'œdème augmente la pression intracrânienne, compresse le système vasculaire et cause des hernies cérébrales que l'on nomme engagement. Selon le type d'engagement, différentes complications peuvent apparaître et entraîner le décès du patient (Dirnagl, 1999).

Tous ces phénomènes pathologiques vont contribuer à augmenter le volume de la lésion. Dans le foyer, la dépolarisation est irréversible et les cellules vont mourir par nécrose. Par contre, dans la pénombre, les cellules parviennent parfois à rétablir leur potentiel membranaire à condition que le débit sanguin local soit rétablit ou grâce à des artères collatérales. La sauvegarde de la pénombre est l'une des principales cibles de la recherche.

1.4.2 Vague de dépolarisation

La forte concentration de K^+ et de glutamate libérés par les cellules dans le milieu extracellulaire va induire le phénomène de « spreading depression » ou de dépolarisation péri-infarctus. Débutant en bordure de la zone ischémique, des vagues de dépolarisation vont se propager dans les tissus environnants. La vague avance à une vitesse allant de 2 à 5 millimètres par minute et elle est suivie d'une période de silence cérébral, caractérisé par une absence d'activité électrique. L'alternance de polarisation-dépolarisation va épuiser les minces réserves énergétiques des neurones de la pénombre. La dépolarisation péri-infarctus contribue à augmenter le volume de la lésion ischémique en transformant les zones de pénombre en zones lésées. Des études menées chez les rats ont démontré que l'administration de MK-801, un antagoniste des récepteurs NMDA (N-méthyl-D-aspartate), réduit le nombre de dépolarisation et diminue le volume de la zone ischémique. Le récepteur NMDA est normalement impliqué dans la formation de la mémoire en prolongeant l'activité synaptique, son ouverture fait

entrer dans la cellule de grandes quantités de Ca^{2+}. Lors d'une ischémie, bloquer le récepteur NMDA aurait comme effet de diminuer l'entrée massive de cet ion dommageable pour les cellules. En effet, en trop grande quantité, il perturbe le métabolisme enzymatique normal des cellules. Ce phénomène n'a pas encore été clairement démontré chez l'homme, mais les concentrations extracellulaires élevées en K^+ et en glutamate laissent présager que le phénomène existe (Iijima, 1992).

1.4.3 Stress oxydatif

Les espèces oxygénées réactives (ROS) font partie du métabolisme cellulaire normal et sont produites par plusieurs voies métaboliques. Elles sont impliquées dans la régulation de la croissance cellulaire, la différentiation, la prolifération ainsi que l'apoptose (Olmez, 2012). Lors de la reperfusion, suite à l'ischémie cérébrale, l'équilibre entre la production de ROS et la production d'antioxydants est brisé. En effet, une augmentation de ROS va causer plusieurs problèmes. La perméabilité des mitochondries est affectée induisant des pores dans leur membrane interne. En plus d'arrêter la production d'ATP, une libération encore plus importante de ROS et de molécules pro-apoptotiques, comme le cytochrome C (Durukan, 2007) est induite. Un excès de ROS va aussi causer une peroxydation des lipides, des dommages aux membranes cellulaires et va dérégler de nombreux processus cellulaires (Durukan, 2007).

L'oxyde nitrique (NO) est une autre espèce oxygénée réactive qui est produite par les oxydes nitriques synthases (NOS). Le NOS se retrouve sous trois isoformes. Il y a la forme endothéliale (eNOS) qui serait bénéfique lors de l'ischémie cérébrale en augmentant la vascularisation (Lee, 2005). D'ailleurs, son inhibition augmenterait la taille de la lésion ischémique (Huang, 1994). Par contre, la production d'iNOS (inductible) et de nNOS (neuronale) serait néfaste. En effet, iNOS, en présence d'ions superoxyde, va former le peroxynitrite, un composé très oxydant, qui va à son tour causer des dommages similaires aux ROS (Olmez,

2012). Il est donc important de considérer l'implication de chaque isoformes dans le processus inflammatoire lorsque vient le temps de mettre au point un traitement.

1.5 Évènements tardifs

1.5.1 Infiltration des cellules immunitaires et intégrité de la barrière hémato encéphalique

Quelques heures (4 à 6) seulement après l'occlusion d'une artère, les cellules immunitaires (leukocytes) vont adhérer à la membrane vasculaire, la traverser et s'accumuler dans le cerveau. Une fois dans la région ischémique, elles vont favoriser l'expression de divers facteurs de transcription comme le facteur nucléaire kappa B (NF-κB), les facteurs induits par l'hypoxie (HIF) et le facteur de régulation de l'interféron (IRF-1). Ces facteurs de transcription stimulent l'expression de médiateurs pro-inflammatoires comme le TNFα et l'interleukine-1 beta (IL-1β) (Wang, 2007). En plus d'être libérées par les cellules immunitaires, plusieurs cytokines sont directement libérées par les cellules endommagées (neurones et glies) du cerveau. Il y a donc un phénomène d'amplification de la réponse inflammatoire lorsque d'autres cellules immunitaires, neutrophiles et macrophages, infiltrent la barrière hémato encéphalique (BBB) maintenant perméable. C'est pourquoi bloquer tôt les cytokines pro-inflammatoires comme l'IL-1β va diminuer le volume de la zone endommagée (Downes, 2010). Par contre, certaines cytokines ont des effets encore mal compris. Par exemple, le TNFα a un effet néfaste et un effet bénéfique sur les cellules selon que ce soit respectivement le récepteur TNFR1 ou le récepteur TNFR2 qui soit activé (Watters, 2011). L'IL-6 aurait elle aussi un double rôle à jouer suite à une ischémie, à court terme elle serait néfaste, mais à long terme elle aurait des effets neurotrophiques (Suzuki, 2009).

L'intégrité de la BBB est aussi affectée par la libération de molécules pro-inflammatoires, mais aussi par le manque d'oxygène, par les radicaux libres et surtout par la destruction de la lame basale par les métalloprotéinases de la

matrice (MMPs). Des études ont démontré que l'activité de MMP-9 est fortement augmentée entre 15 et 48 heures après une ischémie (Danton, 2003). Chez les patients ayant subi une ischémie cérébrale, il existe d'ailleurs une corrélation positive entre la concentration en MMP dans le plasma sanguin et le volume de la lésion ischémique (Danton, 2003). Une fois la barrière perméable, les cellules immunitaires comme les neutrophiles, les monocytes et les lymphocytes, vont pouvoir pénétrer facilement la région ischémique. Les monocytes/macrophages deviendront entre le 5^{ième} et le 7^{ième} jour le type cellulaire prédominant dans la zone ischémique (Danton, 2003). De plus, tous ces leucocytes adhèrent à la paroi endothéliale réduisant le débit sanguin des petits capillaires ce qui nuit à la reperfusion et prolonge l'hypoxie (Stoll, 1998).

1.6 Le rôle de la glie : Astrocytes et Microglies

1.6.1 Les astrocytes

L'astrocyte est le type cellulaire le plus abondant et représente environ 35 % de la masse totale du SNC. Influencé par leur environnement extracellulaire, on distingue deux groupes d'astrocytes morphologiquement différents : les astrocytes de type fibreux et les astrocytes de type protoplasmiques (Panickar, 2005).

Le cytosquelette des astrocytes matures est constitué en grande majorité de filaments intermédiaires de type GFAP (glial fibrillary acidic protein). Cette protéine est l'une des plus synthétisée dans le cerveau et se retrouve en plus grande quantité dans les astrocytes fibreux (Panickar, 2005 et Eng, 2000). La GFAP a un rôle dans la modulation de la mobilité cellulaire et dans le maintien de la morphologie de l'astrocyte (Eng, 2000).

Normalement, les neurones puisent leur énergie du glucose présent dans le sang et des astrocytes qui ont transformés le glucose en lactate (Benarroch, 2014). Les astrocytes servent donc de source énergétique pour les neurones en fournissant les substrats nécessaires lors de période de stress énergétique (Panickar, 2005).

Le cerveau consomme beaucoup d'énergie et paradoxalement, les réserves de glycogène du cerveau sont minuscules comparativement à celles retrouvées dans le foie et les muscles. Afin de supporter les neurones et leur fournir le glycogène, leur principale source énergétique, les astrocytes possèdent des enzymes qui ont la capacité de métaboliser le glycogène. Le glycogène est un polymère de glucose, par contre les astrocytes n'ont pas l'enzyme nécessaire (glucose-6-phosphatase) pour synthétiser du glucose à partir du glycogène (Brown, 2007). Le glycogène est une grosse molécule qui ne peut pas sortir des cellules, il doit donc être préalablement transformé en lactate par les astrocytes. Lors d'une ischémie cérébrale, le glycogène est transformé en lactate, libéré dans le milieu extracellulaire pour être utilisé par les neurones. C'est pourquoi en culture, les neurones et leurs axones fonctionnent normalement lorsque le lactate est substitué au glucose (Brown, 2007).

Suite à ischémie cérébrale, les astrocytes vont adopter une morphologie légèrement hypertrophiée qui peut être causée par plusieurs facteurs. L'une de ces causes serait l'arrêt complet et/ou la baisse de rendement énergétique qui empêcherait le maintien du volume cellulaire normal au détriment d'une membrane électriquement neutre (Panickar, 2005). De plus, les concentrations élevées de potassium, de glutamate, d'acide lactique, de radicaux libres et d'acide arachidonique peuvent causer le gonflement astrocytaire. Un gonflement moyen de l'astrocyte a des effets bénéfiques en augmentant la synthèse de glycogène et en favorisant la libération de taurine. La taurine est un acide aminé qui diminue l'excitotoxicité, en plus d'avoir des propriétés anti-oxydantes et neuroprotectrices (Panickar, 2005). Par contre, un gonflement astrocytaire excessif aurait comme conséquence de réduire davantage l'apport sanguin en compressant les capillaires (Panickar, 2005).

Les astrocytes sont aussi plus résistants que les neurones face à l'ischémie, leur contenu plus élevé en enzymes et en protéines de défense protège les astrocytes. En effet, les astrocytes présentent des niveaux élevés en protéines antioxydantes

(catalase, Superoxyde dismutase) et en protéines anti-apoptotiques comme Bcl-2 (B-cell lymphoma 2). De plus, les astrocytes ont des réserves énergétiques qui leur permettent de survivre plus longtemps que les neurones. Une activité supérieure de l'enzyme pyruvate carboxylase de même que la possibilité d'utiliser les acides gras et les corps cétoniques rendent les astrocytes plus résistants à l'ischémie (Panickar, 2005).
La population des astrocytes est très hétérogène au niveau de leur fonction, de leur contenu cellulaire, de leur emplacement et même de leur résistance face à une ischémie (Brown, 2007). Les astrocytes localisés dans l'hippocampe seraient plus sensibles que les astrocytes corticaux, ce qui serait en grande partie dû à une différence de leur contenu en antioxydants et en protéines anti-apoptotiques (Panickar, 2005).

Une fois activés, les astrocytes vont former une barrière autour de la zone lésée, appelée cicatrice gliale. Le rôle de la cicatrice gliale est indéterminé. Elle représenterait une tentative du SNC pour restaurer l'environnement extracellulaire en contenant la zone endommagée et ainsi favoriser les processus de réparation (Panickar, 2005). L'astrogliose serait bénéfique dans la phase aigüe en limitant l'étendue de la lésion, mais deviendrait néfaste lors de la phase de régénération en nuisant à la régénérescence des neurones (Pekny, 2005).

1.6.2 Les microglies

Les microglies se retrouvent aussi dans le SNC et leur densité varie grandement. Selon la région cérébrale, elles peuvent atteindre de 5 à 20 % de la population cellulaire et comme pour les astrocytes il existe des sous-populations de cellules microgliales (Saijo, 2011). La microglie est un macrophage spécialisé spécifique au SNC. Par contre en immunohistochimie, contrairement aux astrocytes, aucun marqueur n'est spécifique aux cellules microgliales pour les distinguer des macrophages. Pour les identifier, il faut utiliser une combinaison de marqueurs. Les microglies originent de la vésicule vitelline lors des premiers jours

embryonnaires de la souris (E9.5) (Saijo, 2011). Durant le développement murin une vague de cellules primitives progénitrices migrent dans le SNC et se différencient en microglies (E10.5) (Boche, 2013, Saijo, 2011, Ginhoux, 2010). Le renouvellement ainsi que la prolifération des cellules microgliales dans le SNC a longtemps été matière à débat. L'absence d'infiltration dans le cerveau sain adulte suggère fortement qu'il y a un renouvellement à partir des cellules microgliales résidentes (Saijo, 2011, Green, 2014). Le vieillissement affecte les microglies (Norden, 2013). D'ailleurs, chez les personnes âgées on observe des niveaux d'excitation des microglies supérieurs à ceux observés chez les jeunes adultes. Ce phénomène existe aussi chez la souris. L'expression de marqueurs d'inflammation comme le CMH II (complexe majeur d'histocompatibilité), les récepteurs TLR ainsi que plusieurs autres marqueurs augmentent avec l'âge (Norden, 2013). En ce qui concerne le CMH II, il est exprimé par les cellules présentatrices d'antigènes et assure la présentation de l'antigène aux lymphocytes T (Norden, 2013). Le CMH II serait un marqueur d'activation des microglies.

Une fois dans le SNC, la microglie dite « quiescente » est loin d'être inactive. La microglie possède de nombreuses ramifications qui sondent l'environnement, en plus de faire de nombreux contacts avec les neurones et les autres cellules gliales. Dans un cerveau sain, les microglies entretiennent un lien étroit avec les neurones et c'est d'ailleurs les neurones qui maintiennent en partie les microglies sous leurs formes dites « quiescentes ». Les neurones y parviennent grâce à l'expression de CD200 et de fractalkine (Eyo, 2013). Le CD200 est une glycoprotéine exprimée à la surface des neurones. D'ailleurs, on note que les microglies adoptent un phénotype plus amiboïde, caractéristique de leur activation, chez les souris dont les récepteurs CD200R et CX3CR1 (récepteur fractalkine) sont génétiquement absents.

Toujours dans le système nerveux central adulte sain, les microglies ont aussi pour fonction de phagocyter les débris cellulaires provenant des cellules mortes. La phagocytose des cellules nécrotiques et apoptotiques est essentielle au bon

maintien homéostatique du cerveau en réduisant le déversement du contenu cellulaire des cellules mortes dans le milieu. Cela prévient l'initiation d'une réaction inflammatoire et par la même occasion supporte la neurogénèse (Tremblay, 2011). D'ailleurs, les microglies sécrètent des facteurs favorisant la neurogénèse tels que le BDNF, l'IGF1 et le TGF-β (Saijo, 2011). Les microglies sont aussi impliquées dans le remodelage des synapses non fonctionnelles, ce qui favorise la plasticité cérébrale et le maintien d'un cerveau sain (Tremblay, 2011).

La morphologie de la microglie change rapidement lorsqu'elle détecte un agent infectieux ou une anomalie causée par un traumatisme. Suite à une ischémie cérébrale, ses nombreuses ramifications vont se rétracter lui conférant une forme plus amiboïde. Attirée par des facteurs endogènes et chimiotactiques, la microglie va migrer vers la source et proliférera localement au site inflammatoire (Johann, 2012). Cette morphologie typique des microglies dites « activées », la rend difficile à différencier des macrophages qui entrent dans le SNC suite à une ouverture dans la BBB ou simplement par diapédèse.

Ce passage de la forme « quiescente » à une forme « active » a lieu grâce à ses récepteurs membranaires qui sondent l'environnement. Les microglies expriment plusieurs familles de récepteurs qui détectent les PAMPs (pathogen-associated molecular patterns). Cette super famille comprend les TLRs (toll-like receptors), les RLRs (RIG-I-like receptors), les NLRs (NOD-like receptors) et les « C-type lectin receptors » (Saijo, 2011). En plus de détecter les PAMPs, les microglies peuvent aussi reconnaitre les DAMPS (damage associated molecular patterns) (Saijo, 2011).

Quelques minutes seulement après l'ischémie cérébrale, les microglies activées vont s'accumuler dans la zone endommagée et en bordure de la lésion (Xing, 2012). Elles prolifèrent, augmentent leur motricité, activent leur capacité phagocytaire et vont surexprimer les molécules du CMH en plus de produire différentes cytokines, des chimiokines et générer des ROS. La période de

prolifération des microglies atteint un maximum entre 48 et 72 heures après l'ischémie et peut durer jusqu'à plusieurs semaines, voire des mois (Lalancette-Hébert, 2009). Malgré le fait qu'elles génèrent et maintiennent l'inflammation en recrutant d'autres cellules pro-inflammatoires, les microglies sont nécessaires à la récupération fonctionnelle. En effet, elles ont un double rôle, car elles libèrent aussi des cytokines anti-inflammatoires (TGF-β et IL-10) qui auront un effet important sur la neuroprotection ainsi que sur les cellules immunitaires comme les cellules T (Iadecola, 2011). Par exemple, l'ablation sélective des microglies résidentes en prolifération, microglies responsables de la production d'IGF-1, dans un modèle de souris transgénique augmente la mort cellulaire et le volume de la zone ischémique (Lalancette-Hébert, 2007).

1.7 Mort cellulaire

Dans les minutes qui suivent la réduction d'apport sanguin, des dommages aux différentes cellules sont observés. Les cellules vont emprunter deux mécanismes différents pour mourir. Les cellules les plus touchées par les différents évènements pathologiques (dépolarisation de la membrane, stress oxydatif, apport énergétique coupé etc.) vont mourir par nécrose. Les cellules moins affectées et/ou plus éloignées de la zone ischémique vont mourir par apoptose. Ces deux mécanismes de mort cellulaire utilisent des processus différents qui auront une influence sur le développement de la zone ischémique.

La mort cellulaire par nécrose survient après qu'un stress très élevé à l'extérieur de la cellule nuise à son fonctionnement. La nécrose implique la rupture des lysosomes suivie de la rupture de la membrane plasmique. Les lysosomes sont des organites cellulaires contenant des enzymes, dont des lipases et des protéases, qui sont normalement impliquées dans la digestion des déchets cellulaires. Ce type de mort non programmée a pour effet de répandre, dans le milieu extracellulaire, le contenu des cellules touchées induisant une réponse inflammatoire dans les tissus avoisinants, attirant lymphocytes et macrophages.

Le mécanisme de mort cellulaire par apoptose nécessite de l'énergie et entraîne un démantèlement coordonné de la cellule. Cela ne génère pas de réponse inflammatoire puisque le contenu cellulaire n'est pas relargué dans l'environnement. L'apoptose survient après quelques heures voir même quelques jours après l'ischémie cérébrale (Broughton, 2009). Deux voies sont utilisées par les cellules en apoptose, la voie intrinsèque et la voie extrinsèque.

La voie intrinsèque (figure 4) est caractérisée par le dérèglement des mitochondries suite à l'augmentation massive de la concentration en Ca^{2+} à l'intérieur des cellules. Cette augmentation est causée par l'arrêt des pompes qui maintiennent le gradient ionique, qui sont-elles mêmes stoppées par le manque en apport énergétique causé par l'arrêt sanguin. Donc, en plus d'être incapable de fabriquer de l'ATP et de produire des ROS, les mitochondries sont impliquées dans la mort neuronale. Suite à la libération du cytochrome c ou de AIF (apoptosis inducing factor) le cytochrome c va former un complexe, l'apoptosome, entre autre constitué de Apaf-1, proCaspase-9 et de l'ATP.

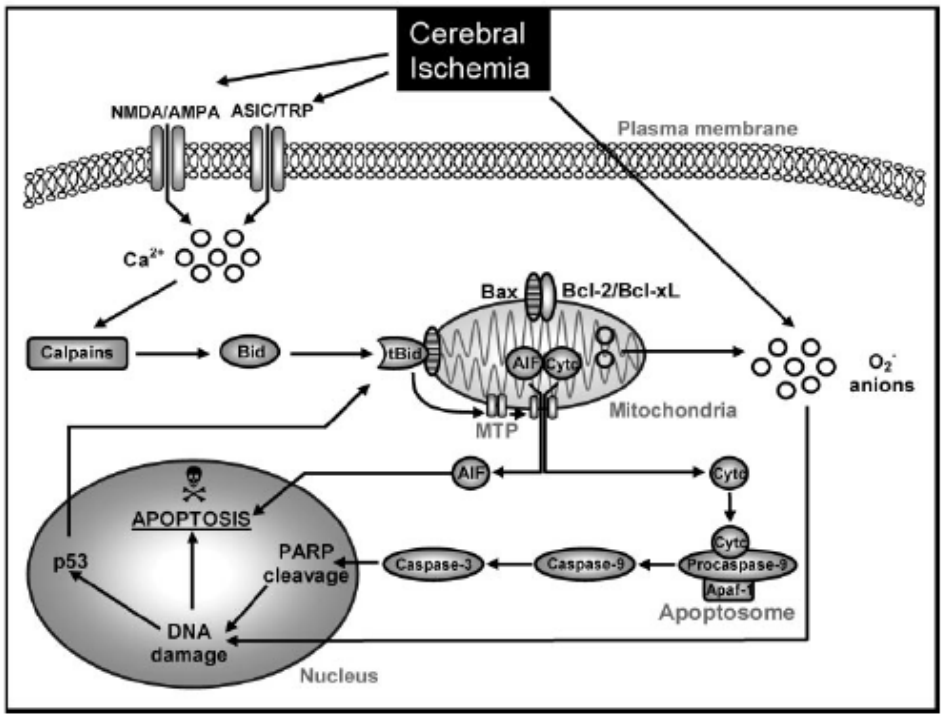

Figure 4. Voie de signalisation intrinsèque de l'apoptose suite à une ischémie cérébrale (Broughton, 2009).

L'apoptosome va activer caspase-3 qui va à son tour inactiver PARP (figure 4). Étant impliqué dans la réparation de l'ADN, l'inactivation de PARP mène à des erreurs pendant la transcription de l'ADN lors du cycle cellulaire entraînant la mort de la cellule. L'inactivation ou l'inhibition de l'un des membres de l'apoptosome ou de la caspase-3 est d'ailleurs un bon moyen de réduire les dommages causés par l'ischémie cérébrale. Une voie n'impliquant pas caspase-3 est aussi présente. Cette voie utilise un deuxième groupe de protéines dont fait partie AIF. Certains la nomment nécrose programmée, alors que d'autres suggèrent que c'est simplement de l'apoptose (Broughton, 2009).

La voie extrinsèque (figure 5), utilise des récepteurs localisés sur la membrane plasmique. Les récepteurs de la famille des tumor necrosis factor receptor (TNFR), ce qui inclut TNFR-1 et Fas, sont stimulés suite à une ischémie cérébrale. Par la suite, un complexe nommé DISC (death inducing signaling complex) va cliver la procaspase-8 en capase-8 qui va à son tour activer caspase-3 et enclencher les mécanismes décrits plus tôt (inactivation de PARP, etc.) (Broughton, 2009).

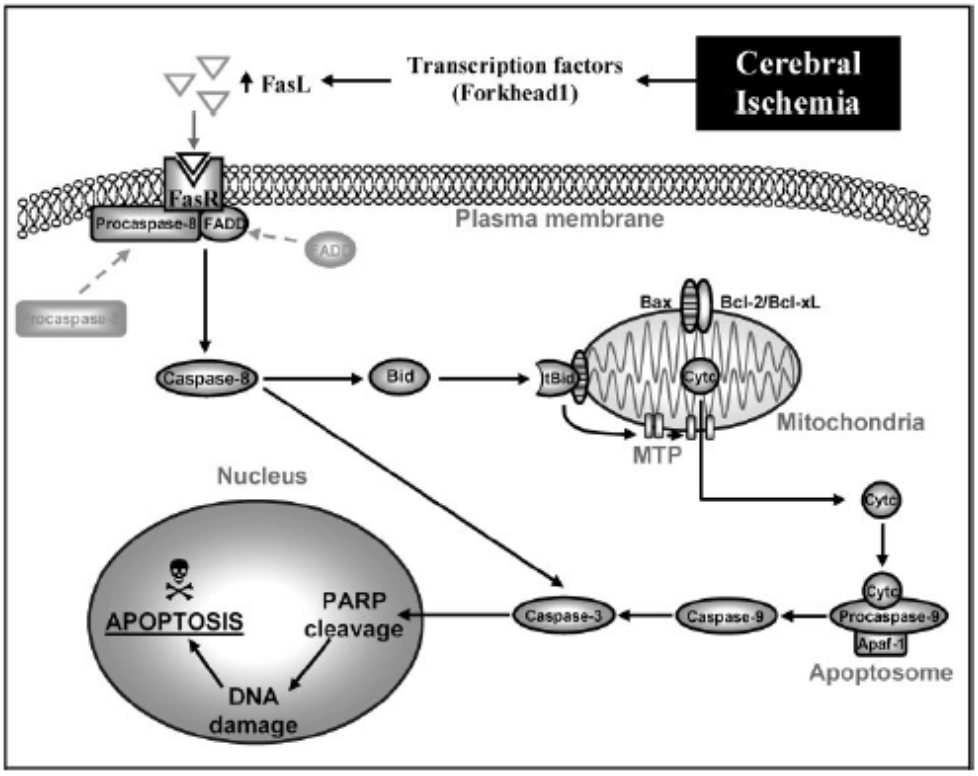

Figure 5. Voie de signalisation extrinsèque de l'apoptose suite à une ischémie cérébrale (Broughton, 2009).

1.8 Interaction entre le système immunitaire et le cerveau ischémique

1.8.1 Les récepteurs de type TLRs

La reconnaissance des microbes et des facteurs virulents est fondamentale au bon maintien de la protection de l'hôte. C'est pourquoi celui-ci est doté de récepteurs de type TLRs, des protéines transmembranaires impliquées dans la défense de l'organisme contre les pathogènes (Kong, 2011). Les TLRs forment des homodimères ou des hétérodimères. Alors que la plupart des récepteurs TLRs forment des homodimères, TLR2 forment des hétérodimères en se liant avec TLR1 ou TLR6 (Werling, 2003). Jusqu'à maintenant, 11 récepteurs TLRs ont été identifiés chez l'homme et 13 chez la souris (Wang, 2011).

On retrouve les récepteurs TLRs sur plusieurs cellules immunitaires comme les neutrophiles, les macrophages, les cellules dendritiques, les lymphocytes B et

les microglies. Ils sont aussi présents sur des cellules qui ne font pas partie du système immunitaire comme les fibroblastes, les cellules épithéliales, les kératinocytes, les myocytes et les neurones (Arumugam, 2009). Les récepteurs TLRs font partie de l'immunité innée et chaque récepteur reconnait un motif spécifique d'un agent pathogène donné. Beaucoup moins complexe que le système immunitaire adaptatif qui peut reconnaître jusqu'à 10^{11} molécules différentes, il n'en demeure pas moins que les récepteurs TLRs sont très importants pour la défense immunitaire (Sasai, 2013). Par contre, le rôle des récepteurs TLR2 serait à la fois néfaste et protecteur en fonction du temps suite à l'ischémie. En effet, le récepteur TLR2 suite à une ischémie cérébrale est fortement impliqué dans la réaction inflammatoire (Kong, 2011 et Lalancette-Hébert, 2009). Par contre, à long terme l'absence du récepteur TLR2 nuit aussi au rétablissement de la souris (Bohacek, 2012).

Les récepteurs TLRs peuvent reconnaitre deux types de ligands : les ligands exogènes (PAMPs) et les ligands endogènes (DAMPs). De plus, les récepteurs TLRs servent de pont entre l'immunité inné et l'immunité adaptative par l'entremise des cellules présentatrices d'antigènes comme les macrophages et les cellules dendritiques (Werling, 2003). Les PAMPs sont rapidement détectées par les récepteurs TLRs. Dans la catégorie des PAMPs, on englobe les lipides, les lipoprotéines, les protéines et les acides nucléiques de différents microorganismes comme les virus, les bactéries, les protozoaires et les moisissures (Arumugam, 2009). Afin d'éviter le développement de maladies auto-immunes, le système immunitaire inné doit être strictement régulé pour éviter toute sur-activation. C'est pourquoi des mécanismes inhibiteurs comme l'expression soluble de TLR2, l'utilisation d'un régulateur négatif intracellulaire, l'expression d'une protéine transmembranaire régulatrice ainsi que la réduction de l'expression du récepteur TLR2 sont tous des moyens utilisés par la cellule pour contrôler son activation (Liew, 2005).

Malgré qu'il y ait plusieurs récepteurs de types TLRs, il existe peu de voies intracellulaires d'activations communes en aval à tous ces récepteurs. Une fois stimulés, les récepteurs TLRs vont activer des facteurs de transcriptions comme le NF-κB, JNK et IRF (O'Neill, 2007). Ces voies métaboliques utilisent une combinaison de cinq protéines adaptatives, la plus connue étant le MyD88. MyD88 est une protéine utilisée par tous les TLRs sauf le TLR3 qui utilise la protéine adaptatrice TRIF. Le NF-κB (figure 6) est finalement activé lorsqu'il y a phosphorylation et dégradation de l'inhibiteur IκB. Une fois libéré, NF-κB est transloqué dans le noyau cellulaire où il y aura transcription de gènes proinflammatoires.

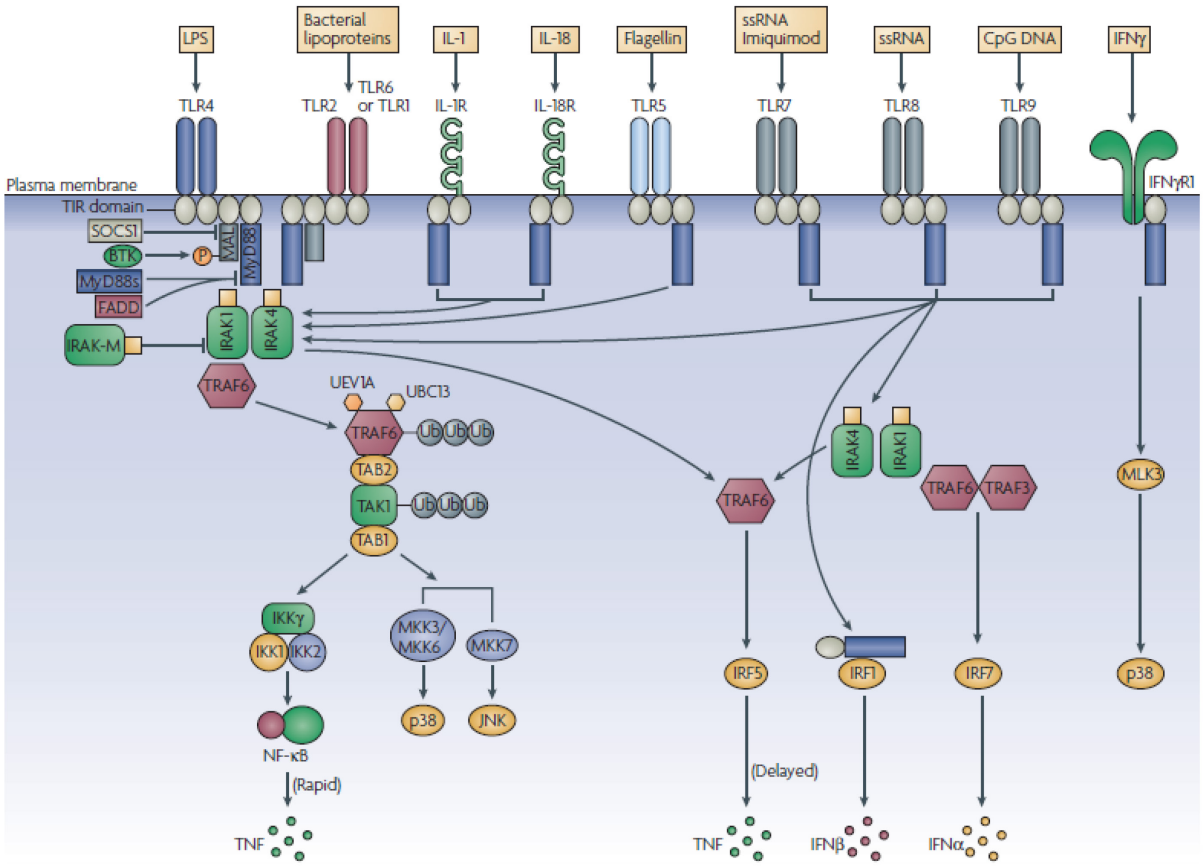

Figure 6. Représentation des récepteurs TLRs et de la voie de signalisation dépendante de MyD88 induisant la neuroinflammation (O'Neill, 2007).

1.8.2 Système immunitaire : inné et adaptatif

La microglie, les macrophages, les cellules dendritiques ainsi que les cellules endothéliales font partie du système immunitaire inné et jouent un rôle important dans l'établissement de toutes réponses inflammatoires (Macrez, 2011). Après l'ischémie cérébrale, la zone lésée se remplit de débris cellulaires et de molécules normalement absentes du milieu extracellulaire. La microglie y perçoit rapidement les changements et s'active (Iadecola, 2011). Parmi les signaux perçus comme dangereux, il y a l'ATP, l'ADN, l'ARN, les HSP (heat shock proteins), le glutamate ainsi que des composantes de la matrice extracellulaire (Pineau, 2009). Toutes ces molécules, qui sont aussi appelées DAMPs (danger- associated molecular pattern molecules) vont activer les récepteurs TLRs exprimés entre autre par les microglies, les cellules endothéliales ainsi que par les macrophages périvasculaires.

De son côté, l'immunité adaptative se développe à la suite de l'immunité innée. L'immunité adaptative se caractérise par le développement d'anticorps spécifiques par le système immunitaire contre un antigène particulier. Une nouvelle rencontre avec cet antigène activera le système immunitaire plus rapidement et fortement grâce au phénomène de «mémoire ». Le système immunitaire adaptatif composé des lymphocytes T et B est aussi impliqué lors d'une ischémie cérébrale. En effet, plusieurs études ont démontré que les cellules immunitaires s'accumulent dans la zone ischémique, mais leur implication à long terme dans la zone lésée est encore mal comprise (Stubbe, 2013). Ce qui distingue les lymphocytes B des lymphocytes T est le relâchement de cytokines et d'anticorps pour les lymphocytes B (Abbas, 2005). Il existe plusieurs types de cellules T. Il y a les cellules T auxiliaires ($CD4^+$), les cellules T cytotoxiques ($CD8^+$), les cellules T régulatrices ($FOXP3^+$), les cellules T de types γδ et les cellules NKT (Abbas, 2005).

À la suite d'une ischémie cérébrale, les lymphocytes T $CD4^+$ et $CD8^+$ sont directement impliqués dans la réaction inflammatoire en libérant plusieurs cytokines. Les cellules $CD4^+$ TH1 libèrent des cytokines proinflammatoires comme

l'IL-2, IL-12, IFN-γ et du TNF-α, alors que les cellules $CD4^+$ TH2 libèrent des cytokines anti-inflammatoires comme l'IL-4, IL-5, IL-10 et le IL-13. Les cytokines pro-inflammatoires, attirent et font augmenter le nombre de leucocytes et de plaquettes dans les petits capillaires nuisant ainsi à la reperfusion suite à l'ischémie cérébrale (Jin, 2010).

Il y a aussi les lymphocytes T régulateurs (T_{reg}) qui sont une sous-population des cellules $CD4^+$ très importante dans la régulation de la réponse immunitaire suite à une ischémie cérébrale. En effet, cette population de lymphocytes T empêcherait la production excessive de cytokines proinflammatoires ce qui diminuerait le volume de la lésion ischémique (Liesz, 2009). Pour y arriver les cellules T_{reg} limitent la production de TNF-α et d'IFN-γ tout en libérant de l'IL-10. Lorsque les cellules de types T_{reg} sont absentes, l'activation des cellules inflammatoires résidentes ainsi que celle des cellules infiltrantes sont augmentées (Jin, 2010).

Les cellules T de types γδ sont une source d'IL-17 et sont impliquées plus tardivement dans le processus inflammatoire. Une étude récente démontre que le volume de lésion chez les souris IL-17KO est en effet inférieur au $4^{ième}$ jour lorsqu'elles sont comparées aux souris contrôles (Shichita, 2009). L'IL-17 produit par ces cellules amplifierait la production de facteurs neurotoxiques nuisant ainsi au rétablissement des tissus touchés.

En conclusion, les différents sous-types de lymphocytes T ont des rôles distincts suite à l'ischémie cérébrale. Ils peuvent donc être une excellente cible thérapeutique à condition de bien prendre soin d'activer les cellules T bénéfiques tout en inhibant les cellules T délétères.

1.9 Rôle des hormones dans l'ischémie cérébrale

1.9.1 La progestérone

La progestérone possède deux récepteurs nucléaires spécifiques (PRA, PRB) qui se retrouvent dans toutes les régions du cerveau. Peu d'études s'intéressent aux effets neuroprotecteurs de la progestérone sur le cerveau suite à une ischémie cérébrale (Liu, 2012). La plupart des études regardent le rôle de l'œstrogène seule ou combinée avec la progestérone. Par contre, les quelques études effectuées chez les souris démontrent un effet neuroprotecteur chez les mâles comme chez les femelles. L'administration de progestérone suite à une ischémie cérébrale diminue la mort cellulaire et augmente la récupération fonctionnelle (Gibson, 2009). Une diminution de médiateurs pro-inflammatoires comme l'IL-1β et iNOS est observée. De plus, la progestérone diminue de façon significative l'œdème cérébral en modulant l'aquaporine (AQP4), l'un des canaux principaux pour le transfert de l'eau dans le cerveau.

1.9.2 Les oestrogènes

Les œstrogènes constituent une famille d'hormones stéroïdiennes retrouvées chez les femelles et, en plus faible quantité, chez les mâles. Les trois différents types d'oestrogènes naturels sont l'oestradiol (E2), l'oestriol (E3) et l'oestrone (E1). Sécrétée par les ovaires, l'oestradiol est l'hormone principale féminine synthétisée, en autre, à partir de la testostérone par l'enzyme aromatase. Dans le cerveau, le 17β-estradiol est un facteur de croissance qui favorise la croissance et la différenciation cellulaire (Toran-Allerand, 2004). Il favorise la stabilisation de la BBB, active les mécanismes anti-apoptotiques, régule les processus inflammatoires en plus de réduire l'excitotoxicité induite par le glutamate (Johann, 2012).

Avant la ménopause, le risque de subir une ischémie cérébrale est moindre chez les femmes comparées aux hommes de même âge. Par contre, après la ménopause, qui se caractérise par une chute d'oestrogènes et de progestérone,

les risques de subir un accident cérébral vasculaire augmentent (Gibson, 2006). Ces hormones ont donc un effet préventif et protecteur chez les femmes et chez les modèles animaux. En effet, l'effet neuroprotecteur observé chez les femelles en réponse à une ischémie cérébrale est perdu après une ovariectomie et est retrouvé après l'administration d'oestrogènes. Chez les mâles, l'œstrogène a aussi un effet préventif et neuroprotecteur suite à son administration (Hoffman, 2006). Le moment entre l'administration de l'œstrogène et la période d'hypoestrogénie (ovx ou ménopause) est important car si le remplacement est tardif l'E2 perd de ses effets neuroprotecteurs et anti-inflammatoires (Suzuki, 2007).

1.9.3 Les récepteurs des oestrogènes

Les récepteurs œstrogéniques se retrouvent partout dans le SNC. Trois types de récepteurs œstrogéniques ont été identifiés dans le SNC, les récepteurs α (Erα), les récepteurs β (Erβ) et les récepteurs couplés aux protéines G. Leur expression et leur localisation vont varier en fonction du stade développemental. Par exemple, en condition normale, les récepteurs ERα sont exprimés seulement lors de la période de différenciation corticale, alors qu'une étude récente a démontré que l'expression du récepteur Erβ varie avec l'âge (Yamaguchi, 2014).

Les neurones, les astrocytes, les cellules de l'endothélium, les plaquettes sanguines et les microglies possèdent des récepteurs œstrogéniques. Pour avoir un effet direct sur la régulation de certains gènes et facteurs de transcription, les oestrogènes ont comme particularité de se lier à l'ADN du gène cible dans une région appelée ERE (estrogen response element) (Toran-Allerand, 2004). Il existe quatres voies d'activation impliquant les récepteurs oestrogéniques et l'oestrogène (figure 7). Premièrement, il y a l'activation directe du gène via les récepteurs œstrogéniques intranucléaires. Lorsque les récepteurs Erα et Erβ sont inactifs, ils forment un complexe avec différentes molécules chaperonnes, dont la protéine de choc thermique 90 (HSP 90). La liaison de l'œstrogène et de son récepteur entraine la dissociation du récepteur avec la protéine HSP90. Ce changement de conformation induit alors une interaction du récepteur avec l'ADN à une région

spécifique du promoteur du gène cible, l'ERE. Cette région régule plusieurs gènes et facteurs de transcription comme le NF-κB qui peuvent être induits après une ischémie cérébrale (Toran-Allerand, 2004). Deuxièmement, l'œstrogène se lie aux récepteurs membranaires puis active un second messager qui par la suite peut activer à son tour les facteurs de transcription (McCullough, 2003). La troisième voie de signalisation s'effectue sans les récepteurs oestrogéniques. De part sa conformation, l'estrogène possède des propriétés anti-oxydantes et peut ainsi limiter la libération de ROS venant des mitochondries endommagées (Cui, 2013). La quatrième voie se caractérise par l'activation des récepteurs oestrogéniques en absence d'œstrogène. Cette voie a la particularité d'être activée par une variété de facteurs comme la dopamine et IGF-1 (Cui, 2013).

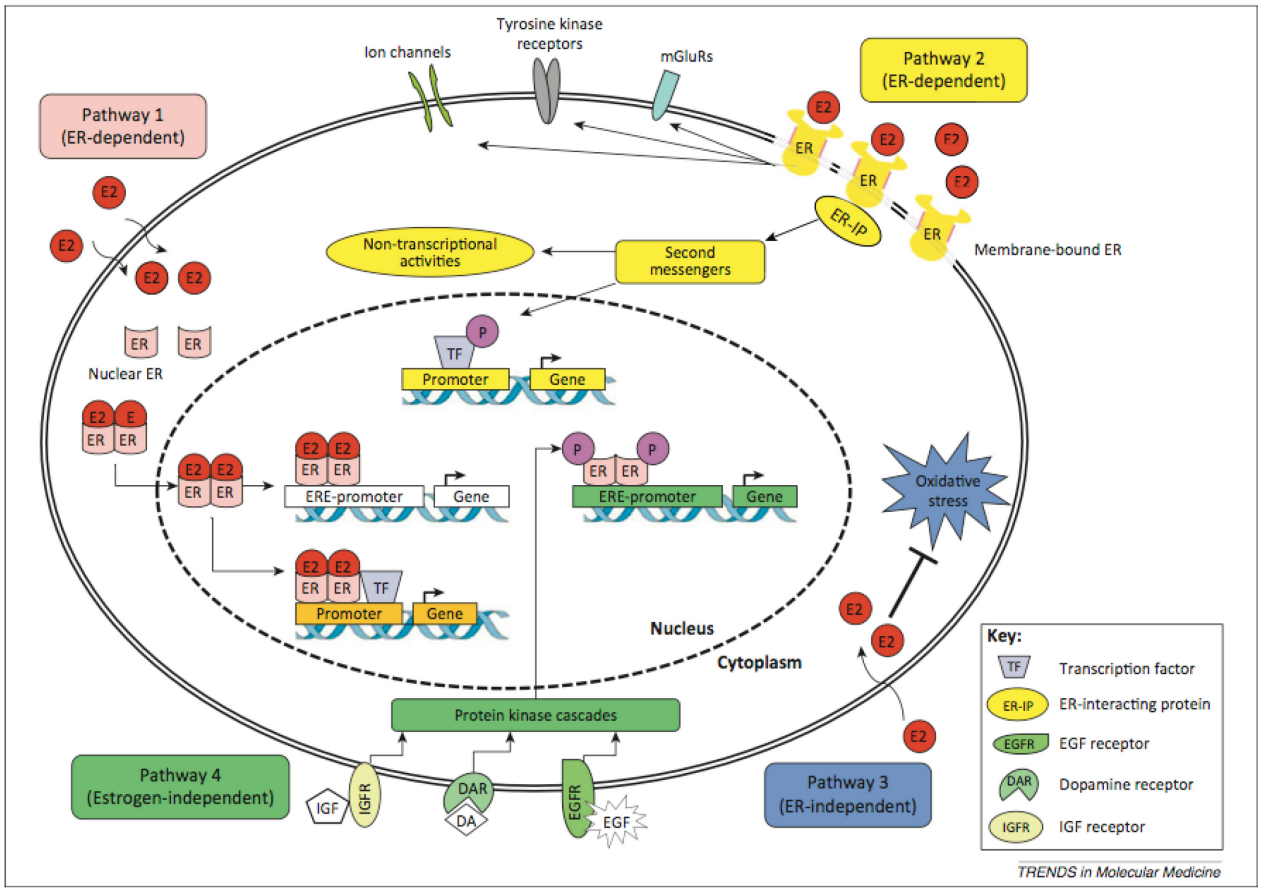

Figure 7. Voie d'activation de l'estrogène ainsi que de ses récepteurs (Cui, 2013).

Il ne fait aucun doute qu'en présence d'E2 les récepteurs oestrogéniques peuvent jouer un rôle neuroprotecteur suite à une ischémie cérébrale (Shin, 2013; Schreihofer, 2013; Zhang, 2011). Par contre, les études effectuées à l'aide de souris KO pour les récepteurs Erα et Erβ ont démontré que le récepteur Erα serait le récepteur le plus impliqué dans la neuroprotection (Schreihofer, 2013). Une étude a démontré chez des souris ovariectomisées supplémentées en E2 que le volume de la lésion est réduit après 24 heures. Par contre cet effet protecteur est perdu chez les souris ErαKO, mais pas chez les souris ErβKO (Dubal, 2000). De plus, une seconde étude a démontré que 24 heures après une ischémie cérébrale transitoire, l'expression des récepteurs Erα est augmentée du côté lésé par rapport au côté non lésé. Les niveaux observés seraient comparables à ceux mesurés lors du développement cérébral, un moment soutenu en neurogenèse. Ces études appuient l'hypothèse de l'importance du récepteur alpha à la suite d'une ischémie cérébrale (Suzuki, 2009).

Par contre, le type de lésion ischémique aurait un effet sur la neuroprotection observée. En effet, le rôle du récepteur Erα serait clairement démontré dans le modèle d'ischémie permanente. Cependant, son rôle dans l'ischémie cérébrale transitoire serait moins bien établit. Lors d'études utilisant des agonistes spécifiques dans un modèle d'ischémies cérébrales transitoires, c'est le récepteur Erβ qui serait le plus impliqué. Il est aussi important de mentionner que chez les singes la quantité de récepteurs Erβ présentes dans l'hippocampe augmente après la ménopause, alors qu'elle diminue chez les rongeurs (Schreihofer, 2013). Le modèle ischémique ainsi que l'espèce animal seraient donc des facteurs à considérer dans ce type d'études.

1.10 Modèles et techniques

1.10.1 Les modèles animaux

Afin d'étudier les mécanismes impliqués lors d'une ischémie cérébrale, plusieurs modèles animaux (souris, rat, chien, lapin, primate) ont été développés.

L’utilisation de souris comporte des avantages lorsque l’on compare celles-ci aux autres modèles. Leur petite taille, la facilité à être manipulées, leur taux de reproduction élevé ainsi qu’un coût d’utilisation relativement bas font de la souris un excellent choix. De plus, pour faire des études mécanistiques ou pharmacologiques, plusieurs modèles de souris modifiées génétiquement sont disponibles. En parallèle, plusieurs tests neurosensoriels et moteurs ont été validés pour mesurer la récupération fonctionnelle des souris après l’ischémie cérébrale. Par contre, l’utilisation de la souris comporte aussi quelques points négatifs. En effet, l'inaptitude à répliquer chez l’homme les avancées scientifiques chez la souris démontre une certaine incompatibilité du modèle et/ou une incapacité à utiliser correctement les modèles murins disponibles.

Il existe 4 modèles d’ischémie cérébrale. Il y a l’ischémie cérébrale complète, l’ischémie globale incomplète, l’ischémie cérébrale focale et l’ischémie cérébrale multifocale (figure 8). L’ischémie cérébrale globale touche la totalité ou la quasi-totalité du cerveau tandis que l’ischémie focale ne touche qu’une région spécifique. L’ischémie cérébrale multifocale touche pour sa part plusieurs régions simultanément (Liu, 2011). Chez l’humain, l’ischémie cérébrale la plus fréquente résulte d’une occlusion embolique ou thrombotique d’une artère cérébrale majeure. L’utilisation chez la souris, du modèle d’occlusion de l’artère cérébrale moyenne s’avère donc un bon modèle d’étude, car il simule bien ce qui survient chez l’humain. Une fois l’artère bloquée, on peut choisir de reperfuser ou non la région lésée (occlusion transitoire ou permanente). Ce modèle génère peu de variabilité dans la taille des lésions si une attention à la température corporelle et une vérification de l’obturation à l’aide d’un laser Doppler sont systématiquement effectuées.

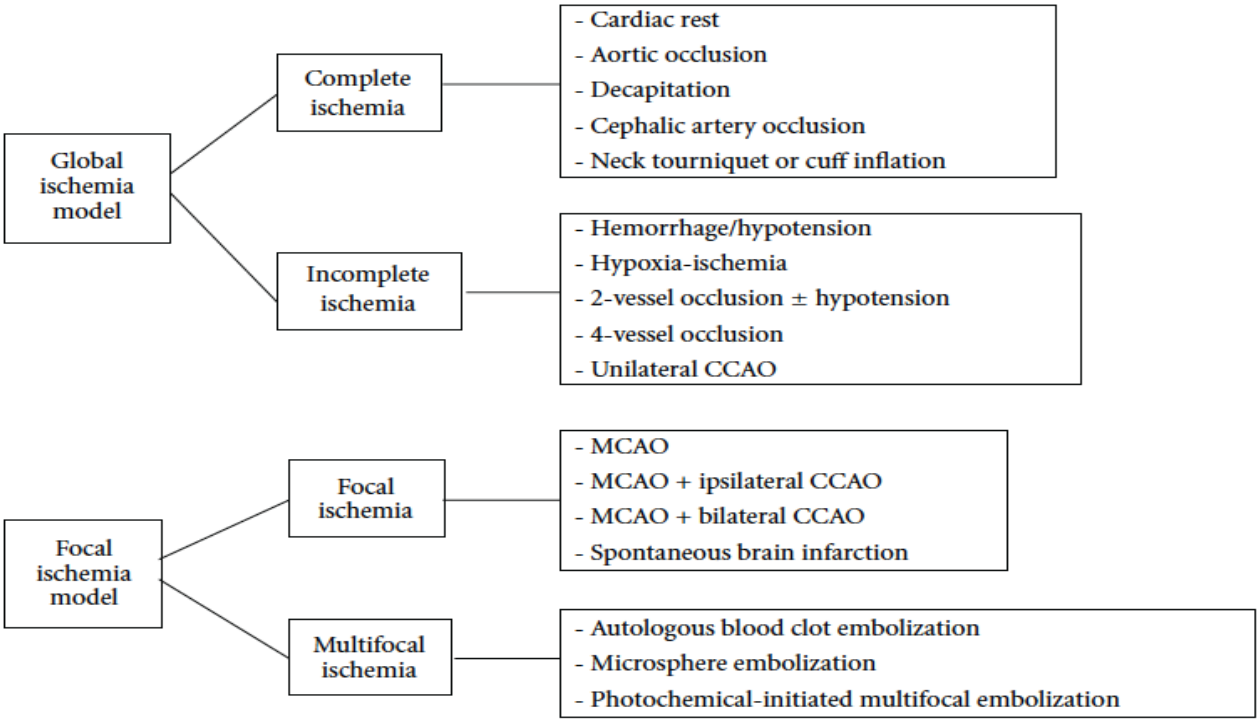

Figure 8. Modèles animaux pour étudier les ischémies cérébrales (Liu, 2011).

1.10.2 Technique

1.10.2.1 La bioluminescence

La bioluminescence ne doit pas être confondue avec la fluorescence. La fluorescence est la capacité que possèdent certains corps d'émettre des photons de longueurs d'onde plus longues (moins d'énergie) que la longueur d'onde du photon absorbé.

La bioluminescence, est la production et l'émission de lumière par un organisme vivant via une réaction chimique. Le gène le plus utilisé dans les études utilisant la bioluminescence code pour l'enzyme de la luciférase provenant de la luciole (*Photinus Pyralis*). Un avantage à utiliser l'enzyme de luciole dans une souris est que la lumière produite possède peu de bruit de fond. C'est d'ailleurs un des avantages que la bioluminescence possède par rapport à la fluorescence. Par contre, contrairement à la fluorescence, pour utiliser cette technique, les animaux

doivent être vivants car la réaction de bioluminescence nécessite de l'oxygène et de l'ATP.

Les photons émis par l'organisme transgénique sont captés à l'aide d'une caméra CCD (capteur à charges défilantes) ultrasensible. La caméra CCD convertit le signal lumineux en signal électrique et par la suite, un programme informatique quantifie l'émission photonique d'une région d'intérêt. Pour être captés par la caméra CCD les photons doivent passer au travers de plusieurs couches de tissus. La lumière diffuse donc dans les tissus autour de la source lumineuse. On peut affirmer que la brillance de la source lumineuse est directement proportionnelle à la radiance à la surface de l'animal (Xenogen, 2004). Dans sa conformation originale, la luciférase, produit une lumière à large spectre culminant à 560 nm, par contre une fraction significative est émise au-dessus de 600 nm (Contag, 2002). Cette fraction est importante puisque pour être captée par la caméra CCD, la lumière émise traversant les tissus est absorbée majoritairement par l'hémoglobine. Les longueurs d'onde les plus absorbées par cette structure, le bleu et le vert, sont celles en-dessous de 600 nm. C'est donc la fraction émise au-dessus de 600 nm qui devient disponible pour les analyses. Afin de rendre la technique encore plus efficace, de nombreuses modifications ont été faites à la luciférase ce qui a permis de déplacer son spectre d'émission encore plus vers le rouge (Contag, 2002).

La bioluminescence est utilisée comme technique de visualisation *in vivo*, car elle permet de suivre de façon non invasive des processus biologiques en temps réel dans les petits animaux de laboratoire (figure 9). La réaction à l'intérieur de la souris débute lorsque l'ATP se lie avec la luciférine préalablement liée à un ion magnésium. Le complexe Mg-ATP sert de support pour la luciférase. Par la suite, ce complexe va réagir avec la luciférase et crée une forme intermédiaire, la luciférine adénylate, entrainant la libération de pyrophosphate. Ce nouveau complexe va alors réagir avec l'oxygène, donnant l'oxyluciférine, un peroxyde qui va rapidement se cycliser après une libération d'AMP. L'oxyluciférine, excitée, va

retrouver sa stabilité en libérant un photon et du CO^2 (Contag, 2002). Il y a ensuite libération de l'enzyme qui peut alors catalyser une autre réaction chimique avec la luciférine. Les photons émis lors de la réaction sont captés par la caméra CCD. Une image créée en couleurs fictives sera superposée à une image prise à l'aide d'une caméra normale, en noir et blanc, pour localiser le signal sur la souris.

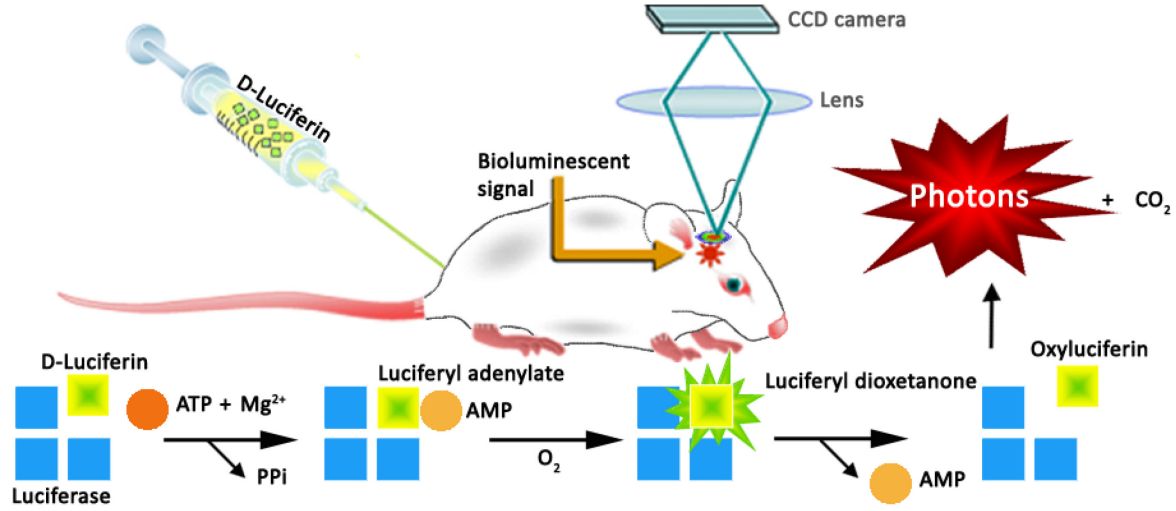

Figure 9. Réactions chimiques à l'intérieur de la souris pour générer un signal bioluminescent (Cordeau, 2012).

1.10.2.2 La reconstruction 3D

La reconstruction 3D est effectuée à partir de formules mathématiques. Le programme utilise la quantité de lumière mesurée à la surface de la souris pour générer une reconstruction 3D mathématique de la provenance de la source lumineuse. Pour ce faire, le logiciel utilise trois types d'images pour effectuer la reconstruction 3D. Il a besoin d'une photographie de la souris en noir et blanc, d'une image faite avec la lumière structurée et des images bioluminescentes prises entre 560-660nm. Pour le deuxième type d'image, l'appareil illumine le spécimen avec une lumière structurée. La lumière dite structurée consiste à projeter sur le sujet des lignes parallèles à l'aide de lasers. Le déplacement, ou autrement dit les courbures de la lumière sur le corps de la souris, va aider à recréer la topographie

du sujet. Le déplacement est la différence entre le lieu où la lumière devrait tomber sur le plateau en absence de l'objet et où la lumière est réellement à cause de l'objet. La topographie du sujet est nécessaire pour modéliser le transport photonique à la frontière de l'interface air-tissu. Pour ce qui est des longueurs d'ondes entre 560-660 nm, elles sont nécessaires, car pour ces longueurs d'ondes les propriétés optiques des tissus de la souris sont très contrastantes. Grâce à ce phénomène, le logiciel calcule la profondeur ainsi que l'intensité de la source lumineuse en fonction de paramètres connus comme la diffusion et la propagation de la lumière dans les tissus (Xenogen, 2004).

1.11 Thérapies et médicaments

Présentement, la seule thérapie efficace contre l'ischémie cérébrale est l'administration de TPA (tissue plasminogen activator) dans une brève fenêtre thérapeutique. En effet, cette protéine doit être administrée dans les 4.5 heures suivant l'ischémie cérébrale. Moins de 5 % des gens ayant un ACV vont recevoir la TPA. La TPA est un agent thrombolytique qui dissout les caillots en activant la transformation du plasminogène en plasmine. Les thérapies visant à contrôler l'inflammation sont plus avantageuses, car la fenêtre thérapeutique est plus grande et on peut l'administrer même aux personnes ayant une ischémie de type hémorragique (Iadecola, 2011).

1.11.1 Les traitements hormonaux

Les oestrogènes ont un effet global sur le cerveau, ils agissent sur les différents types cellulaires et ont un effet potentiellement vasodilatateur sur le système vasculaire. En général, les oestrogènes ont des propriétés antioxydantes qui agissent comme agent neuroprotecteur lors de l'ischémie cérébrale. Lors d'études réalisées sur des cultures corticales murines, il a été démontré que l'oestrogène protège les cellules corticales même si l'on injecte au même moment des antagonistes contre les récepteurs des oestrogènes et des inhibiteurs de la synthèse protéique (McCullough, 2003). Cela démontre clairement un effet

neuroprotecteur indépendant des voies de signalisation utilisées par les récepteurs oestrogéniques et de la synthèse protéique. L'oestrogène y parvient entre autre en récupérant les radicaux libres (Culmsee, 1999). Cependant, lorsque l'on administre des doses physiologiques d'œstrogène, on favorise l'utilisation des récepteurs oestrogéniques et non la récupération des radicaux libres. Il y a alors modulation de l'expression génique ce qui favorise la plasticité synaptique, l'expression de neurotrophines et la production de facteurs favorisant la survie cellulaire (Dubal, 2001).

Une administration d'oestrogène protège aussi le cerveau en diminuant la surexpression de cytokines pro-inflammatoires comme le MCP-1 et l'IL-6. Le MCP-1 est un facteur chimioattractant jouant un rôle nocif en augmentant l'infiltration des cellules immunitaires provenant de la circulation (monocytes et neutrophiles) vers la zone lésée du cerveau (Suzuki, 2007).

Dans les études utilisant les souris ovariectomisées, il fut démontré qu'en plus de la quantité, le moment où l'on administre les oestrogènes est crucial pour obtenir les effets neuroprotecteurs. En effet, après une période d'hypoestrogénicité prolongée, l'administration d'oestrogènes n'offre aucune protection et la diminution de MCP-1 et d'IL-6 n'est pas observée (Suzuki, 2007). Cette découverte a apporté des explications aux études sur les oestrogènes parfois contradictoires effectuées sur des groupes de femmes et de souris ayant subi une ischémie cérébrale. Cette étude a aussi démontré que suite à une ischémie cérébrale chez des souris ayant subi une période d'hypoestrogénie prolongée, le récepteur Erα n'est plus surexprimé. Normalement une augmentation des récepteurs Erα de 300 à 450 % est observée du côté lésé suite à l'ischémie cérébrale (Suzuki, 2007). Comme il fut mentionné plus tôt, le 17β-oestradiol diminuerait l'expression de gènes pro-apoptotiques via le récepteur Erα.

En conclusion, les dommages causés par l'ischémie cérébrale chez les souris en hypoestrogénie vont varier en fonction de la région touchée, du type de lésion, de la dose d'œstrogène et du moment de son administration.

1.12 Hypothèses

Les microglies font parties des premières cellules qui réagissent à tout changement anormal du milieu cérébral. Dans un modèle d'ischémie cérébrale, le passage de la forme quiescente à la forme activée des microglies est associé à une augmentation marquée du récepteur membranaire de type TLR2 (Lalancette-Hébert, 2009) ainsi qu'à la libération de cytokines pro et anti-inflammatoires (Jin, 2010). Les connaissances sur la microglie ont beaucoup avancé dans les dernières années, par contre, le rôle du récepteur TLR2 sur la récupération fonctionnelle à court et à long termes reste à être clarifié. C'est pourquoi dans notre laboratoire, nous avons créé une souris qui nous permet de quantifier l'activation de la microglie et d'étudier de façon longitudinale la réponse inflammatoire *in vivo* suite à une ischémie cérébrale. Le projet de doctorat présenté dans cette thèse a pour objectif de clarifier la dynamique et le rôle de l'activation des microglies. Pour ce faire nous allons dans les futurs chapitres :

Chapitre 2 : Présenter la technique d'imagerie utilisée au cours de mon doctorat.

Chapitre 3: Déterminer le rôle à long terme de l'activation du récepteur TLR2 et des microglies à l'aide de souris TLR2KO. Nous savons que l'activation des microglies peut durer des mois suivant l'ischémie cérébrale (Lalancette-Hébert, 2009), par contre nous ne connaissons pas l'impact à long terme de cette activation sur la zone de lésion. Notre première hypothèse est **que l'absence du récepteur TLR2 nuit de façon significative au profil inflammatoire suite à une ischémie, ce qui résulte à la formation d'une zone de lésion plus grande chez les souris TLR2KO**.

Chapitre 4 : Déterminer si l'environnement peut moduler la réponse des microglies ainsi que la récupération fonctionnelle suite à une ischémie cérébrale. La stimulation multi-sensorielle module la plasticité cérébrale dans le cerveau sain comme dans le cerveau lésé (van Praag, 2000), mais est-ce que l'environnement peut moduler la réponse inflammatoire? Cela reste à être démontré. Notre deuxième hypothèse est **qu'un milieu enrichi favorise la diminution de l'activation microgliale suite à une ischémie cérébrale et ainsi favorise la récupération fonctionnelle tout en diminuant la zone de lésion ischémique**.

Chapitre 5 : Déterminer le lien entre l'inflammation et le récepteur Erα suite à une ischémie cérébrale dans un modèle d'hypoestrogénie chronique. Comme il fut mentionné plus tôt, le récepteur Erα est fortement surexprimé suite à une ischémie cérébrale. Par contre, qu'arrive-t-il au niveau de l'activation microgliale lorsque la souris est en hypoestrogénie chronique en plus d'avoir les récepteurs Erα supprimés génétiquement? Notre troisième hypothèse est **que l'hypoestrogénie chronique va induire des lésions ischémiques plus grandes suite à une activation microgliale plus élevée. De plus, en combinant l'absence du récepteur Erα à l'hypoestrogénie chronique nous allons diminuer l'activation microgliale tout en augmentant la zone de lésion ischémique.**

Chapitre 2. Real time imaging after cerebral ischemia: model systems for visualization of inflammation and neuronal repair.

Contributions des auteurs dans l'article: Real time imaging after cerebral ischemia: model systems for visualization of inflammation and neuronal repair.

Pierre Cordeau et Jasna Kriz ont coécrit le résumé.

Real time imaging after cerebral ischemia: model systems for visualization of inflammation and neuronal repair.

Pierre Cordeau and Jasna Kriz*

Department of Psychiatry and Neuroscience, Faculty of Medicine, Laval University, Centre de Recherche du Centre Hospitalier de l'Université Laval, 2705 boul. Laurier, Québec, QC, G1V 4G2 Canada,

*Corresponding Author:
Jasna Kriz, MD, PhD
Fax:418-654-2761,
Tel:418 654-2296 # 46308
E-mail: jasna.kriz@crchul.ulaval.ca

2.1 ABSTRACT

Brain response to ischemic injury is characterized by initiation of a complex pathophysiological cascade comprising the events that may evolve over hours or several days and weeks after initial attack. At present, spatial and temporal dynamics of these events is not completely understood. To enable better understanding of the brain response to ischemic injury we developed and validated several novel transgenic mouse models of bioluminescence and fluorescence, allowing the non-invasive and time-lapse imaging of neuroinflammation, neuronal damage/stress and repair. These mice represent a powerful analytical tool for understanding *in vivo* pathology as well as the evaluating pharmacokinetics and longitudinal responses to drug therapies. Here, we describe the basic procedures of generating biophotonic mouse models for live imaging of microglial activation and neuronal stress and recovery, followed by a detailed description of *in vivo* bioluminescence imaging protocols used after experimental stroke.

Key words: biophotonic/bioluminescence imaging, stroke, transgenic mice, Firefly luciferase, TLR2, neuroinflammation, GAP-43, brain recovery

2.2 INTRODUCTION

2.2.1 Brain response to ischemic injury: a short overview

Stroke is the leading cause of death and disabilities in industrialized countries (Dirnagl *et al*., 1999; Lo *et al*., 2003). In practice, the term “stroke” refers to an umbrella of conditions caused by the occlusion or hemorrhage of blood vessel supplying the brain. In all instances, stroke ultimately involves dysfunction and death of brain cells. The neurological deficits will reflect the location and size of the compromised brain area. At the present, although progress has been made in understanding the molecular pathway that lead to ischemic cell death, the current clinical treatments remain poorly effective (Dirnagl *et al*., 1999; Lo *et al*., 2003). Here, it is important to emphasize that brain response to ischemic injury is characterized by initiation of a complex pathophysiological cascade. Once

activated the pathological cascade comprises events that may evolve over hours or several days and weeks. This will be followed by the induction of many genes that will initiate post-ischemic inflammation as well as brain recovery. However at present, a spatial and temporal dynamics of these events is not completely understood. To enable better understanding of the brain response to ischemic injury we developed and validated several novel transgenic mouse models of bioluminescence and fluorescence, allowing the non-invasive and time-lapse imaging of neuroinflammation, neuronal damage/stress and repair. The series of our recent studies suggest that biophotonic/bioluminescence signals imaged from the live animals can be used as valid biomarkers to visualize distinct pathological events after ischemic injury (Cordeau *et al*., 2008; Lalancette-Hébert *et al.*, 2009; Gravel *et al*., 2011), screen for novel biocompatible molecules (Maysinger *et al*., 2007; Lalancette-Hébert *et al.*, 2010) and/or analyze early pathogenesis and therapeutic approaches in models of chronic neurological disorders (Keller *et al*., 2009, 2011; Swarup *et al*., 2011)

2.2.2 The value of bioluminescence/biophotonic imaging in stroke research

Bioluminescence is a naturally occurring form of chemiluminescence where energy is released by a chemical reaction in the form of light emission. To date, http://en.wikipedia.org/wiki/Firefly luciferase systems have been and/are widely used in the field of genetic engineering as reporter genes (for review see Contag and Bachman, 2002; Lucker and Lucker, 2010; Close DM *et al*., 2011). In our experiment we generated and used transgenic mice expressing dual reporters, the firefly luciferase (Fluc) and the green fluorescence reporter GFP, whose transcription is dependent upon the selected gene promoter (Lalancette-Hébert *et al*., 2009; Gravel *et al*., 2011). The Fluc bioluminescence is measured and quantified in living intact animals by using high sensitivity/high resolution cooled charged-coupled device (CCD) camera whereas high resolution fluorescence imaging can be done with microscopes equipped with two-photon laser scanning capabilities. These mice represent a powerful analytical tool for understanding *in vivo* pathology of acute and chronic neurological disorders and may be used for

evaluation of pharmacokinetics and longitudinal responses to drug therapies. Here, we describe the procedures of generating biophotonic mouse models for live imaging of microglial activation/innate immune response and neuronal stress and recovery, followed by a detailed description of bioluminescence imaging protocols after the experimental stroke.

2.2.3 Design and generation of DUAL reporter mouse models for in vivo imaging of brain response to ischemic injury

Mouse model for visualization of microglial activation and innate immune response: TLR2/luc/gfp mouse model

Activated microglial cells are the main effectors of the innate immune response in the brain following injuries including ischemia. Although the role of activated microglial cells in ischemia is not yet clear, the activation of microglial cells is characterized by a robust induction of the transmembrane receptor family of Toll-like receptor 2 (TLR2). To selectively image activated microglial cells from the brains of living animals, we generated a transgenic mouse model bearing the dual reporter system luciferase and green fluorescent protein under the transcriptional control of a murine TLR2 promoter (Lalancette-Hébert *et al*., 2009). In this mouse model, transcriptional activation of TLR2 can be visualized in the brains of live animals using biophotonic/bioluminescence imaging and high resolution CCD camera.

Plasmids and vectors:

Internal Ribosome Entry Site (pIRES) vector (BD Biosciences, Mississauga, ON)
Luciferase reporter gene (*luc2*) from pGL4 (Promega, Madison, WI, USA)
Aequorea coerulescens Green Fluorescent Protein (AcGFP) (or any other fluorescent reporter protein of choice) gene from pAcGFP1 (BD Biosciences, Mississauga, ON, Canada)

A fragment of 1548 base pair (bp) from the murine TLR2 promoter was amplified by Polymerase Chain Reaction (PCR) from the 158H14 clone isolated from the RPCI-24 mouse (C57Bl/6J male) bacterial artificial chromosome (BAC) library under standard conditions by using the Expand HiFi PCR System (Roche, Mississauga, ON, Canada) with oligonucleotides corresponding to pGL3-1486 and pGL3 antisense (Musikacharoen, et al., 2001). The PCR-amplified fragments were inserted into the pCR2.1 vector (TA cloning kit; Invitrogen, Burlington, ON, Canada) and completely sequenced to verify their integrity. The Spe1/Pst1 promoter fragments of 1548 bp (TLR2/S) was inserted into the Internal Ribosome Entry Site (pIRES) vector (BD Biosciences, Mississauga, ON, Canada), previously double digested with Spe1 and Pst1 to remove the immediate early promoter of cytomegalovirus ($PCMV_{IE}$). The Nhe1/Sal1 1.7 kb fragment corresponding to the luciferase reporter gene (*luc2*) from pGL4 (Promega, Madison, WI, USA) and the Sal1/Not1 0.7 kb fragment corresponding to the *Aequorea coerulescens* Green Fluorescent Protein (AcGFP) reporter gene from pAcGFP1 (BD Biosciences, Mississauga, ON, Canada) were both inserted into the pIRES recombinant vector. The integrity of the final construct designated pIRES-TLR2-LUC2-AcGFP-p(A) was verified by sequencing. The TLR2 promoter-luciferase-AcGFP transgenes were isolated as a ~5.2 kb Spe1/Cla1 fragment of pIRES-TLR2-LUC2-AcGFP-p(A) and microinjected into the male pronucleus of fertilized C57BL/6 oocytes.

Mouse model for real-time imaging of neuronal responses to brain injuries: GAP-43/luc/gfp mouse model

Plasmids and vectors:
Internal Ribosome Entry Site (pIRES) vector (BD Biosciences, Mississauga, ON)
Luciferase reporter gene (*luc2*) from pGL4 (Promega, Madison, WI, USA)
Aequorea coerulescens Green Fluorescent Protein (AcGFP) (or any other fluorescent reporter protein of choice) gene from pAcGFP1 (BD Biosciences, Mississauga, ON, Canada)

Taking a similar approach as in generation of the TLR2 reporter mouse model (see Fig.1.), to study neuronal responses to injury and repair, longitudinally and in real time, we generated a transgenic mouse carrying reporter genes *luc* and *gfp* under the transcriptional control of the murine growth associated protein-43 (GAP-43), a neuron specific promoter. We selected the GAP-43 gene promoter as a good candidate because of the following characteristics: i) in physiological conditions and in the adult brain it is expressed at very low levels ii) it is highly up-regulated following brain ischemia and in other types of neuronal injuries iii) after brain injury its induction have been mostly restricted to injured neurons, an injury induced induction. Altogether, this mouse model represents a novel and valuable transgenic tool for *in vivo* bioluminescence and fluorescence imaging of neurite outgrowth in development and in the neuronal responses to injury and repair in adult nervous system (Gravel *et al*., 2011).

The Nhe1/Sal1 1.7-kb fragment corresponding to the luciferase reporter gene (*luc2*) from pGL4 (Promega, Madison, WI, USA) and the Sal1/Not1 0.7-kb fragment corresponding to the *Aequorea coerulescens* Green Fluorescent Protein (AcGFP) reporter from pAcGFP1 (BD Biosciences, Mississauga, Ontario, Canada) were both inserted into the Internal Ribosome Entry Site (pIRES) vector (BD Biosciences, Mississauga, Ontario, Canada). A 10kb fragment containing the murine GAP-43 promoter (Zhu *et al*., 1999) was cloned into the pIRES-LUC2-AcGFP recombinant vector. The integrity of the final construct was verified by sequencing. The GAP43-luciferase-GFP transgene was isolated as a Spe1/Cla1 fragment and microinjected into the male pronucleus of fertilized C57BL/6 oocytes. Transgenic mice were generated in the Transgenic and Knockout Facility of the Research Center of the Centre Hospitalier de l'Université Laval (CHUL).

Genotyping

Transgenic animals were genotyped by polymerase chain reaction (PCR) detection of luciferase reporter gene with HotStar Taq Master mix Kit (Quiagen, Mississauga, ON, Canada) in 15 mM $MgCl_2$ PCR buffer with the following primers: (Primer JK3: 5'-GGCGCAGTAGGCAAGGTGGT-3' and JK4:

5’CAGCAGGATGCTCTCCAGTTC-3’). The PCR conditions were as follows: 95°C-15min, 30 cycles (94°C-30sec, 65°C-30sec, 72°C-1 min. 72°C-7 min.) (Cordeau *et al*., 2008; Lalancette-Hébert *et al*., 2009).

Advantages of multi-reporter approach in optical imaging: Why bicistronic constructs?

Majority of mouse models generated and used for bioluminescence imaging are designed by driving expression of reporter gene luciferase under the transcriptional control of the gene promoter of interest. Therefore, in these mouse models there is a delay between initial activation of the promoter and the expression of a sufficient amount of enzyme necessary for detection by *in vivo* visualization technic. Although *in vivo* bioluminescence imaging and the use of luciferases as reporter molecules in whole animal imaging has significant advantages including inherently low background, the light from luciferase enzymes cannot be detected by microscopy or flow cytometry. In addition, luciferase is not readily detectable by available antibodies using standard immunohistochemistry approach. In the majority of available transgenic mouse models the luciferase reporter gene is induced and expressed in multiple tissues, however without means for cell–type specific detection it would be difficult to determine potential functional implications of the bioluminescent signal. For example, the TLR2 up- regulation may not have the same functional significance in microglial cells as compared to neurons. It has been well established that the induction of the TLR2 in microglial cells is a marker of cellular activation, while in neurons the TLR2 induction has been limited to the subset of caspase-3 positive apoptotic cells. To overcome this problem in our reporter mouse models we used bicistronic plasmids co-expressing luciferase together with GFP. As shown in the figure 1, the two reporter genes were connected via an internal ribosome entry site (IRES). Because the previous evidence (Martinez- Salas, 1999) suggests that the use of IRES may lead to lower expression of the coding sequence placed downstream of the IRES therefore in our bicistronic constructs the GFP has been used as a second reporter system. The great advantage of the dual reporter transgenic approach is that the luciferase

light emission can be used for *in vivo* whole animal imaging while the parallel induction of the GFP reporter, in the same subset of cells, will greatly facilitated the cell specific detection and will enable more detailed and meaningful signal analysis (see Fig. 2.). Contrary to luciferase, the GFP is readily detectable by different types of microscopy and the signal can be further increased by the use of commercial anti-GFP monoclonal or polyclonal antibodies. Because in our transgenic models the GFP is induced in parallel with luciferase, these models can be also used for intravital multiphoton imaging. Once transgenic lines are generated we strongly recommend validating transgenic lines in controlled conditions. Superficial analysis of the induced signal can lead to serious mistakes in the interpretation of the obtained results and/or creation of the artifacts. Before engaging in experimental imaging protocols we strongly recommend:

To investigate whether transgene expression follows the expression pattern of the endogenous protein in at least two known experimental models.

To verify whether spatial and temporal dynamics of reporter gene (luciferase) induction follows the predicted pattern of gene promoter activation to a known and controlled stimuli.

Once transgenic mouse models have been properly validated they can be used in more complex *in vivo* imaging experiments. Here, we will describe in details the protocols and procedures for induction of cerebral ischemia followed by *in vivo* bioluminescence imaging of neuroinflammation and neuronal stress/recovery after experimental stroke.

2.3 Induction of cerebral ischemia

Material/equipment

Pre-coated filaments for artery occlusion: Silicon rubber-coated monofilament for MCAO model. Filament size 6-0, diameter 0.09-0.11 mm, length 20mm; diameter with coating 0.23 +/- 0.02 mm; coating length >= 5 mm, Doccol Corporation, www.doccol.com.

Surgical threat: 4-0, 1.5 Metric SOFSILK (waxcoated, braided silk nonabsorbable sutures), Tyco Healthcare Group, LP Norwalk CN, USA

-Sterilized microsurgery set

-Operating microscope

Surgical Procedures –Experimental ischemia

Unilateral transient focal cerebral ischemia was induced by intraluminal filament occlusion of the left middle cerebral artery (MCA) during 1 hour followed by a reperfusion period (Belayev *et al*., 1999; Beaulieu *et al*., 2002; Lalancette-Hébert *et al*., 2007). The middle cerebral artery occlusion (MCAO) is carried out on 2-3 months old transgenic or wild-type (WT) male (20-25 g). The animals are normally anesthetized with 2 % isoflurane in 100 % oxygen at a flow rate of 2 liter/minute (L/min). To avoid cooling, the body temperature has to be regularly checked and maintained at 37ºC with a heating pad. Under an operating microscope, the left common carotid artery and ipsilateral external carotid artery (ECA) are exposed through a midline neck incision and are carefully isolated from surrounding tissue. The internal carotid artery (ICA) is than isolated and carefully separated from the adjacent tissue so monofilament suture can inserted via the proximal ECA into the ICA and then into the circle of Willis, thus occluding the MCA. To induce moderate ischemic brain lesion the MCA was occluded during 1 hour. Depending on the type of imaging protocol the occlusion period is then followed by various reperfusion times, starting from 24-72 hours to several months after initial ischemic injury. After surgery, to avoid cooling for the first 72 hrs the body temperature has to be regularly checked and maintained at 37°C with a heating pad. As previously described (Weng and Kriz, 2007) to confirm successful MCAO at 6 and 24hrs following surgery the animals were examined for early neurological deficits. Only the mice expressing “positive phenotypes” including circling behavior, slight motor deficits of contra-lateral front paw and reduced spontaneous activity were selected for the study. The induction of early TLR2 biophotonic signals can be used as an additional *in vivo* imaging control.

Comment: In our laboratory we use the MCA occlusion/reperfusion model. However described transgenic mice and *in vivo* imaging protocols can be applied to several other experimental models of ischemia and several other types of acute and more chronic brain injuries.

2.4 In vivo Bioluminescence Imaging

Bioluminescence is a naturally occurring form of chemiluminescence where energy is released by a chemical reaction in the form of light emission (Fig. 3.). The luciferase used in our studies belongs to a family of light producing enzymes called Firefly luciferase. In our experiments we used a novel generation of reporters, a pGL4 luciferase reporter vector. These new generation synthetic enzymes are optimized for better expression in mammalian cells, reduced background and due to a removal of cryptic DNA regulatory elements a reduced risk of anomalous transcription. As shown in Figure 3, these enzymes can generate visible light in the presence of enzyme specific substrate (in case of Firefly luciferase it is D-luciferine), oxygen and ATP as a source of energy. In this chemical reaction D-luciferine is converted into oxy-luciferine and part of the chemical energy is converted into visible light. Unlike insects, certain bacteria and some marine organisms, genetically modified mammals do not produce luciferine. Therefore, before every imaging session the substrate has to be injected into mice. D-luciferin is nontoxic and after intraperitoneal injection (i.p.) it is distributed in all tissues including brain. However, when considering steady-state bioluminescent imaging from the brain structures, to avoid artifacts, it is very important to obtain stable concentration of the substrate D-luciferine in the brain. From our experience and in our experimental model it takes between 18-20 minutes after i.p. injection to obtain steady –state bioluminescent signal from the brains of stroked mice. Because these values can be system and model dependent we provide here the detailed description of experimental procedures and some tips for successful and valid bioluminescence imaging.

2.4.1 Preparation of the material: Luciferin solution for in-vivo imaging.

D-luciferin is a small molecule generated in bioluminescent organisms. It diffuses easily across the membranes inlcuding the blood brain barrier, the blood placenta barrier and the blood testis barrier. Furthermore, because of its size the activation of the immune system seems unlikely. Here it is important to mention that D-

luciferin is a molecule sensitive to light, to oxygen and in its powder form to moisture, thus minimizing the exposure of the powder and solution to direct light is important. For these reasons we recommend to work with either amber eppendorfs and/or before experiments, to wrap a regular transparent eppendorf with aluminum foil to keep the luciferin stable. Furthermore, to keep the quality and intensities of the bioluminescent signals stable it is recommended to prepare a fresh solution of luciferin before every experiment. However, in our hands aliquots stored at -80°C have been proven to work really well. They can be kept for at least 6 months without changing the effectiveness. To avoid repeated cycles of freezing and thawing, small aliquots of 1 ml are kept at -80°C. After thawing the luciferin solution is kept at 4°C and used within following day or two.

Material needed to prepare the luciferin solution:

Vial of D-Luciferin firefly potassium salt.
D- Phosphate Buffered Saline (PBS) (with no Mg2+ and Ca+).
Syringe filter, 0,2 um.
Syringe
Dark eppendorf

Procedure: Dissolve the D-luciferin in the D-PBS making a stock solution at a final concentration of 15 mg/ml. For example, dissolve 1 g of D-luciferin in 66.6 ml of D-PBS. Filter the solution with the syringe filter and divide the stock solution in small aliquots (recommended volume is 1 ml) and store at -80°C, in dark eppendorfs until use. Before imaging, thaw the aliquots, on ice or on the bench (both seems to work equally well), and inject 10 ul/g of body weight i.p.. A 20 g mouse will receive 200 ul of solution. In general, an adult mouse can receive i.p. up to 1 ml of solution without any problem. A recommended dose is 150 mg/kg. To avoid injuries, the luciferin should be injected (i.p.) holding the animal abdomen side up, head pointing downwards. This will force the moveable organs up the animal cavity, toward the diaphragm, minimising the risk of injecting or puncturing an organ. In our experiments the animals are injected in the lower left abdominal quadrant using

a 1cc syringe. Avoiding injury and minimising stress is very important element, especially in long term imaging experiment where same animals are imaged (and injected) in repetitive cycles. In our long term experiments (3-4 months) we normally image the same animal 1/week. To date, although we performed several long term imaging studies (Lalancette-Hébert *et al*., 2009; Keller *et al*., 2009, 2011, Gravel *et al*., 2011) we did not observed any luciferin induced toxicity.

2.4.2 Preparation of the imaging session:

In bioluminescence imaging planning is a key to success. Before every imaging session, especially when dealing with more than one group of experimental animals, we suggest to prepare a log book containing the following information:
mice identification number and gender
time of the substrate D-Luciferin injection,
time of induction of anaesthesia,
the acquisition time

Why all these elements are important? First, some of the tissue responses such as neuroinflammation after stroke are gender and estrogen dependent (Cordeau *et al*., 2008). Next, when imaging responses from the brain, it takes between 15-20 minutes after i.p. injection for the luciferin to cross the blood brain barrier and it usually takes approximately 5 minutes to anesthetise one mouse. It's also important to note that programming an acquisition time of two minutes will take a little bit more than two minutes. For example, with the IVIS 200, if you take a two minutes bioluminescence picture at field of view A (4x4 cm, a high resolution field), it will take approximately 150 seconds before you can open the door of the imaging system and place another experimental animal. Because in certain experiments the peak luciferase expression time used in steady-state bioluminescence imaging may be relatively short (5-10 minutes) all of these parameters are extremely important for timely, valid and efficient *in vivo* bioluminescence imaging protocols.

Relevant control groups

Identifying luciferin kinetic curve and peak luciferase expression time
Establishing a baseline curve

To perform quality steady-state *in vivo* bioluminescence imaging for each new transgenic reporter mice and novel experimental paradigm it is necessary to establish the luciferin kinetic curve and the peak luciferase expression time. For example, when imaging microglial activation/innate immune response after stroke in TLR2 reporter mice (Lalancette-Hébert *et al*., 2009) the luciferin kinetic curve and luciferase peak expression time will not be the same if we use different stroke models, i.e., permanent MCA occlusion *vs*. transient MCA occlusion. Furthermore, these important parameters would change if we image animals after stroke using different reporter mouse lines such as GFAP-luc and/or GAP-43-luc/gfp (Cordeau *et al*., 2008; Gravel *et al*., 2011). Therefore, we recommend establishing the luciferin kinetic curve and peak luciferase expression time before every experiment. Namely, before introduction to any new experimental paradigm at least 3-5 transgenic reporter mice should be injected with luciferin and imaged every 5 minutes for 40 to 45 minutes. Once the imaging data is collected and properly analyzed it will be easy to calculate the kinetics and the peak luciferase expression and estimate the duration of the steady state that will used in imaging experiments.
In addition to luciferin kinetic controls, for each transgenic mouse model it is important to analyze the level of baseline reporter gene expression. Depending on the selected gene promoter there is a possibility that even in control conditions (without stroke) we can observe a baseline bioluminescent signal. For that reason in every experiment employing *in vivo* bioluminescence imaging, it is important to establish a baseline curve and compare all the obtained imaging results to appropriate controls.

Protocol for 2D In vivo bioluminescence imaging
In our imaging protocols we use IVIS® 200 Imaging System (CaliperLS, Alameda, CA, USA) however the sequence of events described here can be applied to any of the imaging systems adapted for whole small animals *in vivo* bioluminescence

imaging. As previously described (Cordeau, *et al*., 2008), 25 minutes prior to imaging session, the mice will receive i.p. injection of the luciferase substrate D-luciferin (150 mg/kg - for mice between 20-25g, 150-187.5 µl of a solution of 20mg/mL of D-luciferin dissolved in 0.9 % saline was injected) (CaliperLS, Alameda, CA, USA). In our experiment we always use D-Luciferin from the same provider (note: although the source of luciferin is decided by end user once experiments are initiated we would not recommend changing the source). 10-15 minutes after luciferin injection the mice were anesthetized with 2 % isoflurane in 100 % oxygen at a flow rate of 2 L/min and placed in the heated, light-tight imaging chamber and maintained anesthetized by constant delivery of 2 % isoflurane/oxygen mixture at 1 L/min through an IVIS® anaesthesia manifold (the anaesthesia manifold and adaptors are usually system dependent but equally efficient). Images are collected using high sensitivity (CCD) camera with wavelengths ranging from 300-660 nm. Exposition time for imaging is usually 1 - 2 minutes using different field of views and f/1 lens aperture. We recommend initiating the protocol with default settings for *in vivo* bioluminescence, which are usually 1 min/medium binning. The first bioluminescent images and measurements will normally provide us with initial information about the signal intensities and these parameters will be than adjusted accordingly. For imaging of bioluminescence signals from brain we normally use higher resolution/sensitivity, the 4x4 cm field of view. Focusing on the head provides more detailed images of the signal arising from the brain than imaging a whole mouse (Cordeau *et al*., 2008; Lalancette-Hébert *et al*., 2009; Gravel *et al*., 2011). As previously described, bioluminescence emission is normalized and displayed in physical units of surface radiance, photons per second per centimetre squared per steradian (photons/s/cm^2/sr), as is common in bioluminescence imaging (Zhu *et al*., 2004; Kadurugamuwa *et al*., 2005). The light output is quantified by determining the total number of photons emitted per second using the Living Image 2.5 acquisition and imaging software (CaliperLS). Region of interest (ROI) measurements on the images are used to convert surface radiance (photons/s/cm^2/sr) to source flux or total flux of photons expressed in photons/seconds (p/s). Note, to standardize your

data acquisition, it is very important to use the same ROI measurements over time. In biolumienscence imaging, the data are usually represented as pseudo-colour images indicating light intensity (red and yellow, most intense, or any other colour-code), and overlaid over greyscale reference photographs. After stroke, we usually recommend to image/analyze acute phase (up to 72 hrs after initial stroke), followed by the later stages of tissue response to ischemic injury. The great advantage of *in vivo* bioluminescence and in general optical imaging is that the same animal could be imaged over time. Moreover, using this approach we can visualize the spatial and temporal dynamics of the different elements of the brain response to ischemic injury.

2.5 Protocol for 3D reconstruction of bioluminescent sources

While bioluminescence imaging is a powerful tool for small animal imaging studies, one should be aware of some limitation using this approach. We already discussed here the difficulties of luciferase detection at cellular levels. Another potential problem is accurate detection of the signal from deeper brain structures. Namely, the bioluminescence images are typically two-dimensional and because the light is attenuated approx 10 fold/per cm of tissue the light from superficial sources would be detected in greater extent than they light from deeper tissue structures (Contag and Bachmann, 2002; Luker and Luker, 2010). In stroke imaging this may affect the for example signals arising from cortical infarction vs striatum. To overcome this problem in our imaging experiments we use a protocol for three-dimensional representation of our signals. The technique is called the diffuse luminescent imaging tomography (DLIT). As previously described (Cordeau *et al*., 2008), for the acquisition of 3 dimensional (3D) images, we acquired greyscale photographs and structured light images followed by series of bioluminescent images using different wavelengths (560-660 nm). The 3D reconstruction of bioluminescent sources in the brain is normally accomplished by using diffuse luminescent imaging tomography (DLIT) algorithms (Living Image 3D Analysis Software, CaliperLS, CA, USA).

Diffuse tomography imaging is a technique that analyse the light generated and projected on the surface of the mice to recreate a three-dimensional reconstruction of the zone generating that same light. To generate the 3D image a structured light image of the mouse has to be taken. The structured light image consist of a series of parallel lasers lines projected on the mouse to determine the surface of the mouse. Afterwards the software will analyse the displacement of the laser light to recreate the 3D mouse. This displacement is used to determine the surface topography of the mouse using polygons. Therefore, to remove any artefacts that could be generated by the software, we recommend to comb or to shave the mice before structure light images. After the 3D surface of the mouse is created the software can now localise and quantify the light source in the mouse. To achieve this minimum of two emissions filter (560-660 nm) is needed to localize the light source. Using the different wavelengths, the enzyme with the defined emission spectra (in our case genetically modified Firefly luciferase) and the known tissue properties (bones, muscles, brain, etc.) the software can calculate and map the surface radiance to the photons density for every wavelength. The next step is to divide the interior of the mouse in voxels and to attribute to each voxel the right source strength to generate the photon density measured at each surface element of the mouse (Contag and Bachman, 2002). In our previous work and as shown here in figure 4, we tested several protocols for 3D bioluminescence imaging. Our analysis was further confirmed by immunohistochemistry measurements and revealed that the 3D reconstruction using DLIT algorithms is rather accurate methodology (Cordeau *et al*., 2008).

2.6 Additional tips for successful *in vivo* bioluminescence imaging

Impact of mouse fur color

Here it is important to mention that mouse fur color will affect the capacity of the signal generated by the luciferase chemical reaction with the luciferin to reach the camera. While haemoglobin absorbs the wavelengths below 600 nm, the fraction of light above 600 nm can be blocked by black fur. The pigment that gives the fur its color, the melanin, will absorb light and scatter the signal. Because the majority

of the transgenic and reporter animals used in neuroscience/brain imaging are generated in BL/6 background this may represent a potential problem. To alleviate this problem before imaging session we normally shave the ROI. When removing the fur, precautions must be taken to not harm the skin of the mouse, since cuts or local inflammation will affect the bioluminescence acquisition or emission when working with a mouse model that respond to inflammation. When shaved, over time, some C57BL/6 mice will develop dark skin pigmentation that if covering the ROI can create problems. For that reason it may be advantageous to derive your transgenic lines in C57BL/6 albino background or if possible use any other strain with light fur color.

Covering ectopic and/or saturated signals

When imaging, it is important to keep in mind that some transgenic mice may have ectopic and/or constitutively high transgene (luciferase) expression at the areas potentially interfering with your ROI. For example the GFAP-luc mouse expresses a high level of luciferase in ears. Because during generation of bioluminescent images, the majority of the imaging software will generate a default scales based on the highest recorded signal, if your expected signals is lower than the baseline transgene signal close to your ROI 's you may not observe it. Therefore, it is useful to prepare piece of black paper to cover the area on the mouse that express really high baseline level of the signal. In case of GFAP-luc mouse, if you cover the ears with the black paper you will be able to image a more subtle induction of the signals from the brain area (Keller et al., 2009). Importantly, this procedure has no impact on the amount of light emitted in the non-covered area, it's mainly cosmetic.

Imaging necrotic and hypoxic tissue

Luciferase needs oxygen to complete its reaction, that's why the use of luciferases technology is limited to aerobic environments and living organisms. In environment where the oxygen levels are really low the light produced may not correlate with

the luciferase expression. It's a thing to keep in mind if you are working with a model that implicates large necrosis and/or hypoxia.

2.7 Summary

Unlike many current animal studies that are based on single end point data, the presented reporter mice together with the use of in vivo biophotnic/bioluminescence imaging represent novel powerful analytical tools for understanding in vivo pathology of acute and chronic neurological injuries. In addition, use of in vivo imaging in stroke research may significantly improve the quality of or preclinical drug testing and may lead to more efficient translation of experimental therapies to clinic.

2.8 Acknowledgments

This work was supported by the Canadian Institutes of Health Research (CIHR) and the Heart and Stroke Foundation –Canada. J.K. is recipient of the Career Award from the R&D/and CIHR. P.C. received CIHR Canada Doctoral Scholarships.

2.9 References

Beaulieu, J. M., Kriz, J., and Julien, J. P. (2002). Induction of peripherin expression in subsets of brain neurons after lesion injury or cerebral ischemia. Brain. Res. **946,** 153-61.

Belayev, L., Busto, R., Zhao, W., Fernandez, G., and Ginsberg, M. D. (1999). Middle cerebral artery occlusion in the mouse by intraluminal suture coated with poly-L-lysine: neurological and histological validation. Brain. Res. **833,** 181-90.

Close, D. M., Hahn, R. E., Patterson, S. S., Baek, S. J., Ripp, S. A., and Sayler, G. S. (2011). Comparison of human optimized bacterial luciferase, firefly luciferase, and green fluorescent protein for continuous imaging of cell culture and animal models. J. Biomed. Opt. **16,** 047003.

Contag, C. H., and Bachmann, M. H. (2002). Advances in in vivo bioluminescence imaging of gene expression. Annu. Rev. Biomed. Eng. **4**, 235-60.

Cordeau, P., Jr., Lalancette-Hebert, M., Weng, Y. C., and Kriz, J. (2008). Live imaging of neuroinflammation reveals sex and estrogen effects on astrocyte response to ischemic injury. Stroke **39,** 935-42.

Dirnagl, U., Iadecola, C., and Moskowitz, M. A. (1999). Pathobiology of ischaemic stroke: an integrated view. Trends Neurosci. **22,** 391-7.

Gravel, M., Weng, Y. C., and Kriz, J. (2011). Model System for Live Imaging of Neuronal Responses to Injury and Repair. Mol. Imaging.

Kadurugamuwa, J. L., Modi, K., Coquoz, O., Rice, B., Smith, S., Contag, P. R., and Purchio, T. (2005). Reduction of astrogliosis by early treatment of pneumococcal meningitis measured by simultaneous imaging, in vivo, of the pathogen and host response. Infect. Immun. **73,** 7836-43.

Keller, A. F., Gravel, M., and Kriz, J. (2011). Treatment with minocycline after disease onset alters astrocyte reactivity and increases microgliosis in SOD1 mutant mice. Exp. Neurol. **228,** 69-79.

Keller, A. F., Gravel, M., and Kriz, J. (2009). Live imaging of amyotrophic lateral sclerosis pathogenesis: disease onset is characterized by marked induction of GFAP in Schwann cells. Glia **57,** 1130-42.

Lalancette-Hebert, M., Moquin, A., Choi, A. O., Kriz, J., and Maysinger, D. (2010). Lipopolysaccharide-QD micelles induce marked induction of TLR2 and lipid droplet accumulation in olfactory bulb microglia. Mol. Pharm. **7**, 1183-94.

Lalancette-Hebert, M., Phaneuf, D., Soucy, G., Weng, Y. C., and Kriz, J. (2009). Live imaging of Toll-like receptor 2 response in cerebral ischaemia reveals a role of olfactory bulb microglia as modulators of inflammation. Brain **132:** 940-954.

Lalancette-Hebert, M., Gowing, G., Simard, A., Weng, Y. C., and Kriz, J. (2007). Selective ablation of proliferating microglial cells exacerbates ischemic injury in the brain. J. Neurosci. **27,** 2596-605.

Lo, E. H., Dalkara, T., and Moskowitz, M. A. (2003). Mechanisms, challenges and opportunities in stroke. Nat. Rev. Neurosci. **4,** 399-415.

Luker, K. E., and Luker, G. D. (2010). Bioluminescence imaging of reporter mice for studies of infection and inflammation. Antiviral. Res. **86,** 93-100.

Martinez-Salas, E. (1999). Internal ribosome entry site biology and its use in expression vectors. Curr. Opin. Biotechnol. **10,** 458-64.

Maysinger, D., Behrendt, M., Lalancette-Hebert, M., and Kriz, J. (2007). Real-time imaging of astrocyte response to quantum dots: in vivo screening model system for biocompatibility of nanoparticles. Nano Lett. **7,** 2513-20.

Musikacharoen, T., Matsuguchi, T., Kikuchi, T., and Yoshikai, Y. (2001). NF-kappa B and STAT5 play important roles in the regulation of mouse Toll-like receptor 2 gene expression. J. Immunol. **166,** 4516-24.

Swarup, V., Phaneuf, D., Bareil, C., Robertson, J., Kriz, J., Julien, J. P. (2011). Pathological hallmarks of amyotrophic lateral sclerosis/frontotemporal lobar degeneration in transgenic mice produced with genomic fragments encoding wild-type or mutant forms of human transactive response DNA-binding protein 43. Brain, in press.

Weng, Y. C., and Kriz, J. (2007). Differential neuroprotective effects of a minocycline-based drug cocktail in transient and permanent focal cerebral ischemia. Exp. Neurol. **204,** 433-42.

Zhu, L., Ramboz, S., Hewitt, D., Boring, L., Grass, D. S., and Purchio, A. F. (2004). Non-invasive imaging of GFAP expression after neuronal damage in mice. Neurosci. Lett. **367,** 210-2.

Zhu, Q., and Julien, J. P. (1999). A key role for GAP-43 in the retinotectal topographic organization. Exp. Neurol. **155**, 228-42.

FIGURE LEGENDS

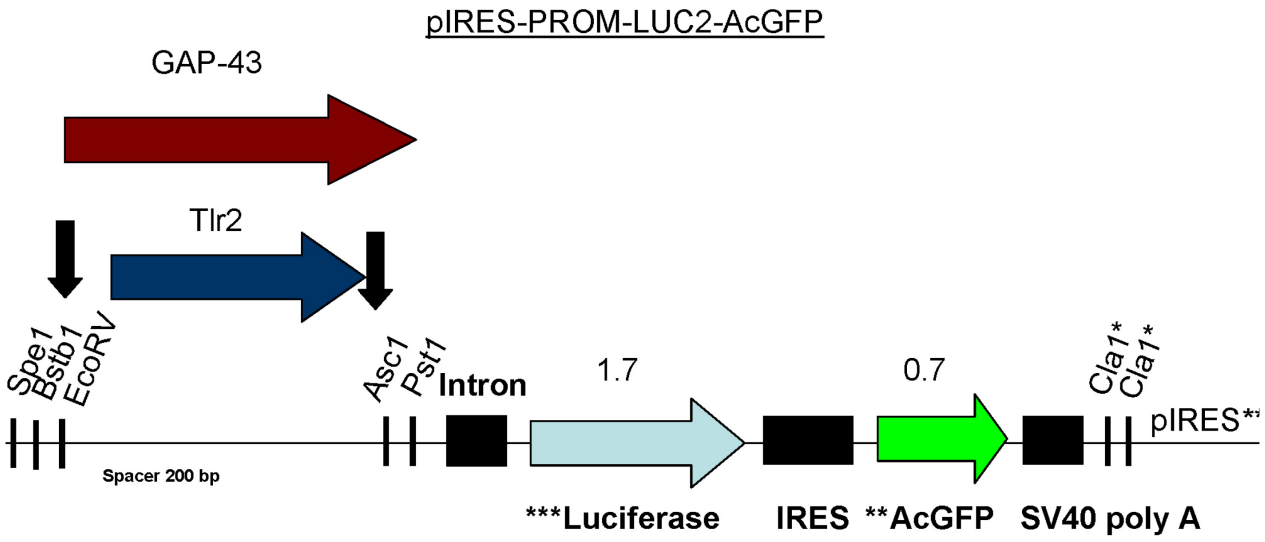

* CpG methylation: needs to be demethylated

** Vector from BD Biosciences

*** From pGL4 (promega)

-Insert is removed with Spe1-Cla1, or BstB1-Cla1, or EcoRV-Cla1

Figure 1. Schematic representation of the DNA constructs used to generate TLR2-Fluc-GFP and the GAP-43-luc/gfp transgenic mice.

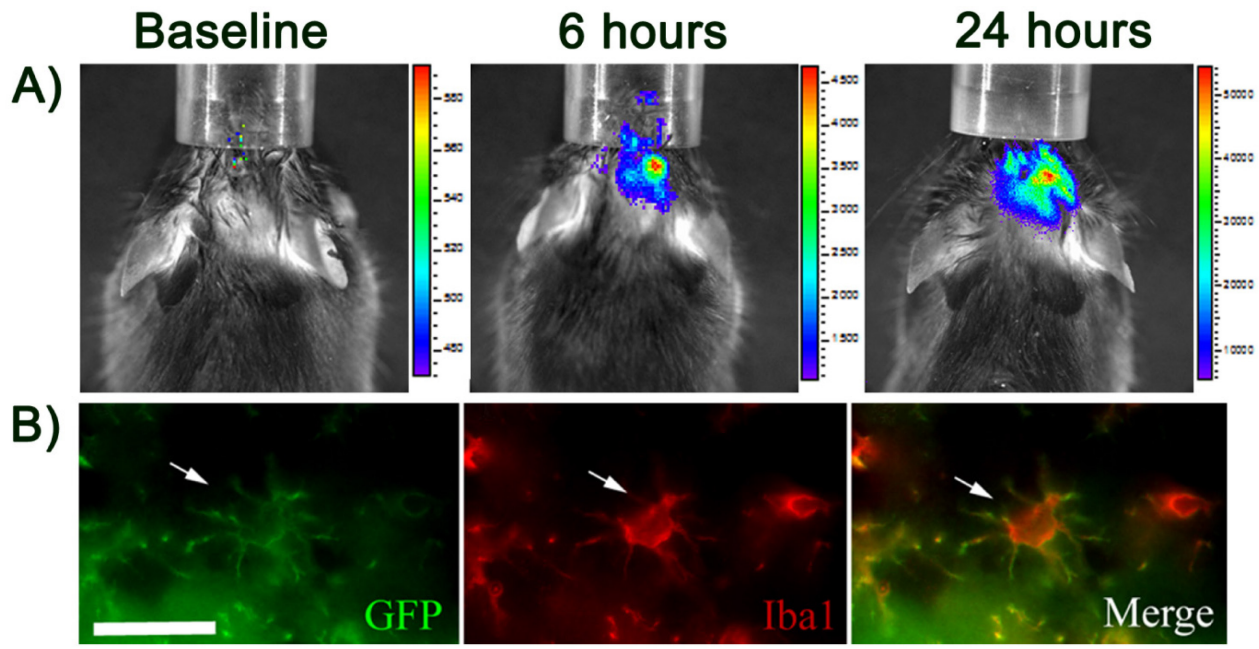

Figure 2. The TLR2-luc/gfp mouse is a bicistronic reporter system in A) the TLR2 induction after LPS injection in the brain of a male mouse at baseline, 6 hours and 24 hours is measured using the luciferase reporter. While in B) to achieve microscope resolution and to identify the induction of the transgene in microglial cells using the microglia specific Iba1 marker the GFP reporter was used. Note co-localization of the Iba1 with the TLR2 driven transgene GFP. Scale bar = 25 µm.

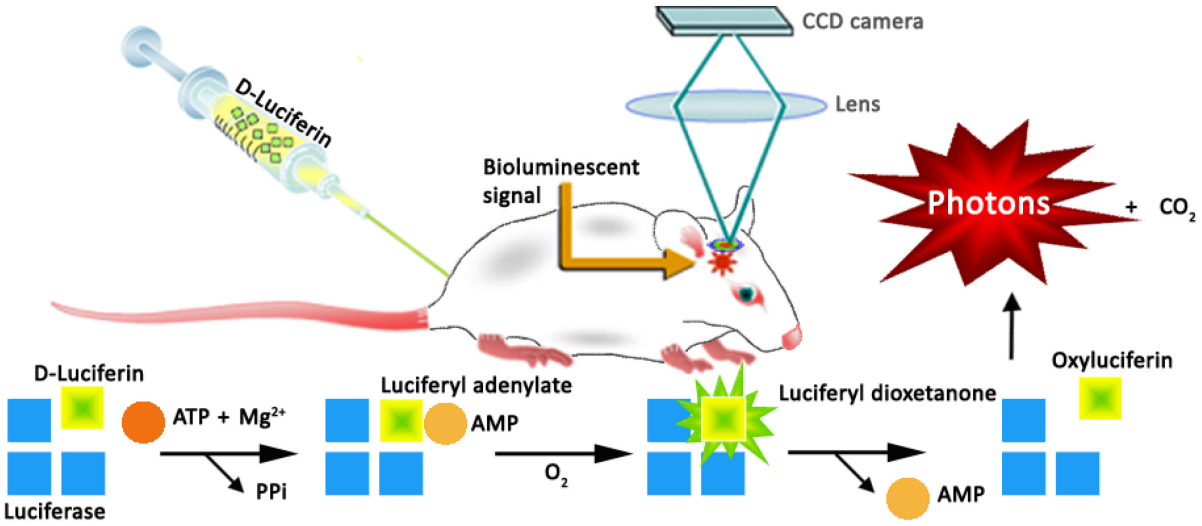

Figure 3. Schematic presentation of the bioluminescent source detection from the brain of living mice. In the presence of ATP and magnesium the luciferin will bind to the luciferase. Afterward, the release of pyrophosphate (PPi) after the creation of AMP will generate luciferyl adenylate. This adenylate will be oxidised to an unstable molecular form after several intermediate stages. To reach molecular stability a photon of light will be release and captured by the CCD camera.

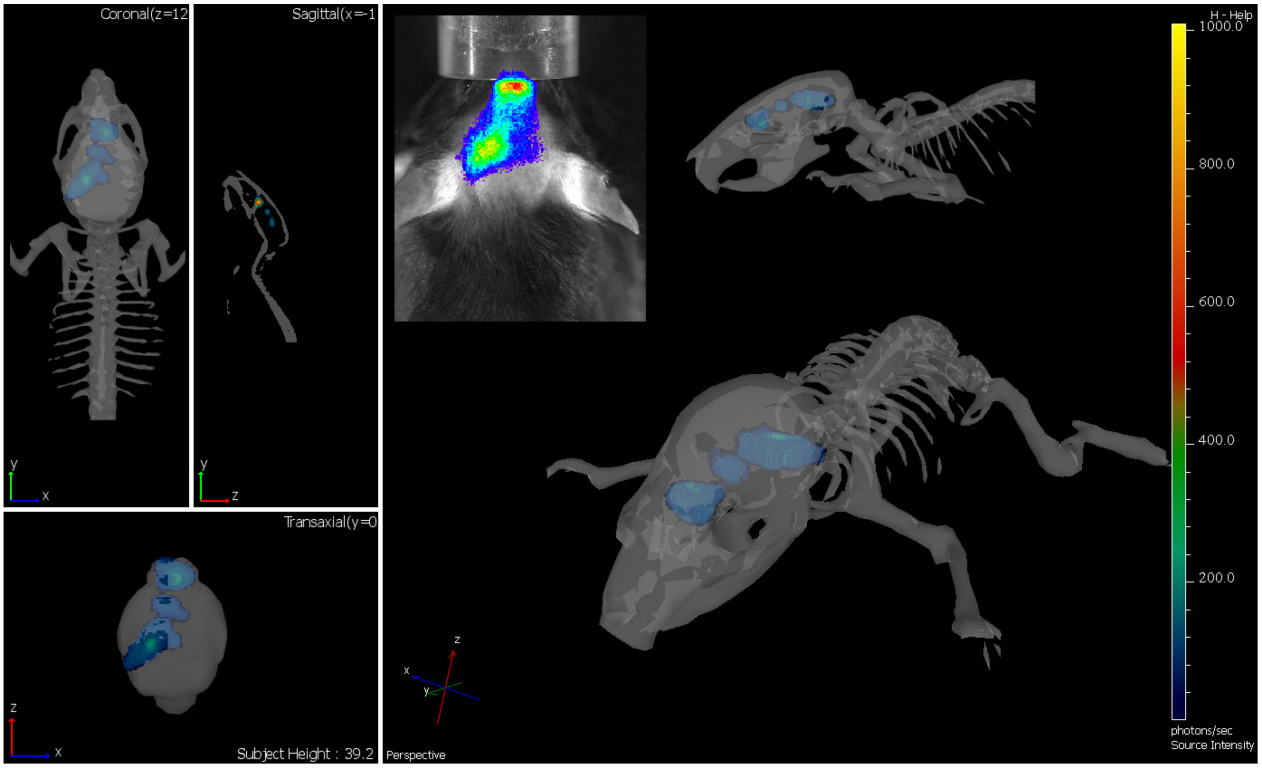

Figure 4. Three-dimensional reconstruction of bioluminescent signals emitted from the brain of a 3 month old TLR2-luc/gfp mouse 24 hours after MCAO. Reconstruction is build using 3 different wavelengths (600 nm, 620 nm and 640 nm) across the emission spectrum of the bioluminescent source (Living Image software, Xenogen). Green area, concentrated in the ischemic lesion, represents areas of the brain with the highest photons emission thus the biggest TLR2 activation. Scales bar on the right are the color maps for source intensity in photons per seconds. Insert image was taken with the A field of view with a 2 minute exposition prior to the 3D sequence image.

Chapitre 3. Toll like receptor 2 deficiency leads to delayed exacerbation of ischemic injury

Contributions des auteurs dans l'article: Toll-like receptor 2 deficiency leads to delayed exacerbation of ischemic injury publié dans le Journal of Neuroinflammation, 2012.

Ivan Bohacek a effectué les immunohistochimies, a utilisé la trousse de cytokines ainsi qu'effectué les FACS. Il a aussi désigné l'expérience et écrit le manuscrit.

Pierre Cordeau a utilisé la trousse de cytokines, fait et analysé les FACS en plus d'aider au design de l'expérience.

Mélanie Hébert-Lalancette a effectué et analysé les hybridations in-situ.

Dunja Gorup a effectué des analyses statistiques.

Yuan-Cheng Weng a effectué les chirurgies.

Srecko Gajovic a participé à la mise en place et la coordination de l'étude.

Jasna Kriz a conçu et coordonné l'étude en plus d'écrire le manuscrit.

Toll like receptor 2 deficiency leads to delayed exacerbation of ischemic injury

Running title: The role of TLR2 in stroke

Bohacek, Ivan, M.D.[1,3], Cordeau, Pierre, M.Sc.[2,3], Lalancette–Hébert, Mélanie, Ph.D.,[2,3] Gorup, Dunja, M.D.[1], Weng, Yuan-Cheng, M.Sc.[3], Gajovic, Srecko, M.D., Ph.D.[1], Kriz, Jasna M.D., Ph.D.[2,3]*

[1]*Laboratory for Neurogenetics and Developmental Genetics, Croatian Institute for Brain Research, School of Medicine, University of Zagreb, Salata 12, Zagreb HR-10000, Croatia,* [2]*Department of Psychiatry and Neuroscience, Faculty of Medicine, Université Laval, Québec, Canada,* [3]*Centre de Recherche du Centre Hospitalier de l'Université Laval, 2705 boulevard Laurier, Québec, QC, G1V 4G2 Canada*

Ivan Bohacek: ibohacek@hiim.hr
Pierre Cordeau: pierre.cordeau@crchul.ulaval.ca
Mélanie Lalancette–Hébert: ml3160@columbia.edu
Dunja Gorup: dgorup@hiim.hr
Yuan-Cheng Weng: yuan_cheng.weng@crchul.ulaval.ca
Srecko Gajovic: srecko.gajovic@hiim.hr

*Corresponding Author
Jasna Kriz, MD PhD
Centre de Recherche du CHUL (CHUQ), T2-52
Université Laval
2705 boulevard Laurier
Quebec City (QC), Canada G1V 4G2
E-mail: Jasna.Kriz@crchul.ulaval.ca

3.1 ABSTRACT

BACKGROUND: Using live imaging approach we have previously shown that microglia activation after stroke is characterized by marked and long-term induction of the Toll like Receptor 2 (TLR2) biophotonic signals. However, the role of TLR2 (and potentially other TLRs), beyond the acute innate immune response and an early neuroprotection against ischemic injury is not well understood.

METHODS: The TLR2 -/- mice were subjected to transient middle cerebral artery occlusion (MCAO) followed by different reperfusion times. Analyses assessing microglial activation profile/innate immune response were performed using *in situ* hybridization, immunohistochemistry analysis, flow cytometry and inflammatory cytokine array. The effects of the TLR2 deficiency on the evolution of ischemic brain injury were analyzed using a cresyl violet staining of brain sections with appropriate lesion size estimation.

RESULTS: Here we report that TLR2 deficiency markedly affects post-stroke immune response resulting in delayed exacerbation of the ischemic injury. The temporal analysis of the microglia/macrophage activation profiles in TLR2 -/- mice and age-matched controls revealed reduced microglia/macrophage activation after stroke, reduced capacity of resident microglia to proliferate as well as decreased levels of MCP-1 and consequently lower levels of $CD45^{high}/CD11b^{+}$ expressing cells as shown by flow cytometry analysis. Importantly, although acute ischemic lesions (24-72hrs) were smaller in TLR2 -/- mice, the observed alterations in innate immune response were more pronounces at later time-points (at day 7) after initial stroke, which finally resulted in delayed exacerbation of ischemic lesion leading to larger chronic infarctions as compared to WT mice. Moreover, our results revealed that TLR2 deficiency is associated with significant decrease in the levels of neurotrophic/antiapoptotic factor IGF-1, expressed by microglia in the areas in- and around ischemic lesion.

CONCLUSION: Altogether our results clearly suggest that optimal and timely microglial activation/innate immune response is needed to limit neuronal damage after stroke.

KEYWORDS: TLR2 -/- mice, microglia/macrophages, neuroinflammation, IGF-1, apoptosis, stroke

3.2 BACKGROUND

Increasing evidence suggest that post-ischemic inflammation plays an important role in evolution of brain injury after ischemia. However, to what extent inflammatory processes are deleterious and/or beneficial to brain recovery is a matter of debate and controversies [1-5]. One of the key features of the brain inflammatory response following ischemic injury is activation of the resident glial cells including microglia. Activation of microglial cells after stroke is characterized by marked up-regulation of the pattern-recognition receptors (PRRs), such as Toll-like receptors (TLRs) [6-14]. TLRs have ability to bind two types of ligands: (i) in response to invading pathogens, pathogen-associated molecular pattern (PAMP) ligands [15], (ii) and endogenous danger associated molecular pattern (DAMP) ligands, recognized in processes that present threat to the structural integrity, such as ischemic injury [12, 16-19]. Recent evidences suggest that TLRs, especially TLR2 may play a key role in evolution of brain damage following cerebral ischemia [9-11; 20-23]. However, the exact role of TLR2 in modulation of the post-ischemic inflammatory response remains unclear. While previous studies were primarily focused on the role of TLR2 only in acute phase 24-72 hrs after experimental stroke, the later phases of the tissue response to ischemia remained unexplored [9, 10, 20, 21, 24]. Our recent work, using *in vivo* imaging approach, revealed that the TLR2 response has a marked chronic component following brain ischemia [11]. Therefore, the aim of the work presented here was to investigate the role of TLR2 signaling and microglial activation beyond the 24-72 hrs time-window.

Here, we report that TLR2 deficiency markedly affects neuroinflammatory response to ischemic brain injury resulting in altered post-ischemic inflammatory cell activation profiles, decreased proliferative capacity of resident microglia, reduced levels of MCP-1 and reduced accumulation of $CD45^{high}/CD11b^{+}$ cells at the site of the ischemic lesion. In addition, reduced levels of neurotrophic and antipoptotic factor IGF-1 expressed by microglial cells were observed in TLR2 deficient mice. Importantly, cumulative effects of the altered post-ischemic inflammatory response resulted in late increase of neuronal apoptosis and delayed exacerbation of ischemic lesion.

3.3 METHODS

3.3.1 Experimental animals

All experiments were carried out on 2-4 months old male TLR2-/- mice obtained from Jackson Laboratories (Bar Harbor, Maine), and WT C57BL/6 as control group. Experimental procedures were approved by the Laval University Animal Care Ethics Committee and are in accordance with *The Guide to the Care and Use of Experimental Animals of the Canadian Council on Animal Care.*

3.3.2 Surgical procedure

As previously described [3, 11, 25, 26], unilateral transient focal cerebral ischemia was induced by intraluminal filament occlusion of the middle cerebral artery (MCAO) during 1 h followed by reperfusion periods of 1, 3, 4, 7 or 14 days. Briefly, all animals were anesthetized with 2% isoflurane, and body temperature was regularly checked and maintained at 37°C with a heating pad in order to avoid hypothermia. After midline neck incision, left common carotid artery and ipsilateral internal and external carotid artery were exposed and isolated from surrounding tissue. 12 mm long 6-0 silicon-coated monofilament suture (Doccol, CA, USA) was inserted via the proximal external carotid artery into the internal carotid artery and then into the circle of Willis, thus, occluding the MCA. After the occlusion period in duration of 1h, monofilament suture was removed, followed by different reperfusion

periods. In our experiments we did not observe any increase in mortality in different experimental groups and in general mortality was very low. Whole operational procedure was conducted under the operating microscope. All animals were allowed *ad libitum* access to water and food before and after surgery.

3.3.3 Tissue collection

After different reperfusion periods, all animals were anesthetized with i. p. injection of chloral hydrate (150 mg/kg, 300-350µl of solution, concentration 10 mg/ml), and transcardially perfused with 30 mL of 0.9% saline, followed by ice-cold borax buffered 4% paraformaldehyde (PFA) at pH 9.5 (for *in situ* hybridization), or PBS buffered 4% PFA at pH 7.4 (for immunohistochemistry, immunofluorescent labeling and cresyl-violet staining). Tissue samples were then post-fixed overnight in 4% PFA and equilibrated in PBS buffered 30% sucrose for 48 h. Brains were embedded in Tissue-Tek (O.C.T. compound, Sakura, USA), frozen at -20°C, cut into 35µm thick coronal sections using cryostat and stored at -20°C.

In order to prepare samples for flow cytometric and cytokine antibody array analysis, animals were anesthetized with chloral hydrate and transcardially perfused with ice-cold 0.9% saline to remove all blood from the nervous tissue. Brain samples were surgically removed and immersed in Hibernate-A medium (for flow cytometric analysis), or immediately frozen in liquid nitrogen (for cytokine antibody array analysis).

3.3.4 *In situ* hybridization

The expression and localization of TLR2 mRNA were detected using S^{35} labeled riboprobes. Protocols for probe synthesis and in situ hybridization were previously described by Lalancette-Hebert et al. [3, 11].

3.3.5 Immunofluorescence

Immunofluorescent labeling (IF) was performed on the brain sections of TLR2-/- mice and WT C57BL6 mice, collected 3 and 7 days after MCAO procedure (all with visible stroke region, n=4 animals/group/stage), according to the previously described procedure [3]. Briefly, brain sections were blocked for 30 minutes in PBS containing 10% goat serum and 0,25% Triton X-100. Sections were then incubated overnight on room temperature with primary antibody [1:250 mouse monoclonal anti-TLR2 (eBioscience, Burlington, Ontario, Canada), 1:500 rabbit polyclonal anti-Iba1 (Wako, Richmond, VA), 1:2000 rat monoclonal anti-CD68 (AbD Serotec), 1:2000 rat polyclonal anti-BrdU (Axyll, Westbury, NY), 1:400 mouse monoclonal anti-BrdU Alexa Fluor 488 conjugated (Molecular Probes, Eugene, OR), 1:500 rat anti-Mac2 (American Type Culture Collection, Manassas, VA), 1:400 rabbit polyclonal anti-cleaved caspase-3 (Cell Signaling, Danvers, MA), 1:300 mouse monoclonal anti-NeuN (Millipore, Billerica, MA), 1:1000 mouse monoclonal anti-GFAP (Millipore), 1: 50 rat monoclonal anti-CD11b (AbD Serotec, Oxford, UK) and 1:50 mouse monoclonal anti-IGF-1 (Millipore, Billerica, MA)]. Afterwards, sections were incubated for 2h at room temperature in corresponding secondary antibody 1:500 (Invitrogen, Eugene, OR). Each of the steps above was followed by four 5 min rinses in PBS-0.25% Triton X-100. In the end of the procedure, sections were coverslipped with Fluoromount G (Electron Microscopy Sciences, Fort Washington, PA) and dried overnight.

3.3.6 Immunohistochemistry

Immunohistochemistry was performed according to the previously described protocol [3, 11]. Brain sections of TLR2-/- and WT mice were collected 3, 7 and 14 days after MCAO procedure (all the stroke region, n=4 brains/group) were used for the experiment. After initial wash in PBS in order to remove O.C.T., endogenous peroxidase activity was attenuated with 0.6% hydrogen peroxide in PBS1X for 15 minutes. Afterwards, sections were blocked for 1 h in PBS1X containing 10% goat serum and 0.25% Triton X-100, and incubated overnight with 1:400 rabbit anti-

cleaved caspase-3 antibody (Cell Signaling, Danvers, MA) in PBS1x containing 0.25% Triton X-100 and 5% goat serum. Sections were then incubated for 2 h with 1:500 goat anti-rabbit biotinylated secondary antibodies (Jackson ImmunoResearch, West Grove, PA). For the amplification of the positive signal, incubation in avidin-biotin solution was performed (Vectastain ABC kit, Vector Laboratories, Burlingame, CA). Staining was developed with nickel-DAB solution (0.3%) (Vector Laboratories). Each of the steps above was followed by four 5 min rinses in PBS-0.25% Triton X-100. On the end of the procedure, sections were dehydrated and coverslipped with DPX mounting medium (Electron Microscopy Sciences).

3.3.7 BrdU labeling

In order to visualize proliferating cells, mice were injected intraperitoneally with 5-bromo-2'-deoxyuridine (BrdU) (50 μg/g of mouse weight in saline), immediately before MCAO procedure and again 2, 24 and 48 h after surgery. 72 h after surgery, mice were anesthetized with i.p. injection of chloral hydrate (150 mg/kg, 300-350μl of solution, concentration 10 mg/ml) and transcardially perfused with 0.9% saline and PBS buffered 4% PFA. Brains were isolated, postfixed overnight in 4% PFA, equilibrated in PBS buffered 30% sucrose for 48 hours, and cut into 35μm thick coronal sections. Afterwards, pretreatment was performed with 2.0 N HCl for protein hydrolysis (30 min, 37.0°C) with further neutralization of HCl with 0.1 M sodium borate (10 min), all diluted with KPBS. Immunofluorescent labeling was later performed on brain samples according to standardized protocol described above.

3.3.8 Flow Cytometric Analysis

In order to analyze the number of mononuclear cells and their proliferation properties after ischemia, flow cytometric analysis was performed on WT and TLR2-/- mice, at 3 and 7 days after MCAO. As previously described [27, 28], mice were injected intraperitoneally with BrdU 12, 24 and 36 hours prior to sacrifice,

according to BrdU Flow Kit protocol (BD, Franklin Lake, NJ, USA). Collected brain samples were prepared for flow cytometric analysis according to previously described procedure [27, 28]. Briefly, tissue was mechanically dissociated with a Teflon homogenizer and incubated with 1X HBSS containing papain (2mg/ml) and DNase I (0,025U/ml) for 30 minutes at 37°C. Afterwards, cell suspension was passed through 70µm nylon cell strainer (BD, Franklin Lake, NJ, USA). In order to isolate mononuclear cell fraction, cell suspension was loaded in 30-37-70% isotonic Percoll gradient (GE Healthcare, Uppsala, Sweden) and centrifuged for 40 min at 500g. After centrifugation, interphase containing mononuclear cells was collected, washed thoroughly, and stained with anti-CD45 conjugated with V500 (BD Horizon), anti-CD11b conjugated with allophycocyanin (APC) (BD, Franklin Lake, NJ, USA). Further, for proliferation analysis, cells were stained with anti-BrdU conjugated with fluorescin isothiocyanate (FITC) antibody, following BrdU Flow Kit procedure (BD, Franklin Lake, NJ, USA). Samples were afterwards analyzed on a flow cytometer (BD LSRII) immediately after end of the staining protocol by a 'blinded' individual. Cells were gated using front scatter (FSC) and side scatter (SSC), to eliminate unviable cells. Further gating was performed using SSC and CD45 in order to select inflammatory cell population. Afterwards, two-color analysis with the use of anti-CD11b and anti-CD45 antibodies was performed in order to delineate $CD45^{low}/CD11b^{+}$ (i.e. microglial) and $CD45^{high}/CD11b^{+}$ (i.e. macrophage-like) cell populations [27, 28]. Proliferation analysis was performed using two-color analysis of anti-CD11b and anti-BrdU antibodies. Non-stroked, BrdU treated animals were used as negative controls for proliferation analysis.

3.3.9 Cytokine array

Expression profile of inflammatory cytokines was performed with a Mouse Cytokine Antibody Array (Raybio Mouse Inflammation Antibody Array 1 (Cat#AAM-INF-1), RayBiotech, Norcross, GA). As previously described [3, 29], protein samples were obtained by homogenization of TLR2-/- and WT brains 1 and 4 days after MCAO (n=3/group) in 1x cell lysis buffer that was included in RayBiotech kit with protease-inhibitor mixture (#P8340, Sigma) added. After extraction, samples were spin down

and supernatant was used for the experiment. Protein concentration was determined for each sample and diluted at 300 µg of total protein in 1x blocking buffer. For each group (3 mice per group) samples were pooled together and incubated with the array membrane overnight at 4°C. After washing in the washing buffer (included in RayBiotech kit), membranes were incubated with biotin-conjugated antibodies overnight. After washing, membranes were incubated with HRP conjugated streptavidin diluted in the blocking buffer for 2 h. Signal detection was performed according to RayBiotech protocol, by exposing membranes to x-ray film (Biomax MR1; #8701302; Kodak), and the obtained results analyzed with ImageJ software.

3.3.10 Assessment of the infarct area

Every sixth coronal cryostat section of TLR2-/- and WT mouse brains collected after reperfusion periods of 3, 7 and 14 days after MCAO, (n=10/group) was stained with cresyl-violet according to the standardized protocol, coverslipped with DPX mounting medium (Electron Microscopy Sciences, Fort Washington, PA) and afterwards digitized. The area of infarction, 'direct stroke area', was quantified with ImageJ program (version 1.42q for Windows, National Institutes of Health, USA), infarct volume was calculated and expressed in mm^3. As previously described [10], correction for edema was applied for brains reperfused for 3 days by calculating the brain swelling. First, 'indirect stroke area' was calculated as contralateral (non-stroked) hemisphere area minus non-stroked area of the ipsilateral (infarcted) hemisphere. Difference between 'direct' and 'indirect' stroke area represented brain swelling. The correction of 'direct stroke area' was performed by subtracting brain swelling volume from 'direct stroke area'. In addition, ‘indirect stroke area’ represents volume of healthy tissue that correlates to the volume of ischemic tissue, not affected by post ischemic shrinkage. Thus, ‘direct stroke area’ reflects lesion consolidation (shrinkage) and glial scar formation and ‘indirect stroke area’ represents lesion progression, i.e. how does altered inflammatory response reflect on surrounding-cell survival and lesion dynamics.

3.3.11 Quantification and statistical analysis

Immunofluorescence

For the quantification of immunofluorescent signal (Iba1, CD68, BrdU, Mac2, IGF-1), four fields of view per section (every sixth section, all stroke area), ten sections per animal were acquired on fluorescent microscope Leica DM5000B, using a 20x Plan Fluotar objective. Immunoreactivity was quantified with the ImageJ software by measuring the integrated optical density (intensity of fluorescence per unit of surface area), and results were expressed in arbitrary units, as previously described [3]. The data were averaged and analyzed by a two-tailed unpaired Student's t-test.

Immunohistochemistry

Every sixth sample section through the brain was used for the immunohistochemical labeling with anti-cleaved caspase-3 antibody. Number of positively stained cells was estimated by the optical fractionator method using Nikon Eclipse 80i microscope equipped with Stereo Investigator software. The ipsilateral (ischemic) hemisphere was traced using a 4 Plan Apochromat and sampled using 60 Plan Apochromat objectives (Nikon, El Segundo, CA). The counting parameters for the experiments were the counting frame size (width and height 100 x 100 μm), sampling grid (500 x 500 μm), dissector height (10 μm) and the guard-zone thickness (1.5 μm). Counts were performed on the entire ischemic area of the ipsilateral (ischemic) hemisphere. Results were expressed as number of cells per mm^3 of ischemic tissue. The data were averaged and statistically analyzed by a two-tailed unpaired Student's t-test.

Cytokine Array

Cytokine expression assays were quantified by measuring optical density of each cytokine spot on the membrane with ImageJ software, as previously described [3, 29]. Cytokines were presented on membranes as duplicates and the analysis was performed twice. The background values were subtracted from cytokine expression values. Data were expressed in arbitrary units relative to appropriate positive

control. Further, data were averaged and analyzed by a two-tailed unpaired Student's t-test.

3.4 RESULTS

3.4.1 Microglial cells up-regulate TLR2 in response to transient ischemic brain injury

To identify whether TLR2 is indeed up-regulated in microglial cells (at mRNA and protein levels) after stroke we performed series of *in situ hybridization* (ISH) experiments followed by double immunofluorescence analysis. In accordance with previous studies [9, 11, 20], 24 hrs after stroke we observed a marked increase of the TLR2 mRNA in the area of ischemic lesion and the peri-infarct zone, showing a positive S^{35} ISH signal (Fig.1A). In contrast, no signal was observed in contralateral, unlesioned hemisphere (Fig.1B). As shown in Figures 1C, D, E, double immunofluorescence analysis of the brain sections after MCAO revealed a co-localization of TLR2 staining with Iba1 (a common marker of microglial cells). The co-localization was observed in activated microglial cells situated in ischemic and peri-infarct regions of the brain at 3, 7 and 14 days post-stroke, suggesting that microglia/macrophages up-regulate TLR2 in early, as well as in more chronic phase of the brain response to ischemic injury (Fig.1C-D). As previously reported [11], few neurons found within the ischemic core area were positive for TLR2, while we did not observe any co-localization between TLR2 and GFAP positive astrocytes (data not shown).

3.4.2 TLR2 deficiency alters microglia/macrophage activation profiles

Because activated microglial activation in response to ischemic injury is characterized by a robust up-regulation of TLR2, we next investigated how and whether this process may be affected in the context of TLR2 deficiency. First, we analyzed expression levels of the distinct microglia/macrophages activation markers such as Iba1 and CD68. The analyses were performed 3 and 7 days following transient MCAO. As expected, immunofluorescent labeling indicated

significant increase of Iba1 immunoreactivity in ischemic side of the brain. The relative increase of Iba1 immunoreactivity (as compared to unlesioned brain controls) was also observed in TLR2 deficient mice. However, comparison of the levels of microglial activation after stroke revealed a marked reduction of Iba1 immunoreactivity in the brain section of TLR2-/- mice as compared to WT mice, at both 3d and 7d time points after MCAO (Fig.2B). Quantitative analysis of Iba1 staining revealed significant reduction at 3 days (1.63-fold) as well as 7 days (1.36-fold) after MCAO in TLR2-/- mice when compared to WT mice (Fig. 2C) (control: WT, 0.48 X 10^9 ± 0.16 X 10^9, n=4; TLR2-/-, 0.54 X 10^9 ± 0.06 X 10^9, n=4, p=0.438; 3d: WT, 2.31 X 10^9 ± 0.12 X 10^9 , n=4; TLR2-/- 1.41 X 10^9 ± 0.06 X 10^9, n=4, p<0.001; 7d: WT, 8.67 X 10^9 ± 0.34 X 10^9, n=4; TLR2-/- 6.37 X 10^9 ± 0.26 X 10^9, n=4, p=0.002). Similar results were obtained following analysis of CD68 immunoreactivity. As shown in Figure 2D, E quantitative analysis of CD68 immunoreactivity revealed no significant difference at the lesion site between WT and TLR2-/- mice, 3 days after transient MCAO. Interestingly however, CD68 immunoreactivity was significantly decreased in TLR2-/- mice 7 days after MCAO, indicating 1.52-fold reduction in signal intensity (Fig.2E) (control (unlesioned): WT, 1.73 X 10^9 ± 0.36 X 10^9, n=4; TLR2-/-, 1.83 X 10^9 ± 0.48 X 10^9, n=4, p=0.258; 3d: WT, 4.65 X 10^9 ± 0.13 X 10^9; TLR2-/- 4.90 X 10^9 ± 0.15 X 10^9, n=4, p=0.265; 7d: WT, 15.19 X 10^9 ± 0.47 X 10^9, n=4, TLR2-/- 9.99 X 10^9 ± 0.60 X 10^9, n=4, p<0.001).

3.4.3 Decreased levels of MCP-1 and $CD45^{high}/CD11b^{+}$ cells in ischemic brains of TLR2 -/- mice

Evidence suggests that pro-inflammatory cytokines such as IL-1β, IL-6 and TNFα may influence the extent of neuronal damage after cerebral ischemia [1, 5]. To determine whether deficient microglial activation in TLR2-/- mice after stroke observed in above presented results induced changes in profiles of pro-inflammatory cytokines we used a standard mouse cytokine antibody array technique to measure over 40 different cytokines from ischemic brains of WT and TLR2 -/- mice [3, 29]. Because production of pro-inflammatory cytokines peaks

within 24hrs following ischemic/reperfusion injury (with the exception of TGFβ levels at 4 days), time points of 1 and 4 days post-stroke were chosen for the analysis [31]. Ischemic injury was associated with a robust increase in the production of pro-inflammatory cytokines both in WT and TLR2 -/- mice. To our surprise, quantitative analysis revealed no significant changes in the levels of pro-inflammatory cytokines such as IL-1β, IL-6 and TNFα between two experimental groups (Figs.3A, B and C) (IL-1β - 1d: WT, 0.026 ± 0.004, n=4; TLR2-/- 0.029 ± 0.002, n=4, p=0.602; 4d: WT, 0.218 ± 0.002, n=4; TLR2-/- 0.202 ± 0.004, n=4, p=0.700; IL-6 - 1d: WT, 0.016 ± 0.002, n=4; TLR2-/- 0.021 ± 0.001, n=4, p=0.082; 4d: WT, 0.011 ± 0.001, n=4; TLR2-/- 0.009 ± 0.001, n=4, p=0.058; TNFα - 1d: WT, 0.028 ± 0.003, n=4; TLR2-/- 0.030 ± 0.001, n=4, p=0.720; 4d: WT, 0.018 ± 0.001, n=4; TLR2-/- 0.019 ± 0.001, n=4, p=0.535). Interestingly however, we observed significant decrease in the levels of MCP-1, 1day after MCAO, (Fig. 4D) in TLR2-/- mice compared to their WT controls (1d: WT, 0.115 ± 0.002, n=4; TLR2-/- 0.095 ± 0.002, n=4, p=0.026; 4d: WT, 0.062 ± 0.007, n=4; TLR2-/- 0.059 ± 0.009, n=4, p=0.841). Because it has been largely acknowledged that MCP-1 plays a pivotal role in monocyte recruitment to the site of injury, we next investigated whether recruitment of infiltrating cells may have been affected in the context of TLR2 deficiency. One of the established protocols for evaluation of the numbers of infiltrating monocytes and resident microglial cells is based on the two-color quantitative and qualitative flow cytometric analysis of $CD45^{+}/CD11b^{+}$ cell populations [27, 28]. Figure 3E presents topographic representation of number of $CD45^{high}/CD11b^{+}$ cells (i.e. macrophage-like)(red) and $CD45^{low}/CD11b^{+}$ cells (i.e. microglia)(green) in control (unlesioned) hemisphere and in ischemic hemisphere 3 and 7 days after stroke in WT and TLR2-/- mice. As shown in Figure 3F quantitative analysis revealed 2.26-fold reduction in numbers of $CD45^{high}/CD11b^{+}$ cells in ischemic brains of TLR2 -/- mice 3 days after MCAO and 2.02-fold reduction 7 days after MCAO compared to WT mice (control (contralateral): WT: 0.35 ± 0.12%, n=4; TLR2-/-, 0.70 ± 0.30%, n=4, p=0.325; 3d: WT, 21.08 ± 2.19%; TLR2-/-, 9.34 ± 3.94%, n=4, p=0.040; 7d: WT, 6.20 ± 0.86%; TLR2-/-, 3.06 ± 0.54%, n=4, p=0.210). We next analyzed numbers of the resident microglial cells

after stroke. The quantitative flow cytometric analysis indicated significant, 1.38-fold reduction in numbers of the $CD45^{low}/CD11b^{+}$ cells in stroked brains of TLR2-/- mice as compared to WT 7d days after stroke (Fig. 3G), suggesting a decrease in population of the resident microglial cells. At 3 days' time point after stroke difference is not statistically significant, but tendency of reduced cell number (1.21-fold reduction) can be observed in TLR2-/- mice compared to WT group (control (contralateral): WT: 5.71 ± 1.15%, n=4; TLR2-/-, 6.23 ± 1.47%, n=4, p=0.793; 3d: WT, 20.44 ± 0.55%; TLR2-/-, 16.91 ± 2.26%, n=4, p=0.137; 7d: WT, 32.44 ± 1.69%; TLR2-/-, 23.55 ± 2.52%, n=4, p=0.026). Our results suggest that early and selective down-regulation of MCP-1 together with significant decrease in the numbers of $CD45^{high}/CD11b^{+}$ and the $CD45^{low}/CD11b^{+}$ cells suggest that TLR2 may have a role in the modulation of monocyte/brain macrophage recruitment to the site of ischemic injury.

3.4.4 Reduced proliferation of resident microglial cells in ischemic brains of TLR2 deficient mice

A highly characteristic feature of the injury-induced microglial activation is massive, but usually transient expansion of microglial cell population, peaking 48-72 hours after initial insult [3, 30]. Our results suggest a decrease in resident microglia numbers. However, at present, it is unclear to what extent the ischemic injury-induced microglial proliferation is affected in the context of TLR2 deficiency. To address this issue, the TLR2-/- and WT mice were injected daily with BrdU. The BrdU-positive/proliferating cells were quantified 3 and 7 days after stroke. In concordance with previous results, quantitative analysis of the BrdU staining (Fig. 4A, B) revealed a robust increase in BrdU immunoreactivity in WT mice. As revealed in Figure 4B, we observed a 24.55% reduction in cell proliferation in TLR2-/- mice (control: WT: 0.03 X 10^8 ± 0.01 X 10^8, n=4; TLR2-/-, 0.04 X 10^8 ± 0.01 X 10^8, n=4, p=0.278; 3d: WT, 4,97 X 10^8 ± 0,13 X 10^8; TLR2-/-, 3,75 X 10^8 ± 0,42 X 10^8, n=4, p=0.048). To further confirm that BrdU is indeed expressed in proliferating microglial cells, double immunofluorescence for BrdU and Iba1, markers of cell proliferation and microglia/macrophages, respectively, 3 days after

transient MCAO was performed. As expected, results demonstrated that the majority of BrdU positive cells were also positive for Iba1 staining (Fig. 4C). To increase the resolution of the results obtained by BrdU signal intensity measurement the microglial proliferative capacity in TLR2-/- mice was assessed by flow cytometry measurement. Proliferation analysis was carried out on the population of $CD45^{low}/CD11b^{+}$ cells – microglial population [27, 28] obtained from TLR2-/- and WT animals injected with BrdU (Fig.4D). The flow cytometric analysis 3 days after stroke revealed a robust, 10- fold increase in the number of $CD45^{low}/CD11b^{+}/BrDU^{+}$ cells in WT mice (Fig. 4D,E). As further shown in Figure 4E, quantitative analysis revealed significant (55.91%) reduction in number of proliferating $CD45^{low}/CD11b^{+}$ cells in TLR2-/- compared to WT mice (control (contralateral): WT: 1.72 ± 0.78%, n=4; TLR2-/-, 1.39 ± 0.63%, n=4, p=0.762; 3d: WT, 18.51 ± 1.41%; TLR2-/-, 8.16 ± 2.14%, n=4, p=0.014). Number of proliferating cells declined by the day 7 and there were no significant difference in numbers of $CD45^{low}/CD11b^{+}/BrDU^{+}$ cells between two experimental groups (Fig.4E).

Previously we have shown that the injury-activated resident microglial cells in proliferation up-regulate galectin-3 (Mac-2 marker of activated microglia) [3]. Further characterization of the proliferating cells in our experimental model revealed that approximately 80% of BrdU positive cells co-localize with Mac-2 (Fig. 4.F). Interestingly, analysis of the Mac-2 immunoreactivity revealed significant 40.52% reduction of the signal in TLR2-/- compared to WT mice (Fig. 4G, H) (control (contralateral): WT, 0.06 X 10^9 ± 0.03 X 10^9, n=4; TLR2-/-, 0.03 X 10^9 ± 0.01 X 10^9, n=4, p=0.448; 3d: WT, 4,17X 10^9 ± 0,20 X 10^9; TLR2-/- 2,48X 10^9 ± 0,75 X 10^9, n=4, p=0.019). Altogether, obtained results indicate that TLR2 deficiency may affect ischemic injury-induced proliferation of the resident microglial cells.

3.4.5 TLR2 deficiency increases delayed neuronal apoptosis and exacerbates ischemic injury

We have demonstrated that activated/proliferating and galectin-3 positive microglial cells exert neuroprotective properties by secreting IGF-1 [3]. To date, it is unclear

whether defective microglial activation/proliferation after stroke may affect evolution of the ischemic injury in TLR2 deficient mice. Although, previous studies have reported smaller acute ischemic lesions in TLR2 deficient mice and/or in mice treated with TLR2 blocking antibodies, the analysis has been limited to the first 24-72 hrs after stroke [9, 10, 20, 21]. We next asked whether initial neuroprotection against ischemic injury in TLR2 -/- mice is also extended to later time-points after stroke. Quantification of the ischemic lesions was performed using cresyl violet stained brain sections of TLR2-/- mice and their WT controls (n=10/group) 3, 7 and 14 days after MCAO. As expected, Figures 5A and 5B, TLR2-/- mice showed significantly reduced direct stroke area (37.03%) compared to WT mice 3 days after MCAO, which is in accordance with previous reports [20, 21]. As described in details in the Methods section and previously reported [10], we analyzed “indirect stroke area” as a measure of contralateral (non-stroked) hemisphere area minus non-stroked area of the ipsilateral (infarcted) hemisphere. Difference between 'direct' and 'indirect' stroke area represented brain swelling. The correction of 'direct stroke area' was then performed by subtracting brain swelling volume from 'direct stroke area'. In addition, ‘indirect stroke area’ represents volume of healthy tissue that correlates to the volume of ischemic tissue, not affected by post ischemic shrinkage. Thus, ‘direct stroke area’ reflects lesion consolidation (shrinkage) and glial scar formation, while ‘indirect stroke area’ represents lesion progression, i.e. effect of altered inflammatory response on lesion dynamics. In that way, ‘direct’ and ‘indirect’ stroke area represent important parameters for adequate characterization of more chronic time-points.

To our surprise, 7 days after transient MCAO, the size of direct stroke area in TLR2-/- mice increased and was significantly larger (31.87%) when compared to controls. Due to a post-ischemic consolidation of the ischemic brain tissue and glial scar formation, in later phase (14 days after transient MCAO), direct stroke area of WT and TLR2-/- mice were reduced compared to 3 and 7 days after MCAO. Still, direct stroke area remained significantly larger in TLR2-/- mice when compared to WT control group (27.99%) (3d: WT, 57.92 ± 4.98, n=10; TLR2-/-, 36.47 ± 3.58,

n=10, p=0.003; 7d: WT, 39.00 ± 2.78, n=10; TLR2-/- 51.43 ± 3.47, n=10, p=0.012; 14d: WT, 22.15 ± 0.96, n=9; TLR2-/- 28.35 ± 2.09, n=6, p=0.010). Quantitative assessment of indirect stroke area (volume of healthy tissue that correlates to volume of damaged, ischemic tissue not affected by post-ischemic consolidation and glial scar formation) 3 days after transient MCAO revealed significant reduction of indirect stroke area (37.58%) in TLR2-/- mice compared to control WT group (Figures 5A and 5C). In addition, 7 days after transient MCAO, indirect stroke area was significantly larger (26.41%) in group of TLR2-/- mice compared to controls. In later phase (14 days after transient MCAO), evolution of ischemic lesion stagnated, and indirect stroke area in TLR2-/- mice remained significantly larger (29.07%) compared to WT control group (3d: WT, 57.82 ± 5.04, n=10; TLR2-/-, 36.09 ± 4.04, n=10, p=0.004; 7d: WT, 42.29 ± 3.24, n=10; TLR2-/- 53.46 ± 2.19, n=10, p=0.010; 14d: WT, 44.10 ± 3.08, n=9; TLR2-/- 56.92 ± 5.43, n=6, p=0.049). Altogether, these results indicate that TLR2 deficiency induces delayed exacerbation in the size of ischemic lesion.

Next, we investigated whether late increase in the size of ischemic lesions detected in TLR2-/- mice is associated with an increase in delayed neuronal cell death. The number of apoptotic cells in both groups was determined using immunohistochemical labeling with anti-cleaved caspase-3 antibody 3, 7 and 14 days after transient MCAO. As shown in Figure 6A and 6B, number of apoptotic cells 3 days after transient MCAO showed 1.35-fold reduction in TLR2-/- mice compared to control WT group, suggesting an early neuroprotective effect of TLR2 deficiency. However, consistent with delayed increase in the size of ischemic lesions, at 7 days after transient MCAO number of cleaved caspase-3 positive cells per mm^3 of infarcted volume in TLR2-/- mice showed 1.37-fold increase compared to group of WT mice. In later time-points, 14 days after transient MCAO, number of cleaved caspase-3 positive cells remained higher in TLR2-/- group compared to WT group, although not significantly higher due to large variation in number of apoptotic cells in TLR2 -/- group. (3d: WT, $2.52 \times 10^5 \pm 0.15 \times 10^5$, n=4; TLR2-/-, $1.87 \times 10^5 \pm 0.18 \times 10^5$, n=4, p=0.046; 7d: WT, $2.99 \times 10^5 \pm 0.27 \times 10^5$, n=4;

TLR2-/-, 4.11 X 10^5 ± 0.35 X 10^5, n=4, p=0.046; 14d: WT, 4.81 X 10^5 ± 0.21 X 10^5, n=4; TLR2-/-, 5.92 X 10^5 ± 0.72 X 10^5, n=4, p=0.2128). In order to investigate which cell types underwent apoptosis, double immunofluorescence labeling of cleaved caspase-3 and neuronal maker NeuN, astrocyte marker GFAP and microglia/macrophage marker CD11b on brain sections of WT mice 3 days after transient MCAO was performed (Fig. 6C, D and E). Cleaved caspase-3 signal co-localized in great majority (>90%) with neuronal marker NeuN (Fig. 6C). As revealed in Figure 6E only few caspase-3 positive cells were also positive for microglia/macrophage marker CD11b (Fig. 6E). We did not observe colocalization of cleaved caspase-3 immunostaining with astrocyte marker GFAP (Fig. 6D). Hence, delayed exacerbation of ischemic injury in TLR2 -/- mice is characterized by delayed increase in neuronal apoptosis.

3.4.6 Reduced levels of IGF-1 in brains of TLR2 deficient mice after transient ischemia

Previous findings demonstrated that activated and proliferating microglial cells produce neurotrophic/antiapoptotic factors such as IGF-1 and thus exert neuroprotection [3, 32, 33]. Because our results demonstrated reduced proliferating capacity/decrease in numbers of microglial cells in TLR2-/- mice, we hypothesized that IGF-1 levels may have been affected in TLR2 deficiency which may have resulted in an increase in delayed neuronal death. To test our hypothesis, we measured IGF-1 levels in control (unlesioned) and lesioned hemispheres of WT and TLR2-/- mice (Fig.7A, B). Analyses were performed 3 and 7 days following transient ischemia. As expected, immunofluorescence labeling indicated significant increase of signal intensity between control (unlesioned) and lesioned hemispheres in WT and TLR2-/- mice. Interestingly, quantitative analysis of IGF-1 signal revealed significant 1.42-fold reduction at 3 days and 2.73-fold reduction at 7 days after MCAO in TLR2-/- mice when compared to WT mice group (Figure 7B) (control (contralateral): WT, 0.004 X 109 ± 0.001 X 109, n=4; TLR2-/-, 0.006 X 109 ± 0.001 X 109, n=4, p=0.283; 3d: WT, 1.24 X 109 ± 0.11 X 109; TLR2-/- 0.87 X 109 ± 0.04 X 109, n=4, p=0.039; 7d: WT, 2.32 X 109 ± 0.29 X 109,

n=4, TLR2-/- 0.85 X 109 ± 0.13 X 109, n=4, p=0.004). To further confirm that the cells expressing IGF-1 after transient ischemia are microglia, double labeling with marker Iba1, was performed 3 and 7 days after stroke. As shown in Figure 7C, D IGF-1 expression on ischemic site was almost exclusive to microglia/macrophages, which is in concordance with previous studies [3, 33]. Same results were obtained on stroked tissue of TLR2-/- mice (data not shown). On site of ischemic lesion, no cell-specific immunostaining was detected for astrocytes or neurons in WT or TLR2-/- in both time points on ischemic lesion site (data not shown). Altogether, these results suggest that defective immune response in brain caused by TLR2 deficiency resulted in reduced amount of microglia-secreted IGF-1 (a very potent antiapototic molecule for stressed neurons) in- and around ischemic lesion site which in terms may have caused an increase in delayed neuronal death and consequent exacerbation of the ischemic injury observed in TLR2 deficient mice.

3.5 DISCUSSION

Microglial activation and innate immune response are key features of the brain inflammatory response to ischemic injury. Using live imaging approach we have previously shown that microglial activation after stroke is characterized by a marked long-term induction of the TLR2 signals, thus suggesting an important role of TLR2 signaling in brain ischemia. In the present study we report altered microglia activation profiles and delayed exacerbation of ischemic injury in the mouse model lacking functional TLR2 receptors. Namely, the TLR2 deficiency resulted in (1) reduced microglia/macrophage activation after stroke (2) reduced capacity of resident microglia to proliferate (3) decreased levels of MCP-1 and consequently lower levels of $CD45^{high}/CD11b^{+}$ expressing cells. Importantly, although acute ischemic lesions (24-72hrs) were smaller in TLR2 -/- mice, the observed alterations in innate immune response were more pronounces at later time-points (at day 7) after initial stroke, which finally resulted in delayed exacerbation of ischemic lesion leading to larger chronic infarctions as compared to WT mice. Finally, reduced microglial activation/proliferation resulted in significant decrease in expression of IGF-1 in microglial cell after stroke. Altogether our

results clearly suggest that optimal and timely microglial activation/innate immune response is needed to limit the extent of neuronal damage after stroke.

Upon activation microglial cells start to express TLRs on their surface [11, 34, 35]. Functional role of TLRs is the signal transduction into the cell via TIR-domain containing adaptor proteins and MyD88 adaptor protein resulting in degradation of IκB proteins and translocation of transcription factor nuclear factor κB (NFκB) into the nucleus, which induces expression of proinflammatory cytokines in response to PAMPs and DAMPs [5, 36, 37]. Among diverse TLRs, it has been reported that after transient cerebral ischemia, induction of TLR2 predominates among TLRs, followed by TLR4 and TLR9 [9]. After brain injury and/or pathogen exposition, TLR2 is mainly expressed in population of microglial cells [11, 20, 38, 39]. In addition, some reports indicate expression of TLR2 in astrocytes, oligodendrocytes, ependymal cells as well as neurons and neuronal progenitor cells [12, 18, 40, 41]. Our results revealed marked induction of TLR2 (mRNA and protein level) that was restricted to ischemic lesion and peri-infarct zones. No signal was observed contralateral, i.e. on non-stroke side. Further, our analysis revealed that in early and late phases of the brain response to transient ischemia up-regulation of TLR2 occurred almost exclusively on activated microglial cells (see Fig. 1C-E). Minor expression was found in limited subpopulation of neurons situated in the ischemic core area and we did not observe any colocalization between TLR2 and GFAP stained astrocytes. These results are in accordance with previous reports on TLR2 induction following brain injury from ours [11] and other laboratories [9, 20, 21, 23, 40, 42].

As discussed, previous studies reported initial neuroprotection against ischemia in TLR2 -/-mice [9, 20, 21]. In keeping with previous work, the results of our study revealed and confirmed that, in TLR2 -/- mice, the early post-stroke period (up to 3 days after transient MCAO) is characterized by smaller infarcts (see Fig.5). Interestingly however, initial neuroprotection was not extended to later time points and we observed progressive and delayed exacerbation of neuronal damage in

TLR2 deficient mice. Thus in TLR2 deficient mice early reduction in microglial responses was associated with initially smaller lesions, a long-term decrease in microglia/macrophage activation and proliferation led to increased neuronal apoptosis and delayed exacerbation of ischemic lesion (Figures 2-6). Previous work suggests that some inflammatory molecules may have time dependent functions [43], however the role of TLR2 (and potentially other TLRs) beyond the acute innate immune response in ischemic injury is not well understood. The results presented in this study suggest that TLR2 has a role in injury induced monocyte/macrophage recruitment as well as in colony proliferation. Increased activation and accumulation of the myeloid cells on the site of lesion after stroke may occur either due to massive proliferation of resident microglia which normally peaks 48-72h after initial activation, or due to increased monocyte recruitment from circulation to the lesion site [3, 30, 44, 45]. Our data suggest that both processes may have been affected in TLR2 -/- mice. Namely, we detected selective decrease in MCP-1 levels 1 day after stroke and consequently lower numbers of $CD45^{high}/CD11b^{+}$ expressing cells in both, 3 and 7 days after onset of ischemia. In addition, TLR2 deficiency was associated with the reduced capacity of resident microglial cells to proliferate. Reduced microglial proliferation was observed in stroked brains of TLR2-/- mice 3 days after MCAO. Although at present we cannot exclude the possibility that detected decrease in microglial proliferation may be due to initially smaller infarcts, it is important to mention that the size of infarction did increase over time in TLR2 -/- mice, however, this was not accompanied by an increase in microglial proliferative response and/or activation,. As shown by flow cytometric analysis the proliferative response stayed low in TLR2-/- mice 7 days after stroke (see Fig4). On the other hand, a decrease in $CD45^{high}/CD11b^{+}$ expressing cells observed at day 3 and 7 and selective decrease in MCP-1 observed in TLR2 -/- mice suggest that TLR2 signaling is needed for adequate recruitment of circulating monocytes. Taken together, these results support in part the hypothesis established on axonal injury model, which suggests that in acute phase TLR2 may modulate proliferation rather than entry of circulating monocytes [23, 30, 46-48].

The question that arises here is how to correlate deficient monocyte/microglia responses observed in TLR2 -/- with delayed exacerbation of the ischemic injury. One of the possibilities is that, as previously reported, rapid phagocytic removal of dead or dying cells prevents the release of proinflammatory intracellular components and contributes to the resolution of inflammation [49]. Reduced CD68 signal intensity may suggest reduced number of phagosomes present on the lesion site TLR2-/- mice, thus implying that the engulfment of cellular debris is altered, with a consequently prolonged inflammation. It is noteworthy that altered microglia/macrophage activation profiles observed in TLR2 -/- mice were more pronounced at day 7 post stroke, which coincided with initial enlargement of ischemic lesions in TLR2 deficient mice. An additional explanation as suggested by our results is that defective innate immune response in brain caused by TLR2 deficiency results in deficient microglia proliferation and consequently reduced levels of IGF-1 which may lead to an increase in delayed neuronal death and exacerbation of ischemic injury.

Based on our results, we may conclude that reduction in numbers as well as aberrant profiles of the activated microglia/macrophages may over time result in microenvironment that is detrimental for neuronal survival and causes exacerbation of ischemic lesion.

3.6 CONCLUSION

Taken together, our data suggest that functional TLR2 signaling is required for modulation of microglia/macrophage responses in injured brain. Moreover, our data also indicate that TLR2 induction may exert temporally differential effects. However, the ischemic injury-induced TLR2 response in the brain is instrumental for timely resolution of the post-ischemic inflammation, finally limiting exacerbation and/or propagation of the initial ischemia-induced neuronal damage.

COMPETING INTERESTS:
Authors declare that they have no competing interests.

AUTHORS' CONTRIBUTIONS:
IB carried out the immunoassays, cytokine array, flow cytometry analysis, quantifications and wrote the manuscript. **PC** participated in cytokine array, flow cytometry and participated in study design. **MLH** performed in situ hybridization and participated in study design. **DG** participated in the study design and performed the statistical analysis. **YCW** performed surgical procedures and helped in tissue collection and cryo-cutting. **SG** participated in study design and coordination. **JK** conceived of the study, participated in study design and coordination and wrote the manuscript.

3.7 ACKNOWLEDGEMENTS:

This work was supported by The Canadian Institutes of Health Research (CIHR) Operating Grant to JK. JK is recipient of the Fonds de la Recherché en Santé Québec (FRSQ) Senior Scholarship. IB, DG and SG received funding from Unity through Knowledge Fund (UKF) grant 35/08. The authors also wish to thank Ms Genevieve Soucy for her technical assistance.

3.8 REFERENCES

Aliprantis AO, Yang RB, Weiss DS, Godowski P, Zychlinsky A: The apoptotic signaling pathway activated by Toll-like receptor-2. *EMBO J* 2000, **19**:3325-3336.

Akira S, Uematsu S, Takeuchi O: Pathogen recognition and innate immunity. *Cell* 2006, **124**:783-801.

Akira S, Takeda K: Toll-like receptor signaling. *Nat Rev Immunol* 2004, **4**:499-511.

Arumugam TV, Okun E, Tang SC, Thundyil J, Taylor SM, Woodruff TM: Toll-like receptors in ischemia-reperfusion injury. *Shock* 2009, **32**:4-16.

Asea A, Rehli M, Kabingu E, Boch JA, Bare O, Auron PE, Stevenson MA, Calderwood SK: Novel signal transduction pathway utilized by extracellular HSP70: role of toll-like receptor (TLR) 2 and TLR4. *J Biol Chem* 2002, **277**:15028-15034.

Babcock AA, Wirenfeldt M, Holm T, Nielsen HH, Dissing-Olesen L, Toft-Hansen H, Millward JM, Landmann R, Rivest S, Finsen B, Owens T: Toll-like receptor 2 signaling in response to brain injury: an innate bridge to neuroinflammation. *J Neurosci* 2006, **26**:12826-37.

Beaulieu JM, Kriz J, Julien JP: Induction of peripherin expression in subsets of brain neurons after lesion injury or cerebral ischemia. *Brain Res* 2002, **946**:153-61.

Bechmann I, Goldmann J, Kovac AD, Kwidzinski E, Simburger E Naftolin F, Dirnagl U, Caso JR, Pradillo JM, Hurtado O, Lorenzo P, Moro MA, Lizasoain I: Toll-like receptor 4 is involved in brain damage and inflammation after experimental stroke. *Circulation* 2007, **115**:1599-1608.

Campanella M, Sciorati C, Tarozzo G, Beltramo M: Flow Cytometric Analysis of Inflammatory Cells in Ischemic Rat Brain. *Stroke* 2002, **33**:586-592.

Cao CX, Yang QW, Lv FL, Cui J, Fu HB, Wang JZ: Reduced cerebral ischemia-reperfusion injury in Toll-like receptor 4 deficient mice. *Biochem Biophys Res Commun* 2007, **353**:509-14.

Cordeau P Jr, Lalancette-Hebert M, Weng YC, Kriz J: Live imaging of neuroinflammation reveals sex and estrogen effects on astrocyte response to ischemic injury. *Stroke* 2008, **39**:935-42.

Gordon S: Pattern recognition receptors: doubling up for the innate immune response. *Cell* 2002, **111**:927-930.

Hailer NP, Grampp A, Nitsch R: Proliferation of microglia and astrocytes in the dentate gyrus following enthorinal cortex lesion: a quantitiative brodmodeoxyuridine labelling study. *Eur J Neurosci* 1999, **11**:3359-364.

Hanisch and Kettenmann: Microglia: active sensor and versatile effector cells in the normal and pathologic brain. *Nat Neurosci* 2007, **10**:1387-94.

Hanisch UK, Johnson TV, Kipnis J: Toll-like receptors: roles in neuroprotection? *Trends Neurosci* 2008, **31:**176-82.

Hill JK, Gunion-Rinker L, Kulhanek D, Lessov N, Kim S, Clark WM, Dixon MP, Nishi R, Stenzel-Poore MP, Eckenstein FP: Temporal modulation of cytokine expression following focal cerebral ischemia in mice. *Brain Res* 1999, **820**:45-54.

Hua F, Ma J, Ha T, Kelley JL, Kao RL, Schweitzer JB, Kalbfleisch JH, Williams DL, Li C: Differential roles of TLR2 and TLR4 in acute focal cerebral ischemia/reperfusion injury in mice. *Brain Res* 2009, **1262**:100-108.

Iadecola C, Anrather J: Stroke research at a crossroad: asking the brain for directions. *Nat Neurosci* 2011, **14**:1363-1368.

Jack CS, Arbour N, Manusow J, Montgrain V, Blain M, McCrea E, Shapiro A, Antel JP: TLR signaling tailors innate immune responses in human microglia and astrocytes. *J Immunol* 2005, **175**:4320-4330.

Janeway JrCA, Medzhitov R: Innate Immune recognition. *Annu Rev Immunol* 2002, **20**:197-216.

Kariko K, Weissman D, Welsh FA: Inhibition of Toll-like receptor and cytokine signaling – A unifying theme in ischemic tolerance. *J Cereb Blood Flow Metab* 2004, **24**:1288-1304.
Kempermann G, Neumann H: Neuroscience. Microglia: the enemy within? *Science* 2003, **302**:1689-1690.

Kriz J: Inflammation in ischemic brain injury: timing is important. *Crit Rev Neurobiol* 2006, **18**:145–157.

Kriz J, Lalancette-Hebert M: Inflammation, plasticity and real-time imaging after cerebral ischemia. *Acta Neuropathol* 2009, **117**:497-509.

Ladeby R, Wirenfeldt M, Garcia-Ovejero D, Fenger C, Dissing-Olesen L, Dalmau I, Finsen B: Microglial cell population dynamics in the injured adult central nervous system. *Brain Res Brain Res Rev* 2005, 48:196-206.

Laflamme N, Echchannaoui H, Landmann R, Rivest S: Cooperation between toll-like receptor 2 and 4 in the brain of mice challenged with cell wall components derived from gram-negative and gram-positive bacteria. *Eur J Immunol* 2003, **33**: 1127–38.
Takeda K, Akira S: Toll receptors and pathogen resistance. *Cell Microbiol* 2003, **5**: 143–53.

Lalancette-Hebert M, Gowing G, Simard A, Weng YC, Kriz J: Selective ablation of proliferating microglial cells exacerbates ischemic injury in the brain. *J Neurosci* 2007, **27**:2596-2605.

Lalancette-Hébert M, Julien C, Cordeau P, Bohacek I, Weng YC, Calon F, Kriz J: Accumulation of dietary docosahexaenoic acid in the brain attenuates acute immune response and development of postischemic neuronal damage. *Stroke* 2011, **42**:2903-9.

Lalancette-Hébert M, Phaneuf D, Soucy G, Weng YC, Kriz J: Live imaging of Toll-like receptor 2 response in cerebral ischaemia reveals a role of olfactory bulb microglia as modulators of inflammation. *Brain* 2009, **132**:940-954.

Lalancette –Hébert M, Swarup V, Beaulieu M, Bohacek I, Abdelhamid E,Weng Y-C, Sato S, Kriz J: Galectin-3 is required for resident microglia activation and proliferation in response to ischemic injury. *J Neurosci 2012, in press*.

Lehnardt S, Lehrmann S, Kaul D, Tschimmel K, Hoffmann O, Cho S, Krueger C, Nitsch R, Meisel A, Weber JR: Toll-like receptor 2 mediates CNS injury in focal cerebral ischemia. *J Neuroim* 2007, **190**:28-33.

Lo EH, Dalkara T, Moskowitz MA: Mechanisms, challenges and opportunities in stroke. *Nat Rev Neurosci* 2003, **4**:399-415.

Matzinger P: The danger model: a renewed sense of self. *Science* 2002, **296**:301-305.

Medzhitov R, Preston-Hurlburt P, Janeway CA Jr: A human homologue of the Drosophila Toll protein signals activation of adaptive immunity. *Nature* 1997, **388**: 394-7.

Nakajima K, Kohsaka S: Microglia: neuroprotective and neurotrohic cells in the central nervous system. *Curr Drug Targets Cardiovasc Haematol Disord* 2004, **4**:65-84.
Nitsch R, Priller J: Circulating monocytic cells infiltrate layers of anterograde axonal degeneration where they transform into microglia. *FASEB J* 2005, **15**:1086-1088.

O'Donnell SL, Frederick TJ, Krady JK, Vannucci SJ, Wood TL: IGF-I and microglia/macrophage proliferation in the ischemic mouse brain. *Glia* 2002, **39**:85-97.

Olson JK, Miller SD: Microglia initiate central nervous system innate and adaptive immune responses through multiple TLRs. *J Immunol* 2004, **173**:3916-3924.
Kielian T: Toll-like receptors in central nervous system glial inflammation and homeostasis. *J Neurosci Res* 2006, **883**:711-730.

Poon IK, Hulett MD, Parish CR: Molecular mechanisms of late apoptotic/necrotic cell clearance. *Cell Death Differ* 2010, **17**:381–397.

Raivich G, Bohatshek M, Kloss CU, Werner A, Jones LL, Kreutzberg GW: Neuroglial activation repertoire in the injured brain: graded response, molecular mechanisms and cues to physiological function. *Brain Res Brain Res Rev* 1999, **30**:77-105.

Rolls A, Schechter R, London A, Ziv Y, Ronen A, Levy R, Schwartz M: Toll-like receptors modulate adult hippocampal neurogenesis. *Nat Cell Biol* 2007, **9**:1081-8.
Hoffmann O, Braun JS, Becker D, Halle A, Freyer D, Dagand E, Lehnardt S, Weber JR: TLR2 mediates neuroinflammation and neuronal damage. *J Immunol* 2007, **178**:6476-6481.

Stoll G, Jander S, Schroeter M: Inflammation and glial responses in ischemic brain lesions. *Prog Neurobiol* 1998, **56**:149-171.

Tang SC, Arumugam TV, Xu X, Cheng A, Mughal MR, Jo DG, Lathia JD, Siler DA, Chigurupati S, Ouyang X, Magnus T, Camandola S, Mattson MP: Pivotal role for neuronal Toll-like receptors in ischemic brain injury and functional deficits. *Proc Natl Acad Sci U S A* 2007, **104**:13798-803.

Wirenfeldt M, Babcock AA, Ladeby R, Lambertsen KL, Dagnaes-Hansen F, Leslie RG, Owens T, Finsen B: Reactive microgliosis engages distinct responses by microglial subpopulations after minor central nervous system injury. *J Neurosci Res* 2005, **82**:507-514.

Ziegler G, Freyer D, Harhausen D, Khojasteh U, Nietfeld W, Trendelenburg G: Blocking TLR2 in vivo protects against accumulation of inflammatory cells and neuronal injury in experimental stroke. *J Cereb Blood Flow Metab* 2010, **31**(2):757-66.

Ziegler G, Harhausen D, Schepers C, Hoffmann O, Röhr C, Prinz V, König J, Lehrach H, Nietfeld W, Trendelenburg G: TLR2 has a detrimental role in mouse transient focal cerebral ischemia. *Biochem Biophys Res Commun* 2007, **359**:574-579.

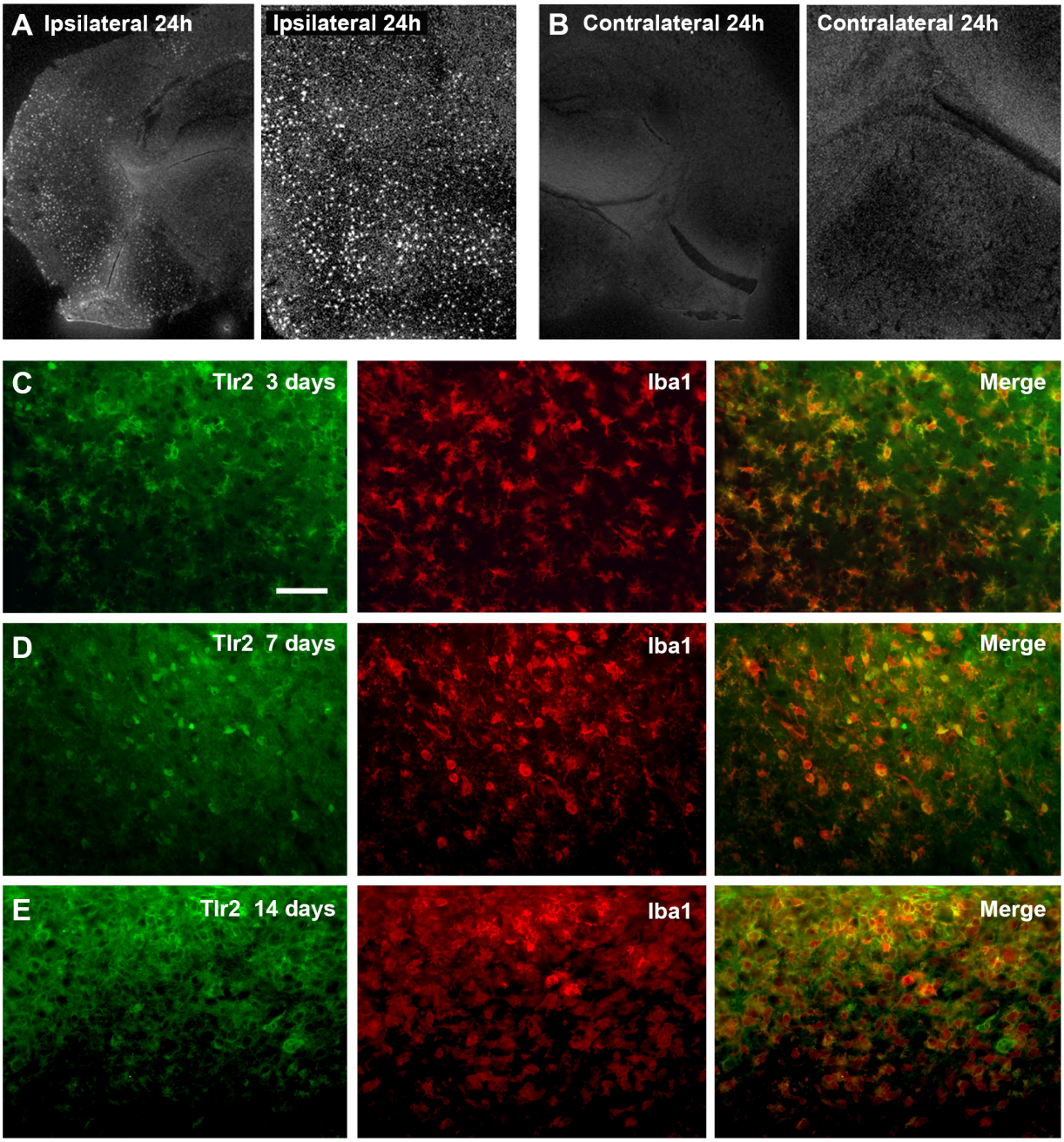
A Ipsilateral 24h
Ipsilateral 24h
B Contralateral 24h
Contralateral 24h
C
Tlr2 3 days
Iba1
Merge
D
Tlr2 7 days
Iba1
Merge
E
Tlr2 14 days
Iba1
Merge

Figure 1. Microglial cells up-regulate TLR2 in response to transient ischemic brain injury. A, B: Photomicrographs of *in situ* hybridization for TLR2 mRNA in WT mice 24 h after ischemic injury indicating marked induction of TLR2 on ipsilateral side shown in low (A, left) and high (A, right) magnification; in contrast to contralateral side where no positive S^{35} signal was observed (B). C, D, E: Double labeling 3, 7 and 14 days after transient MCAO reveals colocalization of TLR2 (green) and Iba1 (red) in WT mice, indicating that TLR2 are expressed almost exclusively by microglia/macrophage cell population in both, early and late phase of response to ischemic brain injury. Scale bar: C, 50 μm.

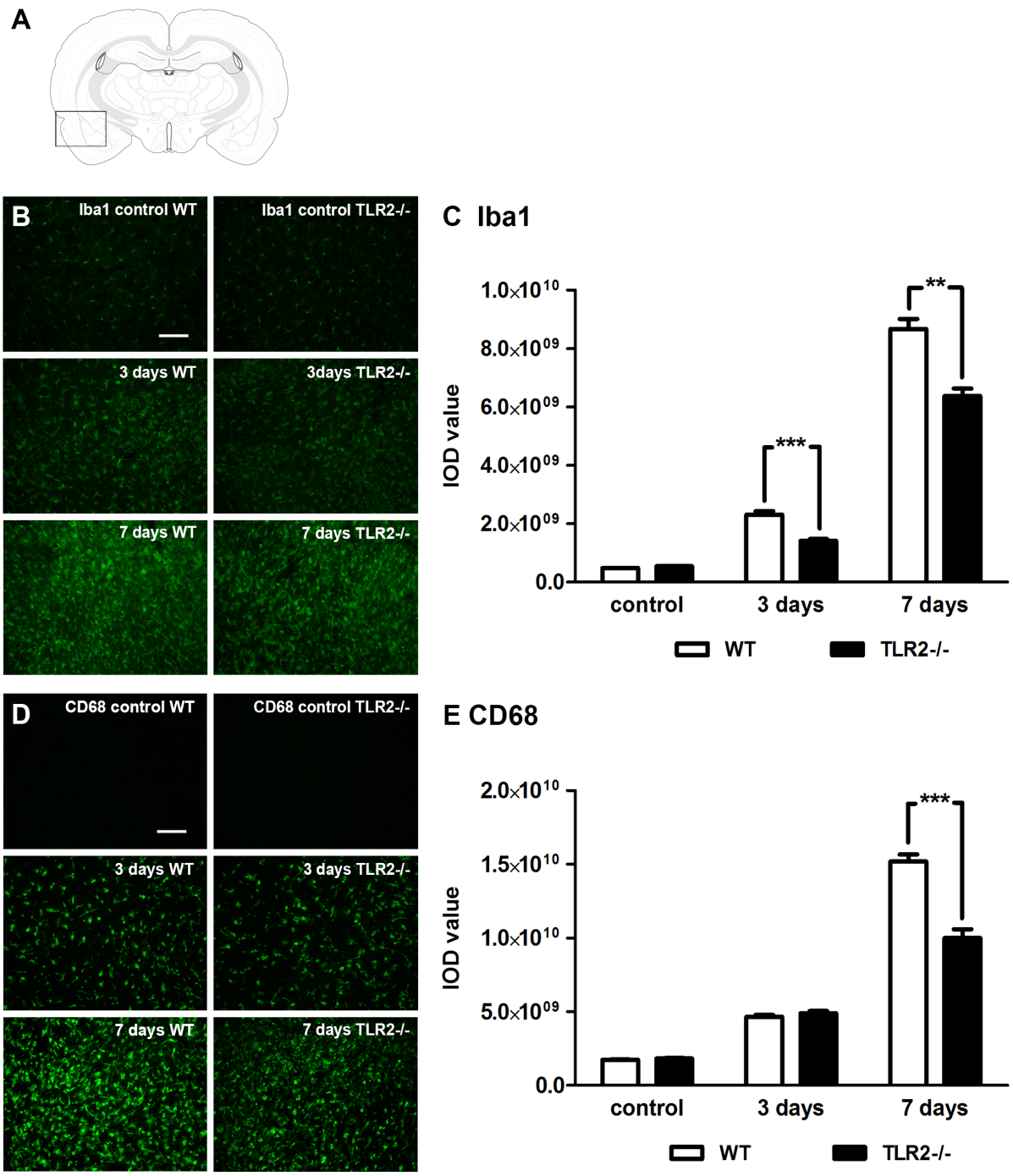
A
B
Iba1 control WT
Iba1 control TLR2-/-
3 days WT
3days TLR2-/-
7 days WT
7 days TLR2-/-
C Iba1
IOD value
1.0×10^10
8.0×10^09
6.0×10^09
4.0×10^09
2.0×10^09
0.0
**
***
control
3 days
7 days
WT
TLR2-/-
D
CD68 control WT
CD68 control TLR2-/-
3 days WT
3 days TLR2-/-
7 days WT
7 days TLR2-/-
E CD68
IOD value
2.0×10^10
1.5×10^10
1.0×10^10
5.0×10^09
0.0
***
control
3 days
7 days
WT
TLR2-/-

Figure 2. TLR2 deficiency leads to altered microglia/macrophage activation profiles. A: Schematic representation of the brain section used for the immunohistochemical experiments. Box represents the area magnified in B and D, and in Figures 3A, 3C, 3F, 3G, as well as in Figures 6 and 7. B: Representative photomicrographs of Iba1 immunoreactivity in control (unlesioned) WT and TLR2-/- mice, as well as 3 and 7 days after transient MCAO, indicate reduced accumulation of Iba1 positive cells in TLR2 deficient mice. C: Quantification of Iba1 immunoreactivity revealed significantly decreased immunoreactivity in TLR2-/- mice compared to WT group of mice 3d and 7d after transient MCAO. D: Photomicrographs of CD68 immunoreactivity in unlesioned (control) WT and TLR2-/- mice and 3 and 7 days after transient ischemic lesion. E: Quantitative analysis of CD68 immunoreactivity in both groups reveals significant reduction of the signal intensity 7 days after MCAO in TLR2-/- group. Values (C, E) indicate mean ± SEM (n=4; **p<0.001 ***p<0.0001). Scale bars: B, D: 100 µm.

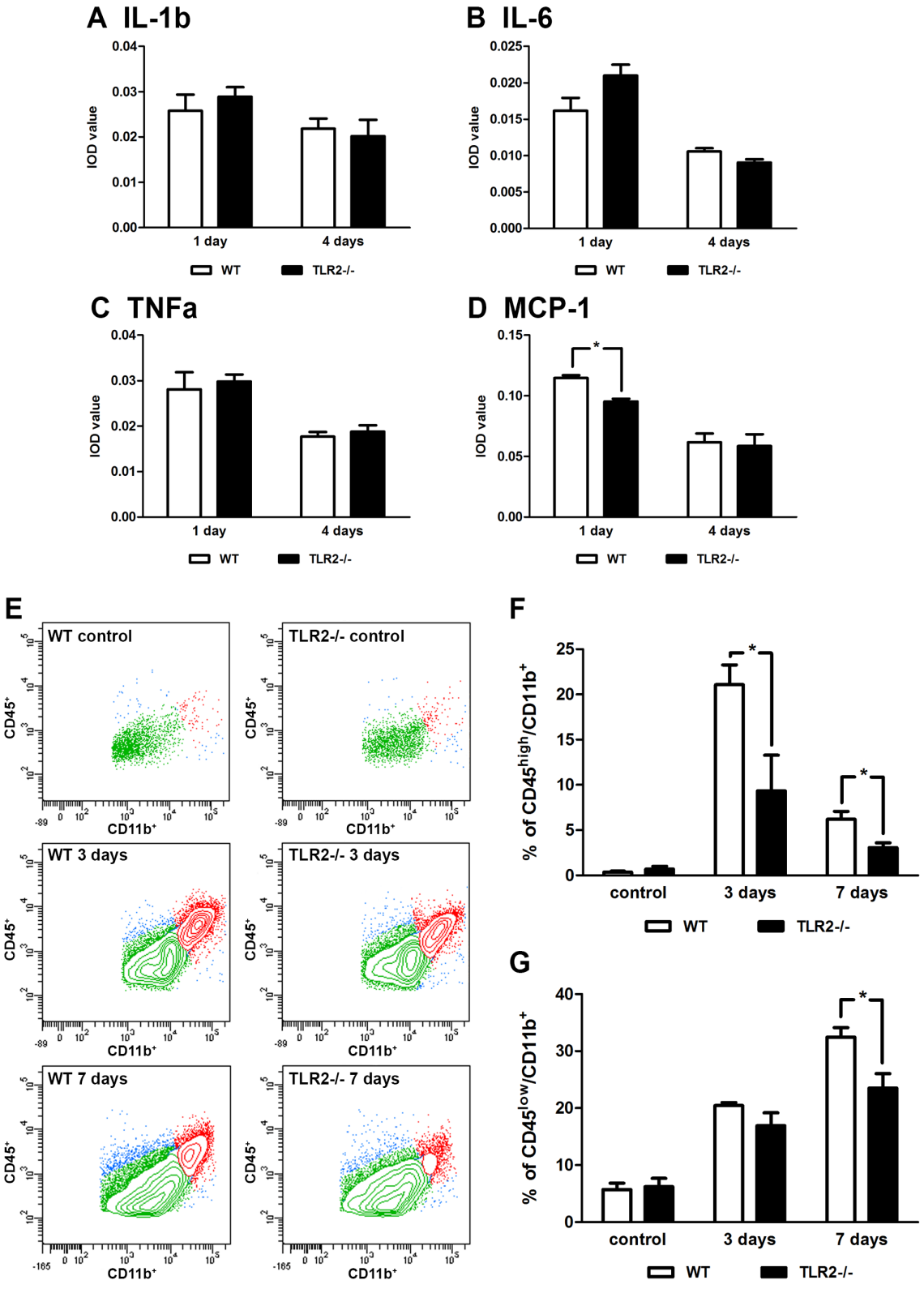
A IL-1b
IOD value
0.04
0.03
0.02
0.01
0.00
1 day
4 days
WT
TLR2-/-
B IL-6
IOD value
0.025
0.020
0.015
0.010
0.005
0.000
1 day
4 days
WT
TLR2-/-
C TNFa
IOD value
0.04
0.03
0.02
0.01
0.00
1 day
4 days
WT
TLR2-/-
D MCP-1
IOD value
0.15
0.10
0.05
0.00
*
1 day
4 days
WT
TLR2-/-
E
WT control
TLR2-/- control
WT 3 days
TLR2-/- 3 days
WT 7 days
TLR2-/- 7 days
CD45+
CD11b+
F
% of CD45high/CD11b+
25
20
15
10
5
0
*
*
control
3 days
7 days
WT
TLR2-/-
G
% of CD45low/CD11b+
40
30
20
10
0
*
control
3 days
7 days
WT
TLR2-/-

Figure 3. Decreased levels of MCP-1 and CD45^{high}/CD11b^{+} expressing cells in TLR2 deficient mice. A-C: Expression analysis of inflammatory cytokines IL-1β, IL-6 and TNF-α on protein level 1 and 4 days after transient MCAO revealed no significant difference between WT and TLR2-/- groups. D: Significant reduction of MCP-1 levels in TLR2-/- group compared to their WT controls, 1day after transient MCAO. E: Topographic representation of isolated brain mononuclear cells from ischemic hemispheres of control, WT and TLR2-/- mice 3 and 7 days after stroke, analyzed using 2-color flow cytometry. Cells were analyzed for the CD45 and CD11b, thus allowing us to distinct two different cell populations: CD45^{high}/CD11b^{+} (i.e. macrophage-like) population (red); and CD45^{low}/CD11b^{+} (microglial) population (green). F: Flow cytometric analysis showed significant decrease in the number of CD45^{high}/CD11b^{+} cells in TLR2-/- mice compared to WT mice in both 3 and 7 days time points after stroke. G: Quantitative analysis of CD45^{low}/CD11b^{+} cells (microglia) indicates significant reduction of cell number in TLR2-/- mice as compared to WT 7d days after stroke, while 3 days after stroke difference is not significant, but tendency of reduced cell number can be occurred in TLR2-/- mice. Values (A-D) are expressed as mean ± SEM (n=4, *$p<0.05$). Data (F, G) are expressed as % of CD45^{+} events ± SEM (n=4; *$p<0.05$).

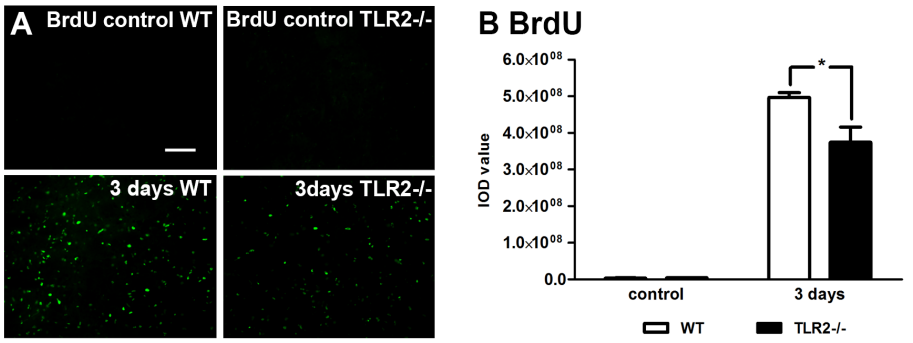
A
BrdU control WT
BrdU control TLR2-/-
3 days WT
3days TLR2-/-
B BrdU
IOD value
6.0×10^08
5.0×10^08
4.0×10^08
3.0×10^08
2.0×10^08
1.0×10^08
0.0
*
control
3 days
WT
TLR2-/-

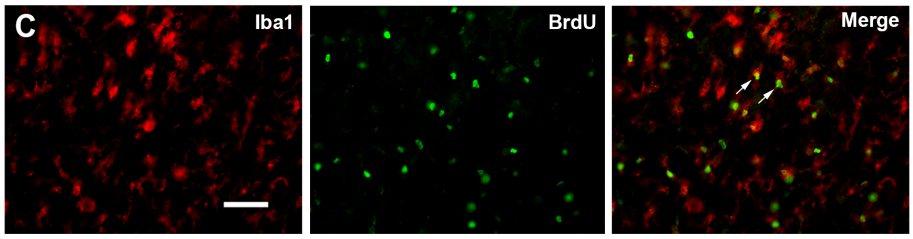
C
Iba1
BrdU
Merge

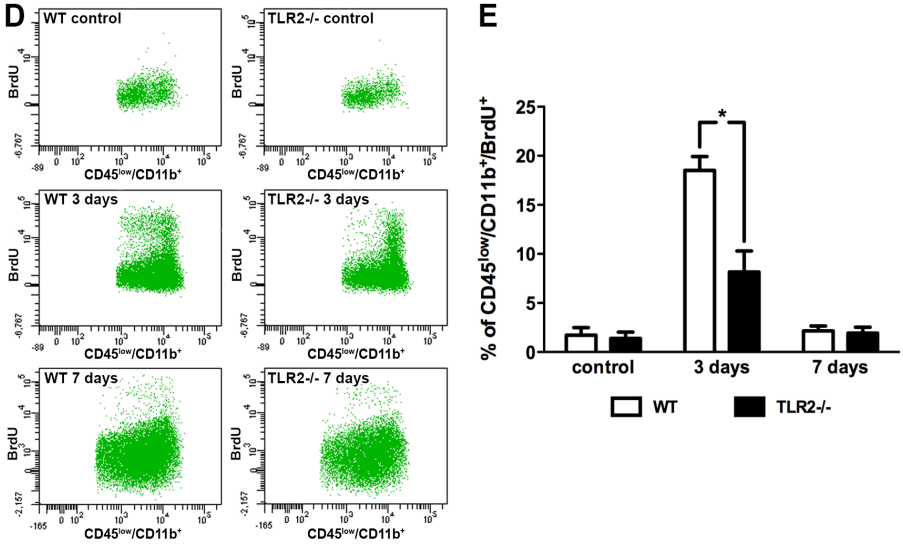
D
WT control
TLR2-/- control
WT 3 days
TLR2-/- 3 days
WT 7 days
TLR2-/- 7 days
BrdU
CD45low/CD11b+
E
% of CD45low/CD11b+/BrdU+
25
20
15
10
5
0
*
control
3 days
7 days
WT
TLR2-/-

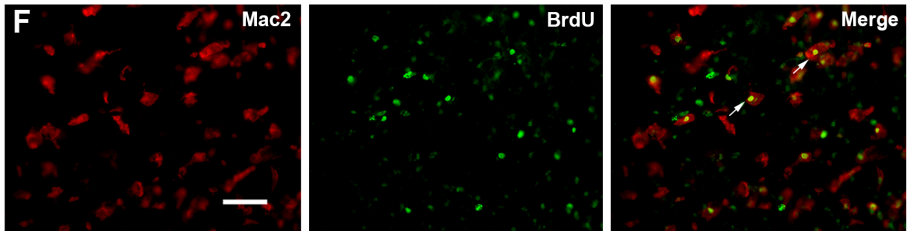
F
Mac2
BrdU
Merge

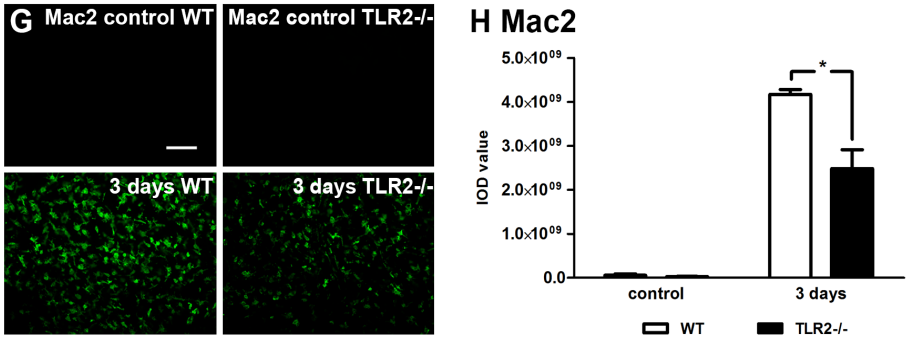
G
Mac2 control WT
Mac2 control TLR2-/-
3 days WT
3 days TLR2-/-
H Mac2
IOD value
5.0×10^09
4.0×10^09
3.0×10^09
2.0×10^09
1.0×10^09
0.0
*
control
3 days
WT
TLR2-/-

Figure 4. TLR2 deficient mice display reduced proliferation of resident microglial cells. A: Photomicrographs of BrdU immunoreactivity in WT and TLR2-/- mice 3 days after transient MCAO and their unlesioned controls, respectively. B: Quantification of BrdU immunoreactivity indicates reduced cell proliferative capacity in TLR2-/- mice compared to WT mice 3 days after transient MCAO. C: Representative photomicrographs of double immunostaining on WT brain sections 3 days after transient MCAO show almost complete colocalization of BrdU (green) positive cells with Iba1(red; white arrows). D: Flow cytometric analysis of $CD45^{low}/CD11b^{+}$ (i.e. microglial) population proliferation in WT and TLR2-/- mice 3 days after MCAO compared to their contralateral (unlesioned) hemisphere controls. E: Graph presents quantification of microglial proliferation measured by flow cytometric analysis. Data indicates reduced microglial proliferation in TLR2-/- mice compared to WT mice 3 days after MCAO. F, Double immunofluorescent labeling reveals colocalization of BrdU (green) and Mac-2 (red; white arrows) in WT brain sections 3 days after transient MCAO. G, Representative photomicrographs of Mac-2 immunofluorescence in WT and TLR2-/- mice observed 3 days after transient MCAO. H, Quantification of Mac-2 immunoreactivity 3 days after transient MCAO revealed reduced signals in TLR2-/- mice compared to WT mice. Data (B, H) are indicated as mean ± SEM (n=4; *$p<0.05$). Data (E) are expressed as % of $CD45^{+}$ events ± SEM (n=4; *$p<0.05$). Scale bars: A, G, 100 µm; C, F, 50 µm.

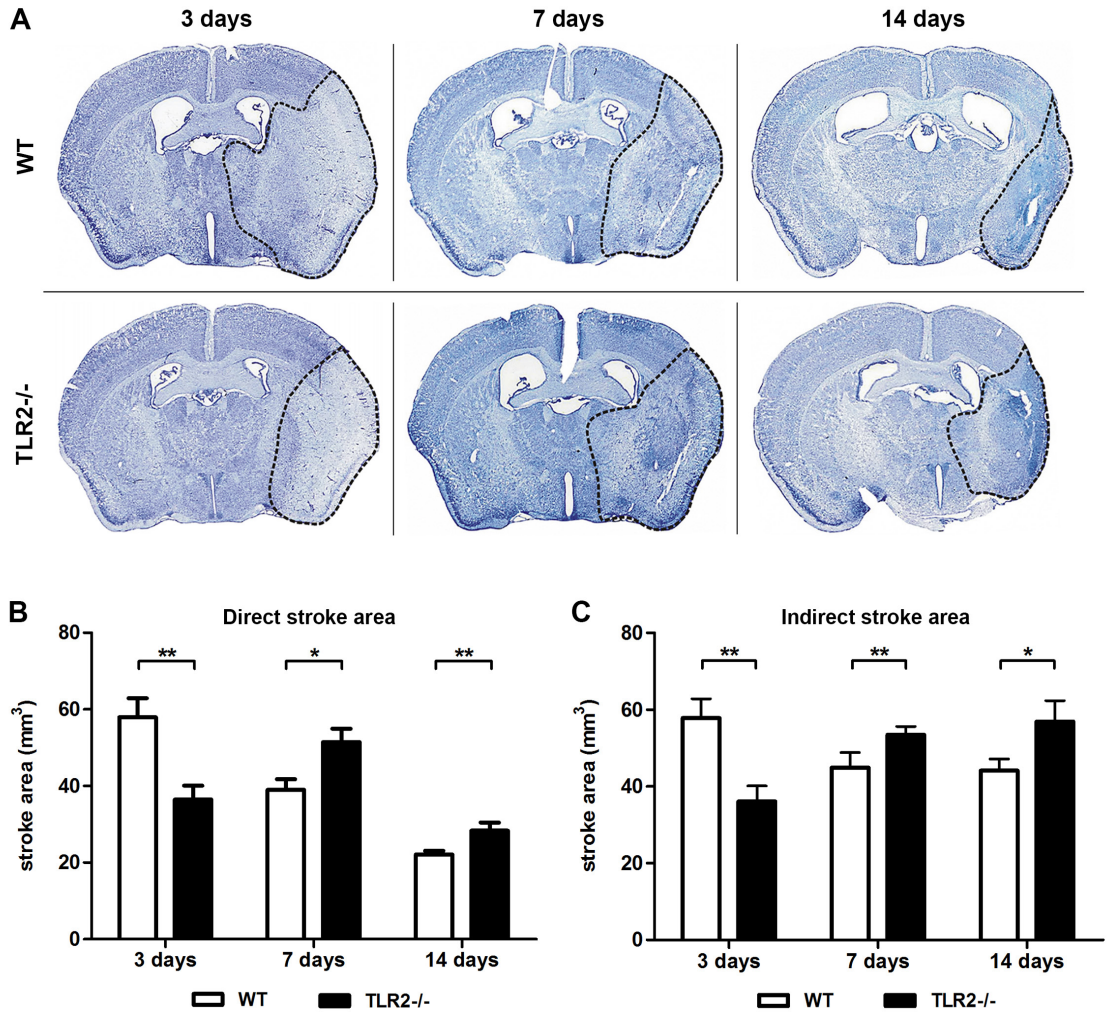

Figure 5. TLR2 deficiency delays evolution of ischemic brain lesion. A: Representative low-magnification photomicrographs of cresyl violet stained brain sections of WT and TLR2-/- mice 3, 7 and 14 days after transient MCAO. Ischemic area is emphasized by black dashed line. B: significantly reduced direct stroke area in TLR2-/- mice 3 days after transient MCAO compared to WT mice, followed by marked lesion exacerbation in TLR2-/- mice 7 days after injury, while lesion in WT mice shows reduction in size. 14 days after injury, evolution of direct stroke area stagnated, indicating significantly larger final lesion size in TLR2-/- mice compared to WT group. C: Smaller indirect stroke area in TLR2-/- mice compared to WT mice 3 days after transient MCAO. In contrast, 7 days after injury, indirect stroke area in TLR2-/- group was larger compared to WT mice, and same relation was observed 14 days after ischemic injury. Values are expressed as mean ± SEM (n=10, *p<0.05, **p<0.001).

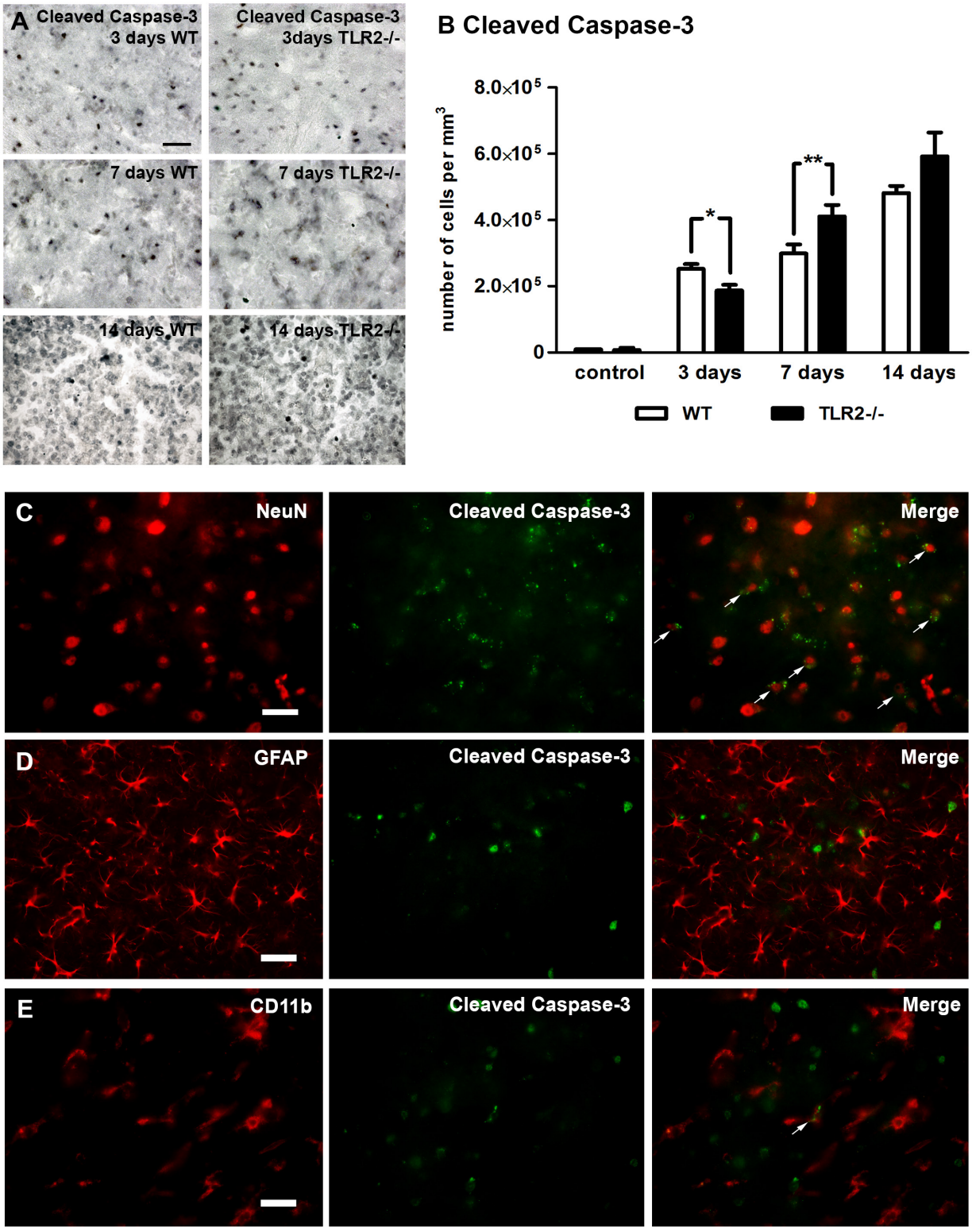
A
Cleaved Caspase-3
3 days WT
Cleaved Caspase-3
3days TLR2-/-
7 days WT
7 days TLR2-/-
14 days WT
14 days TLR2-/-
B Cleaved Caspase-3
number of cells per mm3
8.0×10^5
6.0×10^5
4.0×10^5
2.0×10^5
0
*
**
control
3 days
7 days
14 days
WT
TLR2-/-
C
NeuN
Cleaved Caspase-3
Merge
D
GFAP
Cleaved Caspase-3
Merge
E
CD11b
Cleaved Caspase-3
Merge

Figure 6. Delayed exacerbation of neuronal apoptosis in TLR2 deficient mice. A: Photomicrographs of cleaved caspase-3 immunoreactivity in WT and TLR2 -/- mice 3,7 and 14 days after transient MCAO. B: Quantification of labeled cells showed higher number of apoptotic cells in WT compared to TLR2-/- mice 3 days after injury, while 7 days after injury number of cleaved caspase-3 positive cells was significantly higher in TLR2-/- group compared to WT group of mice. 14 days after transient MCAO, number of cleaved caspase-3 positive cells was higher in TLR2-/- mice, but not significantly, caused by high variation within the group. C: Double immunofluorescence analysis reveals high proportion of cleaved caspase-3 (green) positive cells correlating with neuronal marker NeuN (red, colocalization marked with white arrows). D: No colocalization was observed for GFAP (red) and cleaved caspase-3 (green). E, Only a few cleaved caspase-3 positive cells (green) showed colocalization with Iba1 (red, colocalization marked with white arrow heads), while vast majority was not colocalizing. Data (B) are expressed as mean ± SEM (n=4, *$p<0.05$, **$p<0.001$). Scale bars: A, C, D, E, 25 μm.

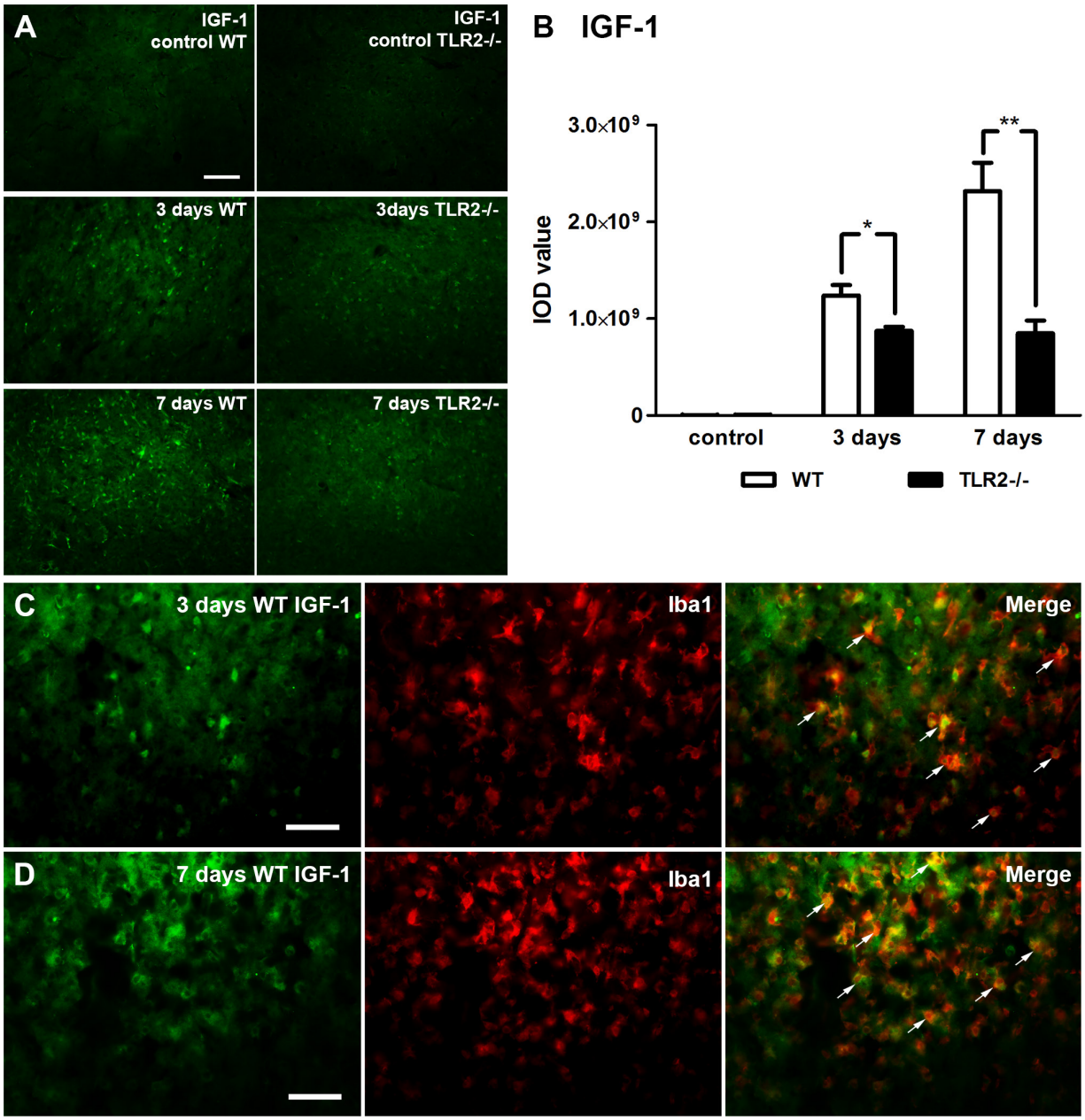

Figure 7. Reduced levels of IGF-1 in brains of TLR2 deficient mice after stroke. A: Photomicrographs of IGF-1 immunoreactivity in control (unlesioned) and lesioned brain hemisphere at 3 and 7days time points after stroke, presenting reduced levels of IGF-1 immunoreactivity in TLR2-/- mice. B, Quantification of signal intensity indicates reduced levels of IGF-1 present in brains of TLR2-/- mice following transient ischemia compared to WT mice. C, D: Double immunofluorescence labeling reveals that IGF-1 expression was exerted by microglia/macrophages within and around the infarcted region in both, 3 and 7 day time points after ischemia. Data (B) are indicated as mean ± SEM (n=4; *p<0.05, **p<0.001). Scale bars: A, 100 µm; C, D: 50 µm.

Chapitre 4. Enriched housing down-regulates the Toll-like receptor 2 response in the mouse brain after experimental stroke

Contributions des auteurs dans l'article: Enriched housing down-regulates the Toll-like receptor 2 response in the mouse brain after experimental stroke publié dans Neurobiology of Disease, 2014.

Mirianna Jlenia Quattromani a effectué les immunohistochimies, les comptes cellulaires, l'acquisition des images en bioluminescence ainsi qu'effectué l'évaluation comportementale. Elle a aussi écrit le manuscrit.

Pierre Cordeau a participé à la mise en place du protocole d'imagerie en plus de diriger les sessions d'imagerie ainsi que l'analyse. Il a aussi apporté une aide technique lors de la chirurgie par photothrombose.

Karsten Ruscher a effectué les chirurgies par photothrombose en plus d'assister lors des sessions d'imagerie.

Jasna Kriz et Tadeusz Wieloch ont coordonné et conçu l'étude en plus d'apporter des correctifs au manuscrit.

Enriched housing down-regulates the Toll-like receptor 2 response in the mouse brain after experimental stroke

Miriana Jlenia Quattromani[1], MSc; Pierre Cordeau[2], MSc; Karsten Ruscher[1], MD; Jasna Kriz[2], MD, PhD; Tadeusz Wieloch[1], PhD

Author affiliations:
[1] Laboratory for Experimental Brain Research, Department of Clinical Sciences, Division of Neurosurgery, Lund University, BMC A13, 22184 Lund, Sweden.

[2] Department of Psychiatry and Neuroscience, Laval University, Le Centre de Recherche de l'Institut Universitaire en Santé Mentale de Québec, 2601, de la Canardière, Québec (Québec), CANADA G1J 2G3.

Corresponding author: Miriana Jlenia Quattromani[1], fax: +46 46 2220615, phone: +46 46 2220609, E-mail: miriana.quattromani@med.lu.se
E-mails: petermavic@gmail.com (Pierre Cordeau); karsten.ruscher@med.lu.se (Karsten Ruscher); jasna.kriz@fmed.ulaval.ca (Jasna Kriz); tadeusz.wieloch@med.lu.se (Tadeusz Wieloch)

4.1 ABSTRACT

Post-ischemic inflammation plays an important role in the evolution of brain injury, recovery and repair after stroke. Housing rodents in an enriched environment provides a multisensory stimulation to the brain and enhances functional recovery after experimental stroke, also depressing the release of cytokines and chemokines in the peri-infarct. In order to identify targets for late stroke treatment, we studied the dynamics of inflammation and the contribution of resident Toll-like receptor 2 (TLR2) expressing microglial cells.

We took advantage of the biophotonic/bioluminescent imaging technique using the reporter mouse-expressing luciferase and GFP reporter genes under transcriptional control of the murine TLR2 promoter (TLR2-luc/GFP mice) for non-invasive *in vivo* analysis of TLR2 activation/response in photothrombotic stroke after differential housing.

Real-time imaging one day after stroke, revealed up-regulation of TLR2 in response to photothrombotic stroke that subsequently declined over time of recovery (14 days). The inflammatory response was persistently down-regulated within days of enriched housing, enhancing recovery of lost sensori-motor function in TLR2-luc mice without affecting infarct size. The number of YM1-expressing microglia in the peri-infarct and areas remote from the infarct was also markedly attenuated.

Using a live imaging approach, we demonstrate that multisensory stimulation rapidly, persistently and generally attenuate brain inflammation after experimental stroke, reducing the TLR2 response and leading to improved neurological outcome. TLR2-expressing microglial cells may provide targets for new stroke therapeutics.

Keywords: bioluminescence/biophotonic imaging; microglia; neuroinflammation; photothrombosis; stroke recovery; transgenic mice

4.2 INTRODUCTION

The evolution of brain injury after stroke and the subsequent recovery of lost brain function due to neuronal damage and neuronal dysfunction, encompass dynamic, complex, heterogeneous and interconnected processes (Endres et al., 2008; Wieloch and Nikolich, 2006), including brain inflammation (Iadecola and Anrather, 2011). These inflammatory events are triggered by the release of chemotactic compounds from the degenerating tissue in the infarct and from cells in the non-injured brain that participate in tissue repair and brain remodeling. This attracts blood-borne inflammatory cells to the injured tissue and activates resident glial cells, including microglia. The activation of microglial cells after stroke is prominent (Kempermann and Neumann, 2003; Kriz and Lalancette-Hébert, 2009; Iadecola and Anrather, 2011), and evident by a pronounced up-regulation of pathogen recognition receptors, such as Toll like receptors (TLRs) (Akira and Takeda, 2004; Ziegler et al., 2010; Lalancette-Hébert et al., 2009). TLRs are expressed by cells of the innate immune system to identify pathogen-associated molecular patterns (PAMPs), which are associated with microbial pathogens or cellular stress (Medzhitov et al., 1997), as well as damage-associated molecular patterns (DAMPs), recognized in processes associated with cell components released during cell damage, such as ischemic injury (Arumugam et al., 2009; Hanisch et al., 2008; Kariko et al., 2004). Recent evidence suggests that TLRs, especially Toll like receptor 2 (TLR2), may have a key role in the evolution of brain damage elicited by cerebral ischemia (Ziegler et al., 2007 and 2010; Lalancette-Hébert et al., 2009; Lehnardt et al., 2007; Tang et al., 2007; Babcock et al., 2006). At present, the spatio-temporal dynamics and the potential long-term role of the TLR2 response to brain damage is not well understood.

Multisensory stimulation by changes in the environment as well as task-driven experience induce brain remodeling and plasticity, in the normal (Draganski and May, 2008), as well as in the injured brain (van Praag et al., 2000; Nithianantharajah and Hannan, 2006; Johansson, 2011). Environmental enrichment refers to housing conditions that facilitate enhanced sensory, cognitive,

motor and social stimulation relative to standard conditions. Enriched housing of the rodents is a strong plasticity inducing agent that can restore lost functions following neurodegenerative disorders or brain damage, such as stroke (Ohlsson and Johansson, 1995; Nygren and Wieloch, 2005). Recently this intervention has been translated to the clinical setting (Janssen et al., 2012). The recovery-promoting effect of enriched housing can be initiated two days after ischemia, without affecting the final infarct volume (Ohlsson and Johansson, 1995). The mechanisms by which enriched housing influences recovery are still poorly understood, but recently it has been proposed to modulate central brain inflammation by depressing the levels of cytokines and chemokines (Ruscher et al., 2009 and 2013).

In order to investigate the spatio-temporal profile of the inflammatory response after photothrombotic stroke and the influence of multisensory stimulation provided by an enriched environment, we assessed the TLR2 response/microglial activation in the TLR2-luc/GFP-expressing mice. We took advantage of the minimally invasive *in vivo* biophotonic/bioluminescence imaging (Kriz and Lalancette-Hébert, 2009) which allows unique and simple longitudinal studies of brain inflammation (TLR2-luc expression) in the same animal for extended periods of time.

4.3 MATERIALS AND METHODS

4.3.1 Experimental animals

The transgenic TLR2sm-fluc-GFP mice were generated and characterized as previously described (Lalancette-Hébert et al., 2009). A total of 32 male TLR2 +/- mice, weighing 20-30 g and 2-4 months old, were used in the study. All animals were housed under a 12 h light/dark cycle with *ad libitum* access to food and water. Experimental procedures were approved by the Laval University Animal Care Ethics Committee and are in accordance with the *Guide to the Care and Use of Experimental Animals* of the Canadian Council on Animal Care.

4.3.2 Photothrombotic stroke

Mice were subjected to unilateral photothrombotic (PT) cortical infarct in the left sensori-motor cortex. During surgery, the body temperature of the animals was kept at 37°C using a self-regulating heating pad. Infarct was induced using a modified method initially described by Watson et al. (1985), and adapted for mice by Schroeter et al. (2002). Briefly, animals were anesthetized using 1.5-2.5% isoflurane (Sigma) in 100% O_2. The skin above the skull was incised; a fiber optic bundle with a 2.5 mm aperture diameter was connected to a cold light source (CL 1500 ECO, Zeiss, Germany) and adjusted to the stereotaxic coordinates of the sensori-motor cortex (Paxinos and Franklin, 2001), 0.5 mm anterior to bregma and 1.5 mm lateral to midline. One intraperitoneal (i.p.) injection of 0.25 ml Rose Bengal (10 mg/ml in 0.9% saline; Sigma-Aldrich, Germany) was given 5 min before the light was turned on for 20 minutes. Care was taken not to exceed 38°C at the skull surface, underneath the fiber optic bundle. Post-surgery, animals were allowed to awake from anesthesia while on a heating pad and returned to the cages with free access to food pellets and water. Temperature and body weight were recorded (Supplementary Table I). Control mice, after skin incision on the skull, were either subjected to Rose Bengal injection without subsequent illumination, or subjected to 20 minute illumination without dye injection. Out of the 32 animals entering the study, one animal spontaneously died at 24 hours of recovery.

4.3.3 *In vivo* bioluminescence imaging

The images were gathered using IVIS® 200 Imaging System (Xenogen, Alameda, CA, USA) as previously described (Lalancette-Hébert et al., 2009). Prior to the imaging session, the mice received an i.p. injection of the luciferase substrate D-luciferine (150 mg/kg, Xenogen), dissolved in 0.9% saline. The mice were then anesthetized with 2% isoflurane in 100% O_2 with a flow rate of 2 L/min and placed in a heated, light-tight imaging chamber. Images were collected with a high-sensitivity CCD camera. Exposure time for imaging was 2 minutes. The

bioluminescence emission was normalized and displayed in physical units of surface radiance (photons/sec/cm^2/sr). Light output was quantified by determining the total number of photons emitted per second with the use of Living Image 2.5 acquisition and imaging software (Xenogen). Region-of-interest (ROI) measurements on the images were used to convert surface radiance (photons/sec/ cm^2/sr) to source the total flux of photons in photons/second. The data are represented as pseudocolor images indicating light intensity (red and yellow, most intense), which were superimposed over gray-scale reference photographs. IVIS images were acquired for each animal, prior to stroke (baseline) and at day 1, 3, 6, 10 and 14 of recovery (Figure 1).

4.3.4 Behavioral assessment and randomization

Studies were subjected to randomization and carried out in a blinded fashion to the investigators who performed the surgeries and behavioral assessment.

Paw placement test: The mouse was held along its rostro-caudal extension on the edge of a bench and both the unilateral front and hind paws were gently pushed along it. The placement of each paw was recorded when the mouse was moved towards the edge (modified from De Ryck et al., 1989; Hunter et al., 2000). Sensori-motor dysfunction was assessed by using a score of 1, 0.5, and 0: (1) - the paw is immediately placed on the table surface; (0.5) - the limb is extended, but with some movements and attempts to place the paw on the surface of the table; (0) - the paw is totally immobilized, hanging down, with no movement. To obtain a neurological assessment during recovery, each mouse was tested at 2, 7 and 14 days after PT stroke.

In order to obtain groups with a similar functional deficit prior to placement of the mice into either standard or enriched cages, selective sorting was performed on day 2 after experimental stroke, a time point of recovery when the infarct development had subsided. Hence, only animals that showed a severe deficit in the paw placement (score = 0) entered the study (n = 14). After selective sorting,

mice were randomly distributed into standard (STD, 17 cm X 16 cm X 34.5 cm) or enriched cages (EE, 30 cm X 27 cm X 43 cm). Multilevel-enriched cages were equipped with various colored objects such as plastic tunnels, small houses, slides and rodent running wheels; the disposition of the objects was changed every second day (Nygren and Wieloch, 2005). Mice were housed in either standard n = 6 (2 animals/cage) or enriched cages n = 8 (5 animals/cage) for 12 days (Figure 1). Animals in standard cages were handled once a day.

4.3.5 Tissue collection

At 14 days after surgery, mice were anesthetized by an i.p. injection of chloral hydrate (150 mg/kg, concentration 10 mg/ml), and transcardially perfused with 0.9% saline followed by ice-cold phosphate-buffered 4% paraformaldehyde (PFA, Sigma) at pH 7.4. Tissue samples were post-fixed overnight in 4% PFA and equilibrated in phosphate-buffered 30% sucrose for 48 h at 4°C. The brains were then sectioned on a microtome at 30-µm thickness in the coronal plane. Sections were collected in 8 subsequent series and stored at -20°C in an antifreeze solution made in phosphate buffer containing 30% glycerol and 30% ethylene glycol.

4.3.6 Infarct volume measurements

For each animal, seven coronal brain sections with a distance of 1.0 mm were immunostained with the NeuN antibody (Neuronal Nuclei, Millipore, Hampshire, UK; dilution 1:1500). Infarcted areas, the non-lesioned area of the infarcted hemisphere and the non-lesioned contralateral hemisphere were outlined on each brain section using the ImageJ software (National Institute of Health, USA). Infarct volume (mm^3) was determined by subtracting the area of the non-lesioned ipsilateral hemisphere from that of the intact contralateral hemisphere, and calculated by volumetric integration for each animal (Swanson et al., 1990).

4.3.7 Immunohistochemistry

Free-floating brain slices were rinsed three times in PBS and quenched in 3% H_2O_2 and 10% MetOH for 15 minutes. After washing in PBS, the sections were blocked with blocking solution (5% normal donkey serum, Jackson ImmunoResearch, UK and 0.25% Triton X-100 in PBS) for one hour at room temperature. The sections were incubated overnight at 4°C with primary antibody (mouse anti-NeuN 1:1500, Millipore, Hampshire, UK; rabbit anti-YM1 1:600, Stem Cell Technologies, Vancouver, Canada) diluted in blocking solution. Following three rinses with 1% normal serum and 0.25% Triton X-100 in PBS, the sections were incubated with appropriate secondary biotinylated antibodies (donkey anti-mouse or anti-rabbit, Vector Laboratories, Burlingame, USA) at a dilution of 1:500 in blocking solution for 90 minutes at room temperature (RT). Visualization was achieved via the Vectorstain ABC kit (Vector) using 3,3-diaminobenzidine-tetrahydroklorid (DabSafe, Saveen Werner, Sweden), 8% NiCl and 3% H_2O_2. Bright field pictures were acquired using an Olympus BX60 microscope (Solna, Sweden).

4.3.8 Immunofluorescence

Free-floating brain slices were rinsed three times in PBS and blocked with blocking solution (5% normal donkey serum, Jackson ImmunoResearch, UK and 0.25% Triton X-100 in PBS) for one hour at room temperature. The sections were incubated overnight at 4°C with primary antibody (rabbit anti-Iba1 1:1000, Wako, Japan; rabbit anti-GFAP 1:2000, Dako, Danmark; mouse anti-NeuN 1:1500, Millipore, Hampshire, UK; rabbit anti-YM1 1:600, Stem Cell Technologies, Vancouver, Canada; rat anti-CD11b 1:50, AbD Serotec) diluted in blocking solution. Following three rinses with 2% normal serum and 0.25% Triton X-100 in PBS, the sections were incubated with appropriate secondary antibodies (donkey anti-mouse/rabbit/rat antibody) conjugated with either fluorescent dyes Cy3/Cy5 (Jackson ImmunoResearch, UK) and Alexa488/555 (Molecular Probes, Invitrogen, USA) at a dilution of 1:500 in blocking solution for 90 minutes at RT. Fluorescent

dyes were imaged using a confocal laser-scanning microscope (Zeiss LSM 510, Jena, Germany).

4.3.9 Cell counting

YM1 positive ($YM1^+$) cells were visualized by immunohistochemistry in bright field. A 10x magnification objective was used to draw the boundaries of the region of interest and to perform the actual cell counts by an investigator blinded to the group identity. We counted $YM1^+$ cells in the somatosensory cortex ipsilateral to the lesion (comprised between peri-infarct cortex and 3 mm from the top of the slice). Distances were defined using an optical grid. We used three coronal brain sections for each animal of the study (levels +0.98, +0.02 and -1.06 in relation to bregma, Paxinos and Franklin, 2001).

4.3.10 Statistical analysis

All data are presented as mean ± SEM, unless otherwise stated. Statistical analysis was performed with the Mann-Whitney *U*-test except for the cell counting, where the data were analyzed by a two-tailed unpaired Student's t-test. $P < 0.05$ was considered statistically significant. Data handling and statistical processing were performed using Microsoft Excel and GraphPad Prism Software.

4.4 RESULTS

4.4.1 Enriched housing enhances recovery of motor function after PT stroke in mice without affecting infarct size

The beneficial effect of enriched housing on brain function after experimental stroke in mice (Nygren and Wieloch, 2005) was confirmed in the present model of PT stroke. Two days after induction of PT in TLR2-luc/GFP mice, the animals were randomly sorted into either standard or enriched cages, and their motor performances assessed with the paw placement test at 7 and 14 days of recovery (Figure 2A). At day 2 of recovery, all standard and enriched animals had a clear

right fore- and hindpaw deficit, with a score of 0. At day 7 after stroke (5 days of differential housing), animals housed in enriched cages showed better performance compared to those housed under standard conditions, and the improvement became significant at 14 days of recovery ($P < 0.001$). The functional score of the right hindpaw did not improve. Function of left paws (ipsilateral to the lesion) were unaffected by the lesion. Also, no paw deficit was seen in sham-operated animals. Photothrombotic stroke caused tissue infarction to the ipsilateral cortex without affecting the subjacent striatum. Importantly, infarct volume at 14 days after PT was 8.6 ± 1.9 mm^3 in the standard housed animals and 8.0 ± 1.9 mm^3 in the enriched group, with no significant difference between the enriched and the standard groups (Figure 2B).

4.4.2 Real-time imaging reveals up-regulation of TLR2 in response to PT stroke

Changes in TLR2 expression, as a marker of the inflammatory response in the brain, were studied in TLR2-luc/GFP mice. Previous work (Lalancette-Hébert et al., 2009) demonstrated a significant increase in TLR2-luc signal after transient MCAO, which was remarkably up-regulated until three months after stroke. Our study shows, for the first time, an elevated TLR2 expression in mice subjected to PT stroke. A robust TLR2 biophotonic signal arising from the injured part of the brain was detected in all injured animals that entered the study. At 24 hours of recovery, real-time imaging revealed a significant up-regulation of TLR2 signal in response to PT in the ischemic lesion site compared to baseline ($P < 0.001$, Figure 3). No increase in TLR2 signal was observed in sham-operated animals (Supplementary Figure I).

4.4.3 Enriched housing attenuates the TLR2 response after stroke

To assess the significance of the TLR2 response after PT stroke, we investigated the effect of housing TLR2-luc/GFP mice in an enriched environment, and compared the TLR2 response of the brain at 3, 6, 10 and 14 days of recovery in mice housed either in standard or enriched conditions (Figure 4). In both groups,

the intensity of the Total Photon Emission signal peaked in the infarcted hemisphere at 24 hours after stroke, and decreased subsequently. For each time point after randomization of the animals into the different housing conditions (2 days of recovery), we found a lower TLR2 signal in enriched housed animals compared to those housed in standard conditions. Starting at 72 hours of recovery, the TLR2 response declined more rapidly in mice housed in enriched conditions, decreasing by 30-40% of that measured in standard housed animals. A significant difference between the standard and the enriched groups was observed at 6 and 14 days of recovery ($P < 0.05$).

4.4.4 TLR2-luc is expressed in microglia of different phenotype

The reporter mouse model used in this study co-expresses luciferase and GFP under transcriptional control of the murine TLR2 promoter, thus, to identify the cell types involved in TLR2 response, *in vivo* bioluminescence analysis was followed by double immunofluorescence microscopy. The TLR2 driven transgene GFP was co-localized with Iba1, a marker for microglial cells, but not with markers of astrocytes (GFAP) and neurons (NeuN) (Supplementary Figure II). In addition, we demonstrated that TLR2 driven transgene GFP is expressed in YM1-expressing microglia, with YM1 being a marker of alternatively activated microglia/macrophage (M/M) (Perego et al., 2011). Fourteen days after PT stroke, the immunoreactivity for YM1 was assessed in three brain coronal sections per mouse. In both experimental groups, YM1 immunoreactivity was evident in ameboid cells in the ischemic core and in the border zone. In the standard housing group, YM1 staining was also observed in ramified cells in both somato-sensory cortices ipsilateral and contralateral to the lesion. Importantly, YM1 expression was essentially undetectable outside the ischemic core and the lesion border in the animals housed in an enriched environment (Figure 5 and 6) and quantitative analysis of immuno-labeling revealed a significant decrease in YM1 immunoreactivity in the enriched housed group of animals compared with the standard one ($P < 0.01$). The YM1 marker is also co-expressed with CD11b, a marker of M/M activation and

recruitment, in the core of both groups of animals and in the somatosensory cortex of standard housed animals (Supplementary Figure III).

4.5 DISCUSSION

Our results revealed that: (1) the bioluminescent signal intensity/TLR2 response is up-regulated within 24 hours after permanent focal ischemia induced by photothrombotic stroke in the mouse brain and then declines over time (14 days) of recovery; (2) subsequently, within 24 hours of multisensory stimulation in an enriched environment, this TLR2 response declines more rapidly, to 30-40% of the one seen in standard housed animals; (3) the TLR2 response originates in the microglial population, including YM1 positive cells in both hemispheres.

The inflammatory response and the related microglial activation after ischemic damage play an important role in the evolution of brain injury and recovery of function after stroke (Iadecola and Anrather, 2011). We have earlier demonstrated that microglial activation after tMCAO is characterized by a marked long-term induction of TLR2 expression, suggesting an important role of TLR2 activation after stroke (Lalancette-Hébert et al., 2009; Bohacek et al., 2012). Microglial cells are the main effectors of the innate immune response in the brain and once activated express different TLRs (Nguyen et al., 2002), including TLR2 (Lehnardt et al., 2007; Bohacek et al., 2012) that interacts with endogenous stress signals such as heat shock proteins (Hsp60 and 70) or extracellular breakdown products of hyaluron lipoproteins (Asea, 2008). Also, NF-kB (nuclear factor kappa-light-chain-enhancer of activated B cells), which stimulates the expression of pro-inflammatory cytokines in response to PAMPs and DAMPs, is activated by TLR2 (Li et al., 2001), linking this receptor to the inflammatory response following brain injuries.

Still, the exact role of TLRs, especially TLR2, in brain injuries remains unclear. Previous studies employing TLR2 knockout mice suggest a detrimental role of TLR2 in cerebral ischemia (Lehnardt et al., 2007; Tang et al., 2007; Ziegler et al., 2007 and 2010), but analyses of TLR2 response using *in vivo* bioluminescence

imaging revealed a more intriguing sequence of events. TLR2 induction in microglia has been shown to serve as a modulator of brain inflammation (Lalancette-Hébert et al., 2009) and, in a recent study, Bohacek et al. suggested that TLR2-deficient mice subjected to experimental stroke exhibited an early reduction (up to 3 days after tMCAO) in microglial response that was associated with smaller lesions. However, later during recovery, this decrease in microglial activation led to increased neuronal apoptosis and delayed exacerbation of the ischemic lesion, suggesting that a balanced innate immune response is needed to limit the extent of neuronal damage after stroke (Bohacek et al., 2012).

Our results show, for the first time, a marked induction of TLR2 signal after focal cortical photothrombotic stroke that decreases with time during recovery, especially in mice housed in an enriched environment. In this context, the positive effects on recovery induced by enriched housing (Ruscher et al., 2009 and 2013) may by explain the decrease in TLR2 signal that we observe in enriched housed animals. This decrease in TLR2 signal reaches significance at 6 and 14 days of recovery, but a tendency is already seen after housing the animals in enriched environment for one day. These results are in accordance with previous studies, which propose an important pathophysiological role of TLR2 in the complex and dynamic post-ischemic cerebral inflammatory response (Lehnardt et al., 2007; Tang et al., 2007; Ziegler et al., 2007 and 2010).

The consistently decreasing TLR2 signal in the enriched-housed animals, measured at all recovery time points, is accompanied by better behavioral performance in this group compared to the standard one, which is evident at 7 days of recovery and becoming significant at 14 days post-stroke. This improvement, predominantly noticeable in the front paw, can be explained by the fact that the enriched-housed animals were probably more subjected to physical activity and experience driven re-learning (Wieloch and Nikolich, 2006; Pekna et al., 2012). Importantly, measurement of the infarct volume showed no significant differences between the enriched and the standard groups, suggesting that the

recovery-promoting effect of enriched housing investigated in our work was not dependent on the size of the infarct but on mechanisms of brain plasticity, at a time when the contribution of inflammation in acute cell death and development of infarction had subsided (Ruscher et al., 2013).

The strong sensori-motor stimulation provided by enriched housing conditions appears to mitigate the general inflammatory response after stroke, also decreasing the number of YM1-expressing microglia, a marker of alternatively activated microglia/macrophages. Here we demonstrate that the impact of environmental enrichment on the brain is still evident at 14 days after stroke and is affecting both hemispheres and, hence, also sites remote from the lesion. An extensive depression of the post-ischemic inflammatory response in mice housed in an enriched environment is in line with earlier results showing a depressed release of cytokines (Ruscher et al., 2009 and 2013) and chemokines (Ruscher et al., 2013).

The question that arises is what could explain the marked depression of microglial activation induced by enriched housing conditions? Previous studies suggest that rodents housed in an enriched environment are exposed to stress (Marashi et al., 2003) since they are subjected to more stimuli and diversity than rodents housed in standard cages. This presumably leads to intermittent hormonal activation and elevated basal corticosterone secretion that help the animals reacting appropriately to the environmental stimuli (Moncek et al., 2004). It has been also extensively shown that glucocorticoids (among which corticosterone) are potent suppressors of the immune response (Webster et al., 2002; Rogatsky and Ivashkiv, 2006), and several studies have indicated the important role of the antigen-presenting cells (APCs) in glucocorticoid-mediated suppression of immunity (Anders et al., 2004; Vieira et al., 1998; Truckenmiller et al., 2005). One explanation could be that environmental enrichment triggers a stress-induced depression of the inflammatory signaling that can be ascribed to the microglial populations, the most potent APCs in the central nervous system. This may then induce a strong shift towards a very

general anti-inflammatory signaling, that could depress the number of TLR2-expressing microglial cells of different phenotype. Alternatively, microglia is deactivated through direct signaling from neural networks stimulated by the multisensory activation of the brain provided by the enriched environment. One possibility is dopamine signaling since levodopa treatment is known to support recovery of stroke patients and, in experimental stroke, attenuates post-ischemic inflammation (Ruscher et al., 2012 a and b).

4.6 CONCLUSIONS

In conclusion, this study reports that the multisensory stimulation provided by enriched housing conditions attenuates the general inflammatory response after stroke reducing the level of the TLR2 signal induction and leading to improved neurological outcome. The TLR2 receptor on microglia may be part of a signaling network that modulates the brain inflammatory response and influences the recovery of neurological function lost after stroke. Understanding the regulation of inflammation elicited by TLR2 receptors after stroke may contribute to the development of new therapeutic strategies that improve recovery in stroke patients.

4.7 Acknowledgments

We thank Carin Sjölund, Kerstin Beirup and Yuan Cheng Weng for excellent technical assistance. This study was supported by the Swedish Research Council (grant No. 2011-2652, TW), the EU 7th work program through the European Stroke Network (grant No. 201024, TW), the Canadian Stroke Network grant (CSN/ESN Initiative, JK), the Swedish Brain Fund (TW) and the Hans-Christian and Alice Wachtmeister Foundation (TW).

4.8 References

Akira S, Takeda K. Toll-like receptor signaling. *Nat Rev Immunol*. 2004;4:499-511.

Anders EP, Monika G, Mark RW, Mogens HC. Induction of regulatory dendritic cells by dexamethasone and 1α, 25-dihydroxyvitamin D3. *Immunol Lett*. 2004;91:63-69.

Arumugam TV, Okun E, Tang SC, Thundyil J, Taylor SM, Woodruff TM. Toll-like receptors in ischemia-reperfusion injury. *Shock*. 2009;32:4-16.

Asea A. Heat shock proteins and Toll-like receptors. *Handb Exp Pharmacol*. 2008;111-127.

Babcock AA, Wirenfeldt M, Holm T, Nielsen HH, Dissing-Olesen L, Toft-Hansen H, et al. Toll-like receptor 2 signaling in response to brain injury: an innate bridge to neuroinflammation. *J Neurosci*. 2006;26:12826-12837.

Bohacek I, Cordeau P, Lalancette-Hébert M, Gorup D, Weng YC, Gajovic S, et al. Toll-like receptor 2 deficiency leads to delayed exacerbation of ischemic injury. *J Neuroinflammation*. 2012;9:191.

De Ryck M, Van Reempts J, Borgers M, Wauquier A, Janssen P. Photochemical stroke model: Flunarizine prevents sensorimotor deficits after neocortical infarcts in rats. *Stroke*. 1989;20:1383-1390.

Draganski B, May A. Training-induced structural changes in the adult human brain. *Behav Brain Res*. 2008;192:137-142.

Endres M, Engelhardt B, Koistinaho J, Lindvall O, Meairs S, Mohr JP, et al. Improving outcome after stroke: overcoming the translational roadblock. *Cerebrovasc Dis*. 2008;25:268-278.

Hanisch UK, Johnson TV, Kipnis J. Toll-like receptors: roles in neuroprotection? *Trends Neurosci*. 2008;31:176-182.

Hunter AJ, Hatcher J, Virley D, Irving E, Hadingham SJ, Parsons AA. Functional assessments in mice and rats after focal stroke. *Neuropharmacology*. 2000;39:806-816.

Iadecola C, Anrather J. Stroke research at a crossroad: asking the brain for directions. *Nat Neurosci*. 2011;14:1363-1368.

Janssen H, Ada L, Karayanidis F, Drysdale K, McElduff P, Pollack M, et al. Translating the use of an enriched environment post stroke from bench to bedside: study design and protocol used to test the feasibility of environmental enrichment on stroke patients in rehabilitation. *Int J stroke*. 2012;7:521-526.

Johansson BB. Current trends in stroke rehabilitation. A review with focus on brain plasticity. *Acta Neurol Scand*. 2011;123:147-159.

Kariko K, Weissman D, Welsh FA. Inhibition of Toll-like receptor and cytokine signaling - a unifying theme in ischemic tolerance. *J Cereb Blood Flow Metab*. 2004;24:1288-1304.

Kempermann G, Neumann H. Microglia: the enemy within? *Science*. 2003;302:1689-1690.

Kriz J, Lalancette-Hébert M. Inflammation, plasticity and real-time imaging after cerebral ischemia. *Acta Neuropathol*. 2009;117:497-509.

Lalancette-Hébert M, Phaneuf D, Soucy G, Weng YC, Kriz J. Live imaging of Toll-like receptor 2 response in cerebral ischaemia reveals a role of olfactory bulb microglia as modulators of inflammation. *Brain*. 2009;132:940-954.

Lehnardt S, Lehrmann S, Kaul D, Tschimmel K, Hoffmann O, Cho S, et al. Toll-like receptor 2 mediates CNS injury in focal cerebral ischemia. *J Neuroim*. 2007;190:28-33.

Li M, Carpio DF, Zheng Y, Bruzzo P, Singh V, Ouaaz F, et al. An essential role of the NF-kappa B/Toll-like receptor pathway in induction of inflammatory and tissue-repair gene expression by necrotic cells. *J Immunol*. 2001;166: 7128-35.

Nguyen MD, Julien JP, Rivest S. Innate immunity: the missing link in neuroprotection and neurodegeneration? *Nat Rev Neurosci*. 2002;3:216-227.

Marashi V, Barnekow A, Ossendorf E, Sachser N. Effects of different forms of environmental enrichment on behavioral, endocrinological and immunological parameters in male mice. *Horm Behav*. 2003;43:281-292.

Medzhitov R, Preston-Hurlburt P, Janeway CA Jr. A human homologue of the Drosophila Toll protein signals activation of adaptive immunity. *Nature*. 1997;388:394-397.

Moncek F, Duncko R, Johansson BB, Jezova D. Effect of environmental enrichment on stress related systems in rats. *J Neuroendocrinol*. 2004;16:423-431.

Nithianantharajah J, Hannan AJ. Enriched environments, experience-dependent plasticity and disorders of the nervous system. *Nat Rev Neurosci*. 2006;7:697-709.

Nygren J, Wieloch T. Enriched environment enhances recovery of motor function after focal ischemia in mice and downregulates the transcription factor NGFI-A. *J Cereb Blood Flow Metab*. 2005;25:1625-1633.

Ohlsson AL, Johansson BB. Environment influences functional outcome of cerebral infarction in rats. *Stroke*. 1995;26:644-649.

Paxinos G, Franklin KBJ. The mouse brain. Second edition. Academic Press, 2001.

Pekna M, Pekny M, Nilsson M. Modulation of neural plasticity as a basis for stroke rehabilitation. *Stroke*. 2012;43:2819-2828.

Perego C, Fumagalli S, De Simoni MG. Temporal pattern of expression and colocalization of microglia/macrophage phenotype markers following brain ischemic injury in mice. *J Neuroinflammation*. 2011;8:174.

Rogatsky I, Ivashkiv LB. Glucocorticoid modulation of cytokine signaling. *Tissue Antigens*. 2006;68:1-12.

Ruscher K, Johannesson E, Brugiere E, Erickson A, Rickhag M, Wieloch T. Enriched environment reduces apolipoprotein E (ApoE) in reactive astrocytes and attenuates inflammation of the peri-infarct tissue after experimental stroke. *J Cereb Blood Flow Metab*. 2009;29:1796-1805.

Ruscher K, Kuric E, Wieloch T. Levodopa treatment improves functional recovery after experimental stroke. *Stroke*. 2012a;43:507-513.

Ruscher K, Kuric E, Wieloch T. Levodopa treatment attenuates inflammation and improves functional recovery after experimental stroke. *Stroke*. 2012b;43:e132-e132.

Ruscher K, Kuric E, Liu Y, Walter HL, Issazadeh-Navikas S, Englund E, et al. Inhibition of CXCL12 signaling attenuates the post ischemic immune response and improves functional recovery after stroke. *J Cereb Blood Flow Metab*. 2013;33:1225-1234.

Schroeter M, Jander S, Stoll G. Non-invasive induction of focal cerebral ischemia in mice by photothrombosis of cortical microvessels: characterization of inflammatory responses. *J Neurosci Methods*. 2002;1:43-49.

Swanson RA, Morton MT, Tsao-Wu G, Savalos RA, Davidson C, Sharp FR. A semiautomated method for measuring brain infarct volume. *J Cereb Blood Flow Metab*. 1990;10:290-293.

Tang SC, Arumugam TV, Xu X, Cheng A, Mughal MR, Jo DG, et al. Pivotal role for neuronal Toll-like receptors in ischemic brain injury and functional deficits. *Proc Natl Acad Sci U S A*. 2007;104:13798-13803.

Truckenmiller ME, Princiotta MF, Norbury CC, Bonneau RH. Corticosterone impairs MHC class I antigen presentation by dendritic cells via reduction of peptide generation. *J Neuroimmunol*. 2005;160:48-60.

Van Praag H, Kempermann G, Gage FH. Neural consequences of environmental enrichment. *Nat Rev Neurosci*. 2000;1:191-198.

Vieira PL, Kalinski P, Wierenga EA, Kapsenberg ML, de Jong EC. Glucocorticoids inhibit bioactive IL-12p70 production by in vitro-generated human dendritic cells without affecting their T cell stimulatory potential. *J Immunol*. 1998;161:5245-51.

Watson, BD, Dietrich WD, Busto R, Wachtel MS, Ginsberg MD. Induction of reproducible brain infarction by photochemically initiated thrombosis. *Ann Neurol*. 1985;17:497-504.

Webster JI, Tonelli L, Sternberg EM. Neuroendocrine regulation of immunity. *Annu Rev Immunol*. 2002;20:125-163.

Wieloch T, Nikolich K. Mechanisms of neural plasticity following brain injury. *Curr Opin Neurobiol*. 2006;16:258-264.

Ziegler G, Harhausen D, Schepers C, Hoffmann O, Röhr C, Prinz V, et al. TLR2 has a detrimental role in mouse transient focal cerebral ischemia. *Biochem Biophys Res Commun*. 2007;359:574-579.

Ziegler G, Freyer D, Harhausen D, Khojasteh U, Nietfeld W, Trendelenburg G. Blocking TLR2 in vivo protects against accumulation of inflammatory cells and neuronal injury in experimental stroke. *J Cereb Blood Flow Metab*. 2010;31:757-766.

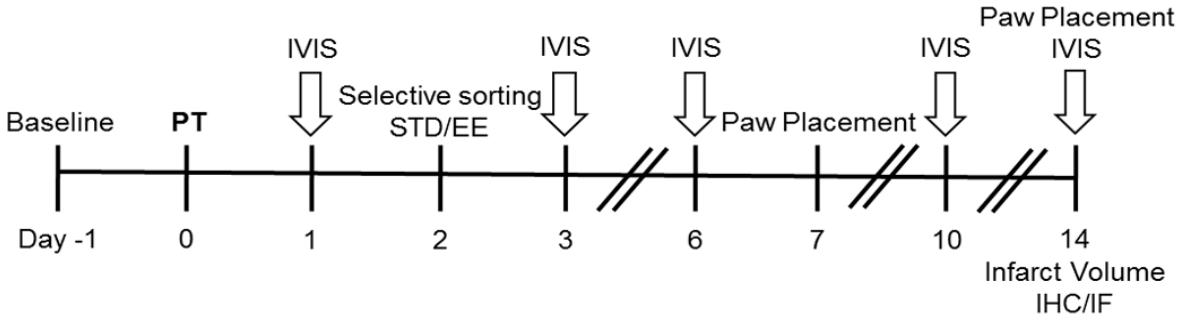

Figure 1. Experimental design. Transgenic TLR2sm-fluc-GFP mice were subjected to photothrombotic stroke. Two days later, neurological deficit was evaluated by the paw placement test and only animals with a test score of 0 were randomized in either standard or enriched groups. IVIS images were acquired, for each animal, prior to stroke and on day 1, 3, 6, 10 and 14 of recovery. At 7 and 14 days after stroke, paw placement was assessed. Mice were then perfused and brains processed for histological analysis. PT = photothrombotic stroke; IVIS = *in vivo* bioluminescence imaging; IHC/IF = immunohistochemistry and immunofluorescence; STD = standard housing; EE = enriched housing.

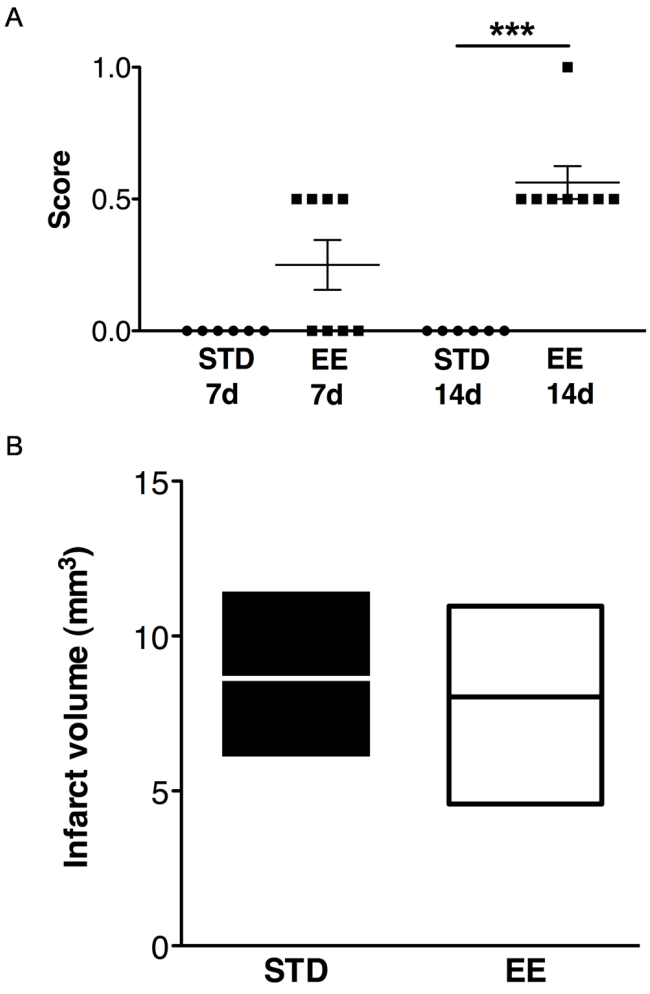

Figure 2. **Effect of enriched environment on functional recovery and infarct volume**. (A) Mice sensori-motor score obtained with the paw placement test. Individual data points are included (14 days, $P < 0.001$). (B) Infarct volumes of standard and enriched animals at 14 days of recovery. Data are presented as mean and floating bars (minimun to maximum). No significant difference in infarct size was seen between the groups. STD = standard housing; EE = enriched housing.

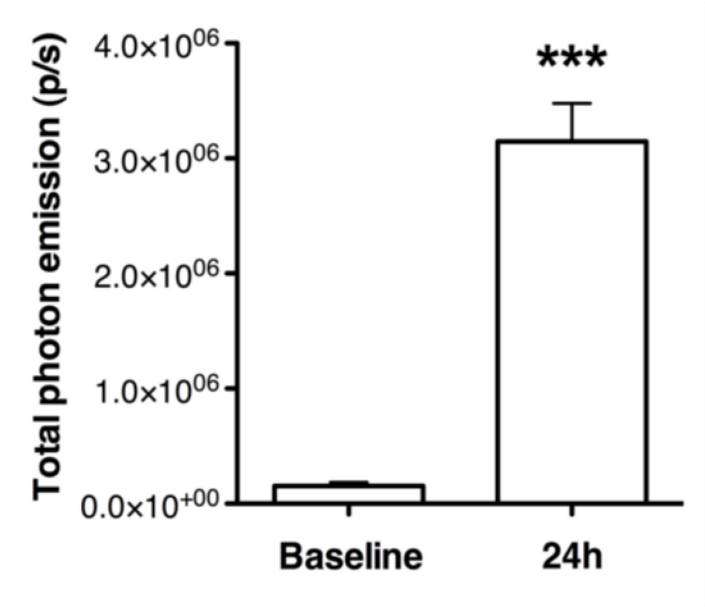

Figure 3. **Up-regulation of Toll-like receptor 2 in response to photothrombotic stroke**. Real time imaging of TLR2 bioluminescent response at 24 hours of recovery reveals a strong up-regulation of Toll-like receptor 2 in response to photothrombosis in the ischemic lesion site compared to the relative baseline ($P < 0.001$).

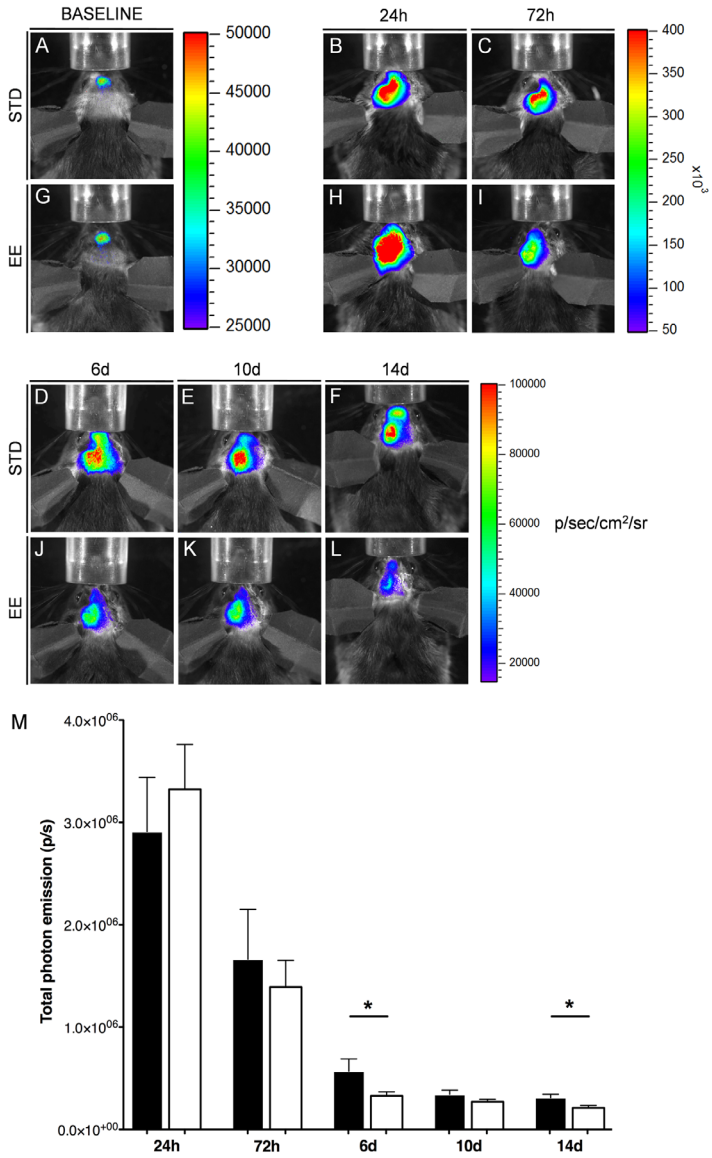

Figure 4. Real-time bioluminescent TLR2 signals after photothrombotic stroke. Representative images of standard (A-F) and enriched (G-L) TLR2-luc mice imaged prior to stroke and at 24, 72 hours, 6, 10 and 14 days of recovery. The images were progressively recorded from the same experimental animal and reveal the dynamics of TLR2 activation throughout the entire duration of the experiment. Scales on the right are the color maps for photon counts. (M) Quantification of luciferase signals revealed a consistent lower TLR2 signal induction in enriched-housed animals after selective sorting (day 2) compared to standard-housed animals (6 and 14 days, $P < 0.05$; black columns = standard housed mice, white columns = enriched housed mice).

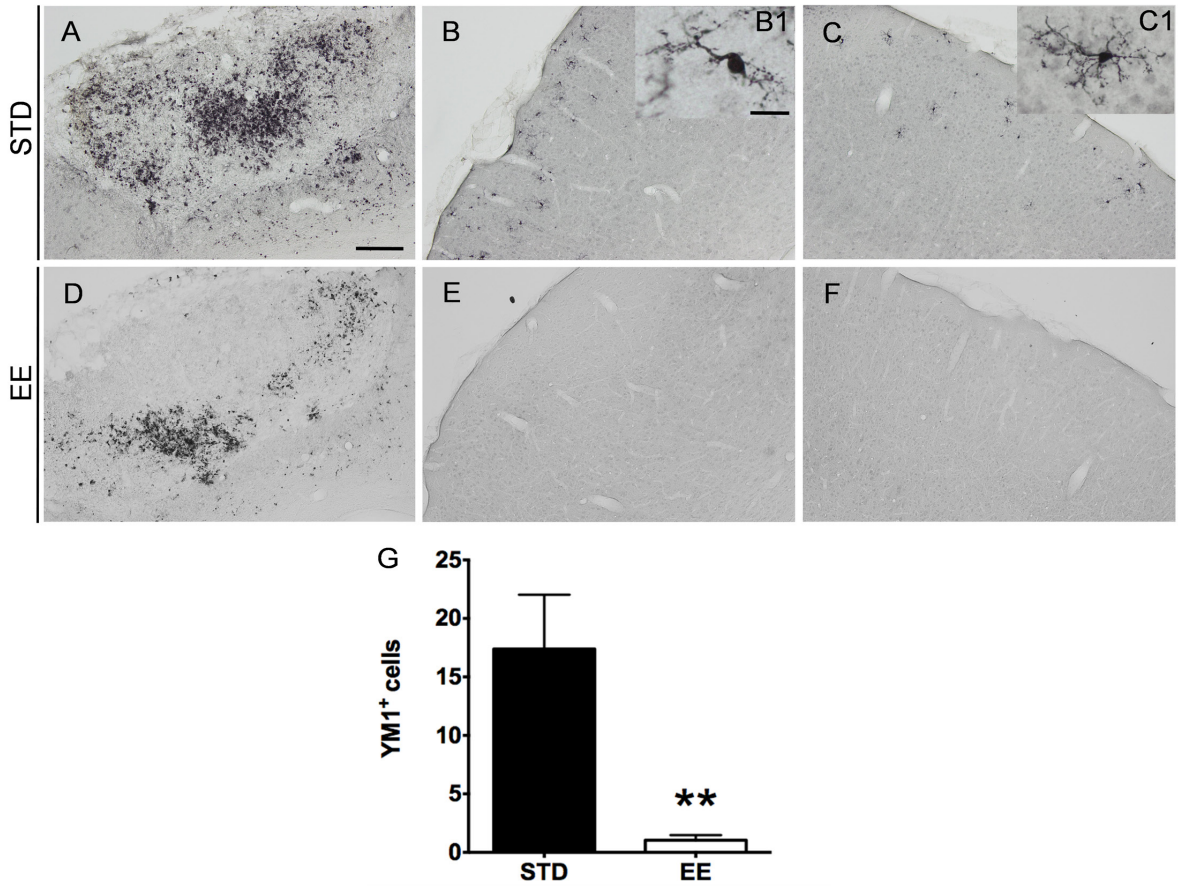

Figure 5. YM1 expression in the mouse cerebral cortex is sensitive to multisensory stimulation provided by EE. (A-F) Representative bright-field micrographs of YM1 immunoreactivity in (A and D) infarct core, (B and E) somatosensory cortex ipsilateral to the lesion, (C and F) somatosensory cortex contralateral to the lesion, scale bar: 100 µm; (B1 and C1) higher magnification, scale bar: 20 µm. (G) Quantitative analysis of YM1 positive cells in the ipsilateral somatosensory cortex revealed a significant decrease in the number of cells in the enriched group of animals compared to the standard group ($P < 0.01$). STD = standard housed mouse; EE = enriched housed mouse.

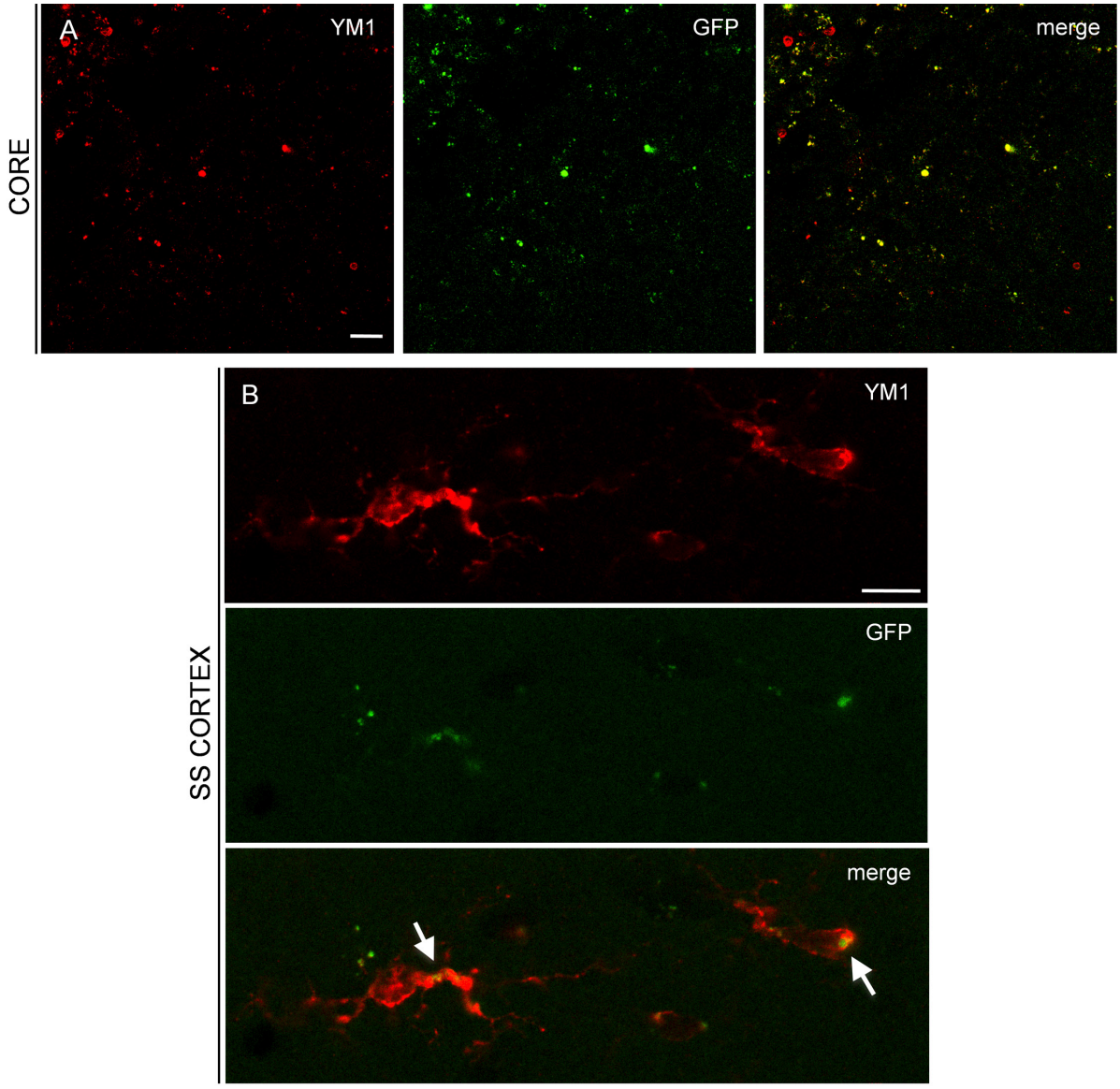

Figure 6. YM1-expressing microglia co-localize with TLR2. Co-localization of YM1-expressing cells (Cy3, red) with TLR2 (GFP, green) in the infarct core (A) and in the somatosensory cortex (B). Confocal images (A) scale bar 20 μm; (B) scale bar 10 μm. CORE = infarct core; SS CORTEX = somatosensory cortex.

SUPPLEMENTARY DATA

Parameters	Time point	Standard	Enriched
Temperature (°C)	0 min[a]	34.8 ± 0.7	35.3 ± 0.8
Body weight (g)[*]	Before[b]	27.5 ± 2.6	24.5 ± 2.4
Body weight (g)[*]	Day 14[a]	25.6 ± 1.9	23.1 ± 1.6

Supplementary Table I. Temperature and body weight of TLR2-luc mice subjected to photothrombotic stroke (PT). Data are presented as mean ± standard deviation. [a]After PT, [b]before PT, [*]statistical difference between the groups, Student's t-test.

SUPPLEMENTARY FIGURE CAPTIONS

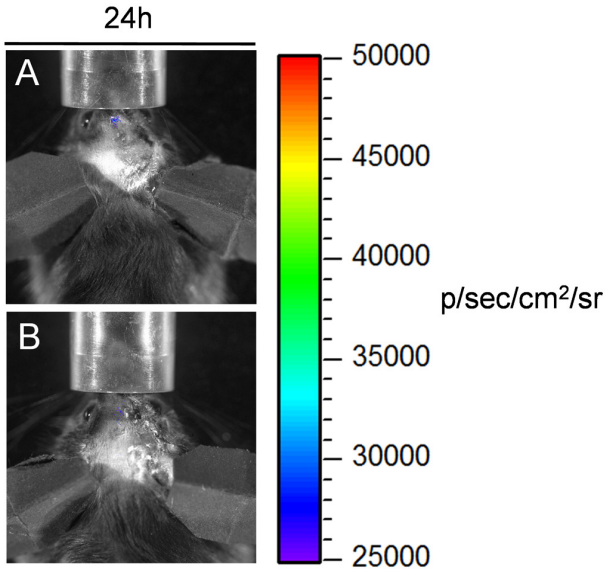

Supplementary Figure I. Real-time imaging visualization of bioluminescent TLR2 signal in sham animals 24 hours after surgery. (A) Sham animal subjected to Rose Bengal injection and no illumination (B) Sham animal subjected to illumination but not to Rose Bengal injection.

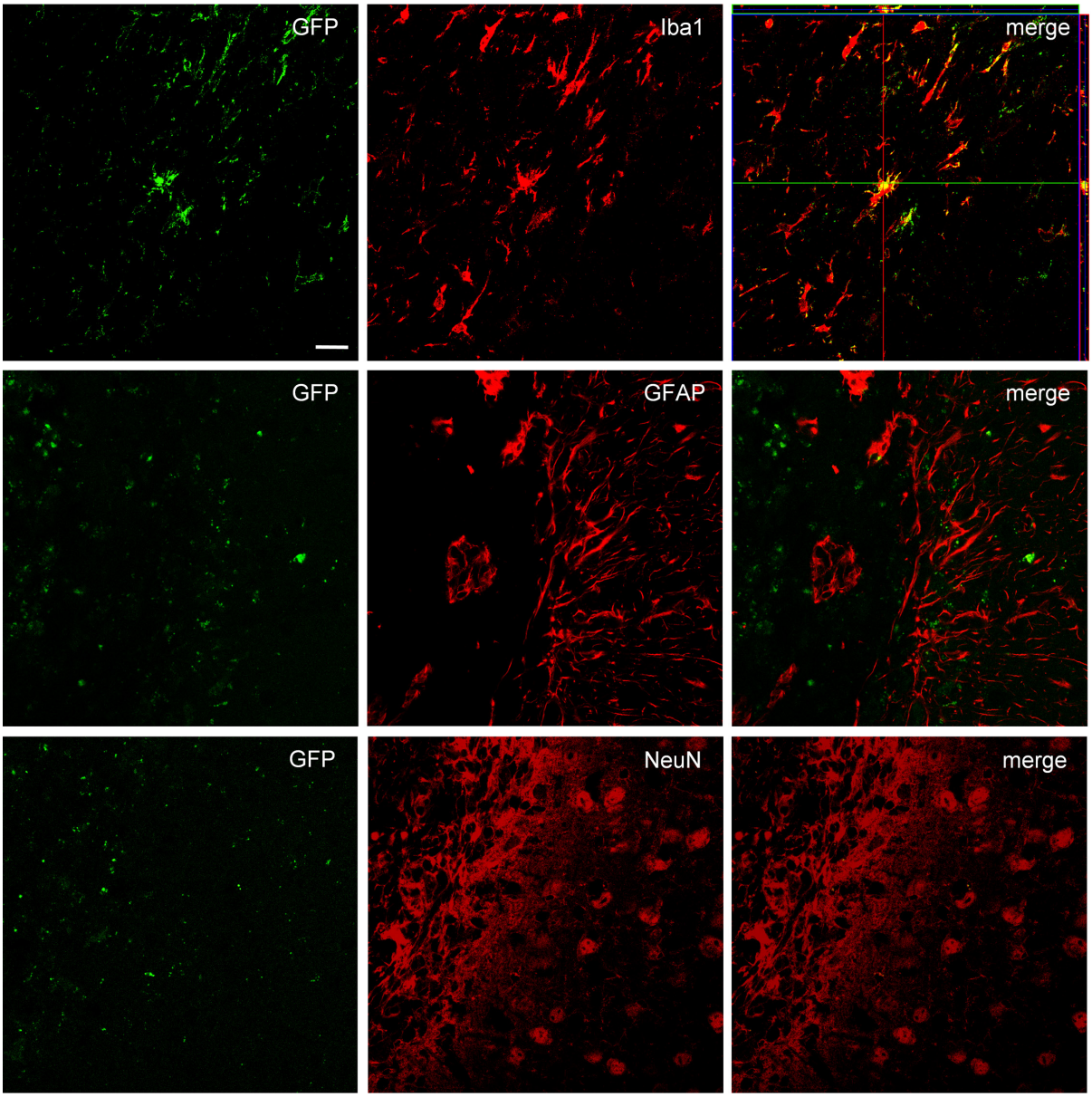

Supplementary Figure II. TLR2 expression occurs predominantly in microglial cells. Co-localization of Iba1 (Cy3, red) with TLR2 (GFP, green). No co-localization has been observed between TLR2 (GFP, green) and GFAP/NeuN (Cy3, red). Confocal images with scale bar 20 μm.

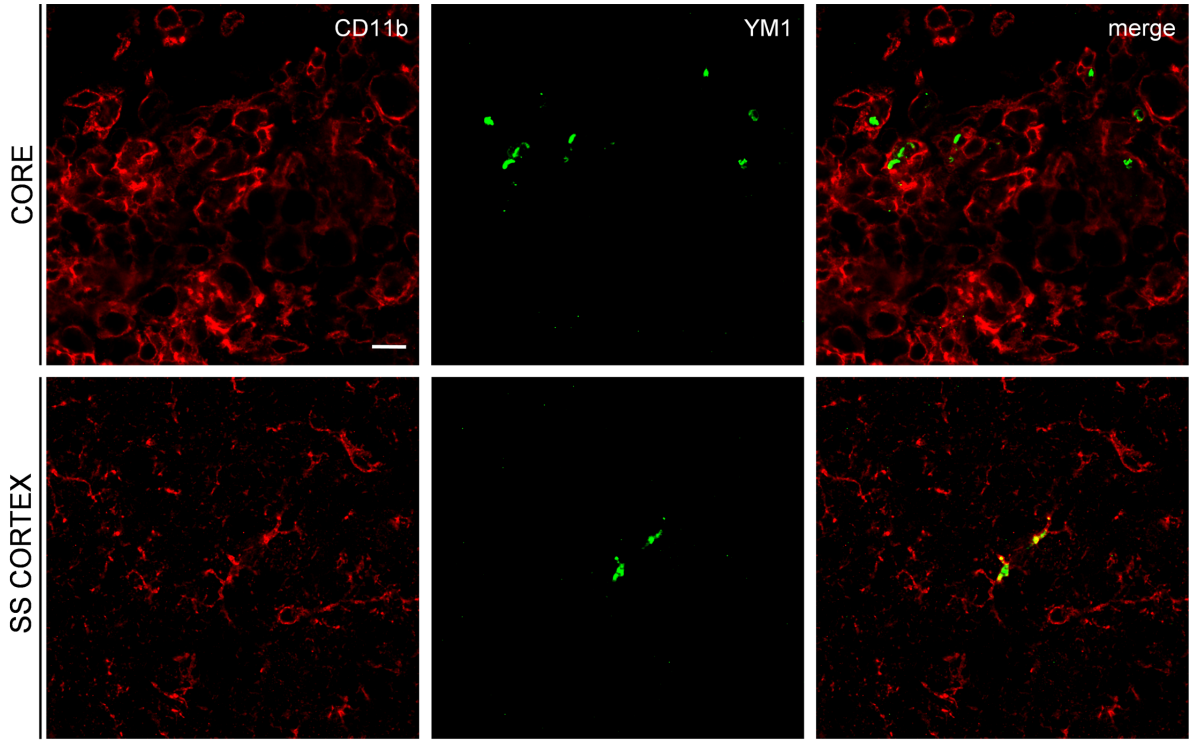

Supplementary Figure III. YM1 is co-expressed with the CD11b marker after PT. YM1 positive cells (CY5, green) co-label with the CD11b marker (Alexa Fluor 555, red) of activated/recruited microglia/macrophages in both phagocytic-like cells in the core and in ramified-like cells of the somatosensory cortex. Confocal images with scale bar 20 μm.

Chapitre 5. Estrogen receptors alpha mediates post-ischemic inflammation in chronically oestrogen- deprived mice.

Contributions des auteurs dans l'article: Estrogen receptors alpha mediates post-ischemic inflammation in chronically oestrogen- deprived mice.

Pierre Cordeau a conçu, effectuer les expériences et écrit le manuscrit.

Mélanie Hébert-Lalancette a écrit le manuscrit.

Yuan-Cheng Weng a effectué les chirurgies.

Jasna Kriz a coordonné et conçu l'étude en plus d'apporter des correctifs au manuscrit.

Estrogen receptors alpha mediates post-ischemic inflammation in chronically oestrogen- deprived mice.

Running title: Oestrogen deprivation affects the innate immune response.

This work was supported by the Canadian Institutes of Health Research (CIHR). P. Cordeau is recipients of the CIHR Canada Doctoral Scholarships.

Pierre Cordeau Jr, Yuan Cheng Weng and Jasna Kriz.

Department of Psychiatry and Neuroscience, Laval University, Centre de Recherche du Centre Hospitalier de l'Université Laval, 2705 boulevard Laurier, Québec, QC, G1V 4G2, CANADA.

Corresponding Author

Jasna Kriz, MD, PhD

TEL: (418) 654-2296 # 46308

Fax: (418) 654-2761

E-mail: Jasna.Kriz@crchul.ulaval.ca

5.1 ABSTRACT

The incidence of stroke increases substantially following menopause with women having worst outcome than men after stroke. While it has been well established that neuroprotective and/or anti-inflammatory effects of estrogen after stroke are mediated by its receptors, notably estrogen receptor alpha (ERα), at present, little is known on how post-ischemic inflammatory response is regulated after menopause. Here we investigated the role of ER in inflammation and microglia activation/innate immune response in ischemic brains of chronically estrogen deprived mice. By using *in vivo* bioluminescence/ biophotonic imaging and Toll like receptor-2 (TLR2) reporter mice, in chronically ovariectomized female mice, we found significantly increased levels of TLR-2 signals in baseline conditions as well as after stroke, increased microglial activation and larger infarctions. Next, because evidence suggests decreased expression levels/function of ERα in aged female brains, the TLR2 reporter mice were derived in ERα knockout background. To our surprise, the *in vivo* imaging analysis revealed that after stroke the TLR2 response was blunted in ERα knockout mice. Analysis of the pro- and anti-inflammatory cytokine profiles revealed selective, 5.7-fold increase in levels of IL-6 and 4.7-fold increase pSTAT3 suggesting an over-activation of JAK/STAT3 pathway and larger infractions in ERα knockouts chronically deprived of estrogen. Taken together, our results suggest that in estrogen deprived mice, ERα is involved in regulation of innate immune response and ischemic- injury induced production of IL-6. Based on our results, we propose that loss of functional ERα, observed during aging, may additionally contribute to increased vulnerability to ischemic injury in aged females.

5.2 INTRODUCTION

To date, studies have clearly demonstrated difference on stroke outcome between genders (Cordeau, 2008, Wise, 2007, Gibson, 2013). In fact, women are less vulnerable to stroke when their level of oestrogen are elevated. Interestingly

however, this gender effect is completely reverted after menopause. Namely, the incidence of stroke increases substantially following menopause with women having worst outcome for stroke than men. Moreover, while it has been widely established that increased immune response is prominent feature of aging in both genders, recent evidence suggest proportionally higher activation of immune related genes in female brain (Berchtold, 2008). Estrogens are well known to exert neuroprotective as well as immune-modulatory effects. The effects of estrogen are mediated through estrogen receptors ERα and ERβ, both widely distributed through various tissues and organs including brain. As previously reported, ERs are expressed in many cell types including microglial cells. Previous work clearly demonstrated that in different experimental models (in *in vitro* and *in vivo* conditions) inflammatory response and activation of microglial cells can be modulated via ERα and ERβ (Vegeto, 2003, Ghisletti, 2005, Baker, 2004, Wu, 2013). While incidence of stroke increases with aging, at present little is known about the role of ERs in the brain response to ischemic injury in aged female brains and in the context of menopause. Evidence suggests that ERα expression and /or function is decreased with aging. Namely, Ishunina and colleagues (Ishunina, 2008, 2009) reported that elderly women show increased expression of the ERα splice variants that act as dominant negative regulators of the ERα mediated transcriptional activation and function, thus suggesting a loss of receptor function with advanced age. Given its well established neuroprotective role in physiological condition, the described progressive decline/loss of function of ERα in concert with increased expression of pro-inflammatory genes in aged female brains, may represent an additional risk factor for increased vulnerability following stroke.

Cerebral ischemia is associated with the strong inflammatory and glial responses that may contribute to neuronal damage and/or provide a trophic support (Kriz, 2009, Iadecola, 2011, Kamel, 2012). Using live imaging approach, we previously showed the effects of estrogens and gender on neuroinflammation after stroke (Cordeau, 2008). In the present study, we investigated how ischemic-injury induced microglial activation and innate immune response are regulated in the mouse model of menopause and aging. To do this, we took advantage of

transgenic mouse model, a TLR2-luc-GFP reporter model developed earlier in our laboratory (Lalancette-Hebert, 2009). In this model, microglial activation and innate immune response can be visualized in real time from the brains of live mice using *in vivo* bioluminescence/biophotonic imaging. Using this model, we visualized in real time the effects of oestrogen deficiency and the absence of ERα on microglial activation after cerebral ischemia. We report here that chronic estrogen deprivation markedly increases microglial activation profile and the innate immune responses (TLR signals) before and after stroke. To our surprise the absence of Erα in chronically ovariectomized females blunted innate immune responses. However, the observed attenuation of the TLR2 response in chronically estrogen deprived females was associated with distinct pro-inflammatory cytokine profile, a selective hyperexpression of IL-6 and over activation of JAK/STAT3 pathway leading to a further increase in the size of ischemic lesion.

5.3 MATERIAL AND METHODS

5.3.1 Generation of transgenic mice and genotyping

The transgenic TLR2-luc/GFP mice derived in C57BL/6 background were used as described (Lalancette-Hebert, 2009). Transgenic animals were identified by PCR detection of luciferase. The genotyping was performed as previously described (Lalancette-Hebert, 2009). To derive double transgenic colonies as a first step the TLR2-luc/GFP mice were then crossed with an oestrogen receptor alpha heterozygous mouse and in the second step of breeding we obtained the TLR2-luc/GFP mice in ERα KO background (Jackson Laboratory, strain name: B6.129P2-Esr1^{tm1Ksk}/J).

5.3.2 Surgical procedures:

Ovariectomy

As previously described (Cordeau, 2008) 2 month old transgenic female mice were anesthetized with 2 % isoflurane in 100 % oxygen at a flow rate of 2 L/min. Under anesthesia both flanks of the animal were shaved prior to incision. A 5mm, dorsal/ventral incision was made through the skin, the ovarian fat pad was located and the ovaries were removed bilaterally.

Middle cerebral artery occlusion

As previously described, the unilateral transient focal cerebral ischemia was induced by intraluminal filament occlusion of the left middle cerebral artery (MCAO) during 1 hour followed by a reperfusion period of 48 hours or 7 days (Lalancette-Hebert, 2007, 2011, 2012). The surgery was carried out on 2-4 months old females TLR2-Luc-GFP; Erα^{KO} and their wild-type (C57BL/6) littermates. The animals were anesthetized with 2 % isoflurane in 100 % oxygen at a flow rate of 2 L/min. To avoid cooling, the body temperature was regularly checked and maintained at 37ºC with a heating pad. All experimental procedures were approved by the Laval University animal care ethics committee and are in accordance with The Guide to the Care and Use of Experimental Animals of the Canadian Council on Animal Care.

5.3.3 Vaginal smears and hormone detection

As previously described, to avoid the effects of physiological fluctuation of estrogen levels on inflammatory response we regularly controlled the vaginal smears (Cordeau, 2008). The vaginal epithelial cells were obtained from mice and smeared onto cleaned slides. Slides were then evaluated for the presence of white blood cells and the morphology of epithelial cells to determine the stage of the oestrus cycle. For the female control group, they were cycled to perform the MCAO at the end of the diestrus period

5.3.4 *In vivo* bioluminescence imaging

The images were gathered using IVIS 200 Imaging System (Xenogen, Alameda, CA, USA). Prior to imaging session, the mice received intraperitoneal (i.p.) injection of D-luciferine, a luciferase substrate (150 mg/kg, Xenogen, Alameda, CA, USA) dissolved in 0.9 % saline. The mice were then anaesthetized with 2 % isoflurane in 100 % oxygen at a flow rate of 2 L/min and placed in the heated, light-tight imaging chamber. Images were collected using high sensitivity CCD camera with wavelengths ranging from 300-600 nm. Exposition time for imaging was 2 minutes using the smallest field of views and f/1 lens aperture. As previously described, bioluminescence emission was normalized and displayed in physical units of surface radiance, photons per second per centimeter squared per steradian (photons/sec/cm2/sr) (Lalancette-Hebert, 2009, Cordeau, 2008, 2012). The data were represented as pseudo-color images indicating light intensity (red and yellow, most intense), which were superimposed over grayscale reference photographs.

5.3.5 Tissue collection

The animals were anesthetised via an i.p. injection of 0.1ml/10g of ketamine (10mg/ml) /xylazine(1mg/ml) and transcardially perfused with 30 ml of 0.9% NaCl, followed by PBS 1X buffered 4% PFA at pH 7.4. Tissue sample were then postfixed overnight in 4% PFA and equilibrated in phosphate-buffered 30% sucrose for 48 hours. Brains were embedded into Tissue-Tek (O.C.T. compound, Sakura, USA) and freeze at -20°C and cut into coronal section with a Cryostat (25 µm thick) and store at -20°C.

5.3.6 Size of Infarct

For measurements of the lesion size, WT littermate and transgenic mice were anaesthetized 48 hours after the tMCAO. The brains were then removed from the skull, cut in 1 mm thick slices and stained with 2,3,5-phenyltetrazolium chloride (TTC) (Lalancette-Hebert, 2007, 2012). The infarct volume was calculated for each

section of brain and quantified by using the Scion Image program (Scion Corporation). 3-4 mice were used for each experimental group.

5.3.7 Cytokine array

The protein expression analysis of inflammatory cytokines was performed with a mouse antibody array (RaybioMouse inflammation antibody array 1; catalog #AAM-INF-1-4; RayBiotech, Norcross, GA). Protein lysates were obtained by homogenization of brains of control and transgenic mice in 1x cell lysis buffer (included in the RayBiotech kit) with protease-inhibitor mixture (#P8340; Sigma). The protein concentration was determined for each sample and diluted at 300 µg in 1x blocking buffer. Samples for each group (three mice/group) were pooled and incubated with the array membrane overnight at 4°C. After washes, the membranes were incubated with the biotin-conjugated antibodies overnight at 4°C. The membranes were then processed according to RayBiotech protocol. Membranes were exposed to x-ray film (Biomax MR1; #8701302; Kodak) and analyzed by Raybio® Analysis tool (RayBiotech, USA) and ImageJ software (Lalancette-Hebert, 2007, 2012).

5.3.8 Western blots

Mice were sacrified after isoflurane anaesthesia. The brain was dissected in two hemispheres: ipsilateral and contrateral from the lesion site. After this was done it was rapidly frozen in liquid nitrogen and stored at –80°C until used for protein extraction. Whole protein lysates from the mouse were extracted by homogenization of the tissues in the same buffer used with the cytokines kit. The protein was quantified and diluted in 15% glycerol, 5% SDS, 80 mM Tris–HCl, pH 6.8, 5% β-mercapto-ethanol and 0.01% bromophenol blue. Each sample (50 µg) was run on a SDS/glycine polyacrylamide gel and then transferred electrophoretically to a PVDF membrane (Perkin Elmer Boston, MA, U.S.A). The

blots were blocked in 5% non-fat milk/0.1% Tween 20 in phosphate-buffered saline (PBS) and probed with antibodies diluted in the blocking buffer: STAT3 (1:1000, Cell Signalling, Whitby, Ontario), SOCS3 (1:1000, Cell Signalling), Iκbα (1:800, Cell Signalling) and Bax (1:750, Cell Signalling). Immunodetection was performed with an HRP-labelled secondary antibody (Jackson ImmunoResearch Laboratories ins.), and the detection was performed with the Immobilon Western kit (Millipore Corporation, Billerica, MA, U.S.A). The blots were then re-probed with an anti-actin antibody to document equal loading. Quantification of western blots was carried out using ImageJ software and normalized against actin.

5.3.9 Immunofluorescence

Brain sections were blocked in PBS containing 10% goat serum and 0.25% Triton X-100 for 1 hour. The sections were then incubated overnight at room temperature in 1% goat serum and 0.1% Triton X-100 in primary antibody (rabbit polyclonal anti-Iba-1 1:750 (Wako, Richmond,VA), mouse monoclonal anti-GFP 1:500 (Millipore), rat polyclonal CD68 1:1000 (Millipore, Billerica, MA) and rat polyclonal CD11b 1:500 (Serotec, Raleigh, NC) and rat monoclonal galectin-3 (American Type Culture Collection, Manassas, VA).This step was followed by six, 10 min rinses in PBS-0.1% Triton X-100. Incubation for 3 hrs at room temperature in corresponding secondary donkey fluorescent antibody (1:500; Jackson ImmunoResearch, West Grove, PA) was performed. The sections were mounted with Vectashield (Vector, Burlingame, CA) after six, 10 min washes in PBS.

5.3.10 Statistical analysis

All data are presented as mean ± SEM. Statistical analysis was performed by one-way ANOVA followed by post hoc comparison test (Tukey-Kramer test). $P < 0.05$ was considered statistically significant.

5.4 RESULTS

5.4.1 Real time imaging reveals marked increase in microglial activation/TLR2 signals in chronically estrogen deprived mice

Microglial cells are the main effectors of the innate immune response following brain injuries including stroke. Microglial activation is a hallmark of brain inflammatory response to ischemic injury and growing evidence suggest that any changes in activated microglial phenotype may significantly affect the outcome after stroke. It has been widely established that ageing is associated with distinct age-dependent shift in brain inflammatory profile and primed (more activated) microglial cells. Interestingly however, the results of the recent studies revealed that pro-inflammatory genes profiles is more pronounced in aged female brains as well as in immune cells (Cribbs, 2012, Hart, 2012). Another hallmark of microglial activation after stroke is a robust up-regulation of the Toll like receptor 2 (Lehnard 2007, Tang, 2007, Ziegler, 2007 Lalancette-Hebert, 2009). While in physiological, resting condition, the TLR2 expression in the mouse brain is weak, its expression is strongly induced in microglia following stroke. In our previous work we clearly demonstrated the capacity of the transgenic TLR2-Luc-GFP mouse to visualize and assess the microglial response after a cerebral ischemia (Lalancette-Hebert, 2009). In this study, using the same transgenic model, we first asked how TLR2 induction/microglial activation after stroke is affected in the context of estrogen deprivation. Our previous studies suggest that a chronic lack of estrogen markedly affected astrocytes response to ischemic injury (Cordeau, 2008). As schematically presented in Figure1, to assess the role of estrogen deprivation on microglial activation profile *in vivo* the mice were divided in 3 different groups; control female mice, acutely estrogen deprived mice (MCAo performed 14 days after OVX) and chronically estrogen deprived mice (MCAo performed 40 days after surgery). Prior to all surgery a baseline levels of microglial activation state was acquired using *in vivo* biophotonic/ bioluminescence imaging. Interestingly, the baseline TLR2 activation level was higher in the chronically OVX group as compared to the acutely OVX mice and controls (Control female: 1.13e5 ± 1.28e4 p/s; 14 days ovx:

8.94e3 ± 1.34e4 p/s; 40 days ovx: 1.97e5 ± 1.46e4 p/s) (Figure 2A, F, K). After the MCAO, the microglial activation continued to be longitudinally monitored in all the groups for 14 days. In all the groups, the same pattern could be observed, the TLR2 level rise after the stroke, peak around 48 hours and decrease afterward. The female deprived of estrogens for a longer period of time had a higher TLR2 activation when compared to the other groups for the first 72 hours (Control female: 6.69e5 ± 8.01e4 p/s; 14 days ovx: 4.19e5 ± 1.00e5 p/s; 40 days ovx: 9.62e5 ± 1.10e5 p/s after 48 hours). Hence chronic estrogen deprivation is associated with higher microglia activation profiles and significantly higher TLR2 signal induction levels as measured in our *in vivo* imaging protocols. To confirm that the TLR2 biophotonic signal induction is indeed arising from activated microglial cells we next analyzed expression pattern of the TLR2 driven transgene GFP (Figure 3). As expected, the double immunofluorescence analysis 48 hrs after MCAo revealed a co-localization between GFP and the microglial marker Iba1 staining in the brain sections of the control, acutely and chronically OVX mice. Note more ramified microglia morphology in the controls and in the 14 days ovx mice as compared to chronically OVX mice. No expression of the TLR2-driven GFP transgene was observed in the contralateral side of the ischemic brain (data not shown).

5.4.2 Chronic lack of estrogen is associated with larger infarction

Our previous *in vivo* imaging work demonstrated that the level of astrocyte activation measured as induction of the GFAP signals did not correlate with the size of ischemic lesion/neuronal damage in male mice as they did with the female mice (Cordeau, 2008). This suggests that inflammatory response to ischemia may have gender specific biomarkers of brain damage. To determine whether significant induction of the TLR2 signals observed in chronically estrogen deprived females is associated with larger ischemic lesions, we analyzed and quantified the size of the ischemic areas in control mice and compared them with acutely vs.

chronically estrogen deprived mice. As shown in Figure 4A and B, 48 hours after stroke, quantitative analysis revealed significantly larger infarction in the mice with chronic estrogen deprivation. As further confirm by Western blot analysis, larger ischemic lesions detected in chronically OVX mice were associated with increased expression levels of Bax protein, a known marker of apoptotic cell death (Figure 4C, D).

5.4.3 Estrogen receptor alpha mediates TLR2 response after stroke

Evidence suggests that in addition to chronic estrogen deficiency, the process of aging in the female brain has been associated with a marked decline in functional ERα. Moreover, decreased expression of ERα in certain brain regions such as hippocampus is found in some neurological diseases such as Alzheimer's disease (Ishunina, 2009). Here it is important to mention that ERα is expressed on many cell type including microglial cells. Previous studies revealed that E2 is able to inhibit microglial activation through ERα (Vegeto, 2003). Therefore, we hypothesized that in addition to chronic estrogen deficiency progressive loss of ERα function may be underlying cause of alterations of immune responses and increased vulnerability to stroke in elderly women. To further determine the role of ERα in modulation of inflammatory responses after stroke in the context of chronic estrogen deficiency, the TLR2-luc-GFP mice were derived in $ER\alpha^{KO}$ background. As described previously (figure 1) the double transgenic mice were ovariectomized (TLR2-luc-GFP and TLR2-luc-GFP, $ER\alpha^{KO}$) and the strokes were induced 40 days after initial surgery. Non-ovariectomized TLR2-luc-GFP mice and TLR2-luc-GFP; $ER\alpha^{KO}$ were used as additional controls.

The analysis of the *in vivo* imaging results revealed that, in baseline conditions and as in previous experiments, the TLR2-luc-GFP OVX mice show higher levels of the TLR2 activation when compare to non-OVX female mice before stroke (TLR2-luc-GFP: 1.19e5 ± 1.06e4 p/s, TLR2-luc-GFP OVX 1.91e5 ± 1.30e4 p/s) (fig 5A, E).

The baseline levels of the TLR2 signal were also elevated in TLR2-luc-GFP; ERα^{KO} OVX mice (1.66e5 ± 1.11e4 p/s). After stroke, we observed a marked up-regulation of the TLR2 signals in all groups reaching a peak at 48 hours and then started to decline with time (Figure. 5Q). Here it is important to mention that induction of the TLR2 signal after stroke was significantly higher in the chronically estrogen deprived mice, the TLR2-luc-GFP OVX, as when compared to all other groups (Figure 5A-H). Because evidence suggests a progressive loss of function of the ERα in aged female brains, we next analyzed the TLR2 responses in chronically estrogen deprived TLR2-luc-GFP; ERα^{KO} mice. The TLR2-luc-GFP; ERα^{KO} mice were used as additional controls. To our surprise, the overiactomized and chronically estrogen deprived TLR2-luc-GFP; ERα^{KO} and the non ovariectomized TLR2-luc-GFP; ERα^{KO} mice showed very similar pattern of the TLR2 signal induction after stroke (fig 5I-P, Q) (TLR2-luc-GFP: 6.02e5 ± 6.20e4 p/s, TLR2-luc-GFP OVX: 9.24e5 ± 1.04e5 p/s, TLR2-luc-GFP; ERα^{KO}: 3.40e5 ± 5.35e4 p/s, TLR2-luc-GFP; ERα^{KO} OVX: 5.42e5 ± 1.25e5 p/s at 48 hrs). Indeed as shown in figure 5, the lack of ERα (in OVX group) resulted in attenuation of TLR2 signals when compared to OVX mice. It has been widely established that ERα^{KO} mice have higher levels of estrogen. Namely, the level of oestrogen is 10 times higher in the ERα^{KO} when compared to control mice (Couse, 1995). On the other side, in the context of chronic OVX, the ERα^{KO} females are clearly estrogen deprived. Thus, our results strongly suggest that ERα is indeed involved in modulation of microglia activation and innate immune response following cerebral ischemia. Suggesting that, at least, part of the ischemic injury-induced inflammatory response is mediated by ERα and is estrogen independent.

At the present, it is unclear how estrogen deficiency in concert with an age-dependent functional downregulation of ERα may affect microglial activation and innate immune responses after stroke. We therefore analyzed expression of distinct microglial markers known to be involved in microglia-response to stroke including Iba1, CD68 and Gal-3 (Lalancette-Hebert, 2007, 2009, Bohacek, 2012). The brain sections were examined 48 hrs after stroke because the results obtained

in the live imaging experiments demonstrated that this point is associated with the most prominent differences in the TLR2 signal intensities between different experimental groups (Figure 6). The immunofluorescence analysis revealed a marked robust increase in microglial marker Iba1 and CD68 in all experimental groups (fig 6 A-H). Interestingly, analysis of the Gal-3 (Mac-2) immunoreactivity revealed a decrease in signal intensities in chronically estrogen deprived TLR2-luc-GFP; ERα^{KO} mice (fig 6C, F, I, L).

5.4.4 Over-expression of IL-6 and shift towards JAK/STAT pathway in ERα mice.

To further investigate the differences in pro-inflammatory cytokine profiles, we took advantage of cytokine array technic (Lalancette-Hebert, 2007, 2012). In order to determine the impact of the lack of Erα and/or estrogen on the pro-inflammatory molecules expression, we perform quantitative cytokines array in four different mice group 48 hours after stroke. As shown in figure 7 and in accordance with imaging results, analysis of the different cytokines revealed a significant increase in pro-inflammatory cytokine levels (Figure 7A-F). The increase in levels of TNF- α and IL-1β and IL-17 was significantly higher in OVX and TLR2-luc-GFP; ERα^{KO} OVX mice when compared to adequate controls (Figure 7A-D). Intriguingly however, as shown in figure 7C, in estrogen deprived mice the lack of ERα was associated with a selective 4-fold increase in the level of IL-6. The main intracellular pathway used by downstream signalling of the IL-6 cytokine family is the JAK/STAT pathway; however other pathway including NF-κB or PI3/Akt, MEK/Erk can also be activated. We first focused on JAK/STAT and NF-κB. Therefore, to delineate whether dysregulation of the IL-6 response in TLR2-luc-GFP; ERα^{KO} OVX mice after stroke leads to activation of JAK/STAT and/or NF-κB pathway, we perform western blot analysis and looked into protein levels of Ikbα, phospho-Stat3 (pSTAT-3) and suppressor of cytokines-3 (SOCS3), proteins members involved downstream events of NF-kB signalling and IL-6. Of particular interest, was an experimental group the TLR2-luc-GFP; ERα^{KO} OVX mice that showed over-expression of IL-6 after stroke. While we did not observed significant

differences in the levels of Ikbα between OVX and TLR2-luc-GFP; ERα^{KO} OVX mice (Figure 7J) the high level of phospho-Stat3 and significant decrease in the level of SOCS3 is observed by western blot in the mice deprived of oestrogen when Erα is absent (Figure 7K, L). These results indeed correlate well with over-expression of IL-6 seen in this group. Next, activation of JAK/STAT pathway leads to induction of suppressors of cytokines signaling molecules (SOCSs), in particular SOCS3 (Tan, 2005). The functional role of SOCS3 is to act as negative feedback inhibitor of the JAK/STAT pathway by preventing STAT3 phosphorylation. In accordance with the high level of p-STAT3, the level of SOCS3 is lower in the TLR2-luc-GFP; ERα^{KO} OVX when compared to all non OVX groups. Hence, these observations suggest that ERα in response to ischemic injury specifically act through the IL-6/JAK/STAT pathway.

5.4.5 ERα deficiency induces increased infarction in estrogen deficient mice

Inflammatory response can help or hinder recovery after stroke depending of the timing, the context and/or type of brain injury (Kriz, 2009). Moreover, it has been suggested that after cerebral ischemia, IL-6 can play a role in both cell survival and neurodegenerative processes (Suzuki, 2009). Thus we next asked whether observed over-expression of IL-6 in TLR2-luc-GFP; ERα^{KO} OVX mice is a part adaptive or maladaptive neuroinflammatory response to ischemic injury. Namely, as shown in figure 8A the analysis of the stroke area between different experimental groups revealed significantly larger infarcts in TLR2-luc-GFP; ERα^{KO} OVX mice thus suggesting the overexpression of IL-6 in the context of chronic estrogen deprivation and lack of ERα is deleterious.

In fact, the higher expression of IL-6 correlates with the size of brain damage as showed by a larger stroke area in TLR2-luc-GFP; ERα^{KO} OVX when compared to all experimental group. Taken together our results suggest that ERα in the context of chronic estrogen deficiency is involved in regulation of IL-6 level. Because

altered regulation and increased levels of IL-6 has been associated with aging, it is possible that chronic estrogen deficiency together with downregulation of functional ERα may contribute to increased brain vulnerability to stroke observe in our model.

5.5 Discussion

It has been widely established that after menopause women are more vulnerable to stroke induced damage than men, however underlying mechanisms are not well understood. Although increased vulnerability could in part be explained by estrogen deficiency, the lack of beneficial effects on stroke after estrogen replacement therapy suggests more complex mechanisms (Wise, 2005; Schreihofer, 2013). Using bioluminescence /biophotonic imaging and TLR-luc/gfp reporter mice previously generated in our laboratory, we were able to visualize microglial/activation and TLR2 responses from the brains of chronically estrogen deprived female mice as well as in the estrogen deprived mice lacking ERα. The rationale for using ERα knockout mice lays in the fact that for women, aging comes (in addition to with a drastic loss of ovarian hormones) with a functional changes in ERα and an increased expression of the splice variant that acts as a dominant negative regulator of receptor activity (Ishunina, 2008, 2009). We provide here first *in vivo* evidence revealing that following ischemic injury ERα plays an important role in mediation of microglial activation and innate immune responses –TLR2 upregulation. Namely, while chronic estrogen deprivation was associated with higher level of microglial activation the TLR2 responses at baseline levels and after stroke our *in vivo* imaging revealed a blunted up-regulation of TLR2 receptor in ERαKO mice. The up-regulation was attenuated in chronically estrogen deprived ERα as well as in non-OVX ERα^{KO} suggesting a ligand independent role of the receptor in stroke. Further analysis of the pro-inflammatory cytokine profile revealed rather selective increase in the levels of IL-6 in OVX ERα^{KO} mice, followed by 6 fold increases in pSTAT. Importantly, increased levels of IL-6 observed in OVX ERα^{KO} were associated with significant increase in the size of

ischemic lesion thus suggesting that change of microglia activation profiles and marked shift towards IL-6/JAK/STAT signaling contributes to ischemic injury.

To date, many studies have demonstrated neuroprotective effects of estrogen and ERα following experimental ischemic injury (Rusa, 1999; Dubal, 2001, 2006, Behl, 2002). Brain response to ischemic injury is associated with an early activation of the microglia, a key cell in the innate immune system, to activate the brain inflammatory processes. Microglial activation causes release of a wide range of inflammatory mediators that can be toxic or protective for the surrounding cells (Patel, 2013). At present, little is known about ERα- mediated mechanisms of microglial activation in stroke, especially in the context of chronic estrogen deficiency. ERα is one of tree receptor that binds oestrogen (Schreihofer, 2013). Those receptors are not uniformly distributed into the brain and within cells types, thus their implication in stroke outcome varies greatly (Schreihofer, 2013). ERα can act as a ligand-activated transcription factor, but also have ligand-independent mechanisms of signalisation. However, by using a cell type specific ERα-mutants *in vivo* model of stroke, Elzer and colleagues (Elzer, 2010) revealed that neuronal rather than microglial expression of ERα mediates neuroprotective effects of estrogen. The effects were measured in young mice treated with E2 and, as mentioned previously, it is unclear how ERα can affect microglial activation profiles after stroke in the context of menopause and associated estrogen deficiency.

Aging can be a sufficient stressor to induce a chronic activation of microglial cells and macrophages. Actually, aging comes with a pro-inflammatory status that intensifies with time. For women, aging comes also with a drastic loss of ovarian hormones associated with progressive decline and loss of the functional ERα leading to menopause. In experimental models, ovariectomy, a surgery that induces E2 deprivation in mice, can induce a state of ‘inflamm-aging’ that mimics post-menopausal women. Our *in vivo* imaging results are consistent with this notion. In fact, as shown in figure 2, the absence of oestrogen for a long period induces exaggerated microglial activation in basal condition and also after stroke,

leading to bigger lesion. Likewise, in menopausal women, the loss of ovarian hormones leads to changes in the neuroinflammatory response of the brain; levels of pro-inflammatory cytokines like IL-6 and TNF-α increase leading to cognitive impairment and neurodegeneration (Brown, 2010).

The most striking finding that emerged from our live imaging study is a marked attenuation of TLR2 signals in TLR2-luc-GFP; ERα^{KO} OVX mice in response to cerebral ischemia. Intriguingly, the downregulation of the TLR2 response was not associated with the decrease in pro-inflammatory cytokine levels but rather in change in pro-inflammatory post-ischemic profile. Namely, the analysis of the pro-inflammatory cytokine profile revealed that after stroke the TLR2-luc-GFP; ERα^{KO} OVX mice have the comparable level of TNFα, IL-1β and IL-17 as compared to TLR2-luc-GFP OVX mice. However, we observed a rather selective increase in the level of IL-6 associated with 4-fold increase in pSTAT level (Figure 7) suggesting a shift towards IL-6 /JAK/STAT pathway. This cytokine is known to exert pleiotropic effects from inflammatory to neurotrophic depending of the pathological context (Suzuki, 2009). ERα is shown to directly interact with IL-6 and NF-κB (Stein, 1995; Kurebayashi, 1997) and exerts indirect negative regulatory effect on IL-6 activity (Matthews, 2005). The IL-6 cytokine activate the JAK/STAT pathway and the level of STAT3, an important member of the signalling cascade, can be affected by the presence of E2 (Bjornstrom, 2002). In our experiments, we show that the level of STAT3 is indeed increased in the TLR2-luc-GFP; ERα^{KO} OVX at the same extend as IL-6 compared to other mice group suggestion that the strong production of IL-6 induces JAK/STAT pathway activation. Furthermore, the level of the suppressors of cytokine signalling 3 (SOCS3) is very low in the same group. SOCS3 is the more powerful protein to inhibit the signal of IL-6 and its low expression found in TLR2-luc-GFP; ERα^{KO} OVX mice can in part explain the strong IL-6 production. Here it is important to mention that altered regulation of IL-6 has been associated with aging (Daynes, 1993) and it may represent increased risk and disadvantage for longevity.

In conclusion, we demonstrated that 1) that chronic estrogen deficiency is associated with more activated microglial phenotypes and increased pro-inflammatory cytokine levels 2) ERα can act in a ligand independent manner after stroke and modulate microglial activation and innate immune response 3) in model of menopause loss of ERα leads to over-expression of IL-6 production, over-activation of JAK/STAT pathway and increased ischemic damage. We propose here that the early suppression and/or regulation of the IL-6-JAK/STAT pathway rather that estrogen-based therapy may be beneficial in stroke after menopause.

5.6 ACKNOWLEDGMENTS

This work was supported by the Canadian Institutes of Health Research (CIHR) J.K. is recipient of the FRQS Senior Scholarship Award.

5.7 REFERENCES

Alkayed, N.J., et al., *Gender-linked brain injury in experimental stroke.* Stroke, 1998. 29(1): p. 159-65; discussion 166.

Baker, M.E., *Co-evolution of steroidogenic and steroid-inactivating enzymes and adrenal and sex steroid receptors.* Mol Cell Endocrinol, 2004. 215(1-2): p. 55-62.

Behl, C., *Oestrogen as a neuroprotective hormone.* Nat Rev Neurosci, 2002. 3(6): p. 433-42.

Berchtold, N.C., et al., *Gene expression changes in the course of normal brain aging are sexually dimorphic.* Proc Natl Acad Sci U S A, 2008. 105(40): p. 15605-10.

Bjornstrom, L. and M. Sjoberg, *Mutations in the estrogen receptor DNA-binding domain discriminate between the classical mechanism of action and cross-talk with Stat5b and activating protein 1 (AP-1).* J Biol Chem, 2002. 277(50): p. 48479-83.

Bohacek, I., et al., *Toll-like receptor 2 deficiency leads to delayed exacerbation of ischemic injury.* J Neuroinflammation, 2012. 9: p. 191.

Brown, C.M., et al., *Production of proinflammatory cytokines and chemokines during neuroinflammation: novel roles for estrogen receptors alpha and beta.* Endocrinology, 2010. 151(10): p. 4916-25.

Cordeau, P., Jr., et al., *Live imaging of neuroinflammation reveals sex and estrogen effects on astrocyte response to ischemic injury.* Stroke, 2008. 39(3): p. 935-42.

Cordeau, P. and J. Kriz, *Real-time imaging after cerebral ischemia: model systems for visualization of inflammation and neuronal repair.* Methods Enzymol, 2012. 506: p. 117-33.

Couse, J.F., et al., *Analysis of transcription and estrogen insensitivity in the female mouse after targeted disruption of the estrogen receptor gene.* Mol Endocrinol, 1995. 9(11): p. 1441-54.

Cribbs, D.H., et al., *Extensive innate immune gene activation accompanies brain aging, increasing vulnerability to cognitive decline and neurodegeneration: a microarray study.* J Neuroinflammation, 2012. 9: p. 179.

Daynes, R.A., et al., *Altered regulation of IL-6 production with normal aging. Possible linkage to the age-associated decline in dehydroepiandrosterone and its sulfated derivative.* J Immunol, 1993. 150(12): p. 5219-30.

Dubal, D.B., et al., *Differential modulation of estrogen receptors (ERs) in ischemic brain injury: a role for ERalpha in estradiol-mediated protection against delayed cell death.* Endocrinology, 2006. 147(6): p. 3076-84.

Dubal, D.B., et al., *Estrogen receptor alpha, not beta, is a critical link in estradiol-mediated protection against brain injury.* Proc Natl Acad Sci U S A, 2001. 98(4): p. 1952-7.

Elzer, J.G., et al., *Neuronal estrogen receptor-alpha mediates neuroprotection by 17beta-estradiol.* J Cereb Blood Flow Metab, 2010 30(5): p. 935-42.

Ghisletti, S., et al., *17beta-estradiol inhibits inflammatory gene expression by controlling NF-kappaB intracellular localization.* Mol Cell Biol, 2005. 25(8): p. 2957-68.

Gibson, C.L., *Cerebral ischemic stroke: is gender important?* J Cereb Blood Flow Metab, 2013. 33(9): p. 1355-61.

Hart, A.D., et al., *Age related changes in microglial phenotype vary between CNS regions: grey versus white matter differences.* Brain Behav Immun, 2012. 26(5): p. 754-65.

Iadecola, C. and J. Anrather, *Stroke research at a crossroad: asking the brain for directions.* Nat Neurosci, 2011. 14(11): p. 1363-8.

Ishunina, T.A. and D.F. Swaab, *Age-dependent ERalpha MB1 splice variant expression in discrete areas of the human brain.* Neurobiol Aging, 2008. 29(8): p. 1177-89.

Ishunina, T.A. and D.F. Swaab, *Estrogen receptor-alpha splice variants in the human brain.* Gynecol Endocrinol, 2008. 24(2): p. 93-8.

Ishunina, T.A. and D.F. Swaab, *Hippocampal estrogen receptor-alpha splice variant TADDI in the human brain in aging and Alzheimer's disease.* Neuroendocrinology, 2009. 89(2): p. 187-99.

Kamel, H. and C. Iadecola, *Brain-immune interactions and ischemic stroke: clinical implications.* Arch Neurol, 2012. 69(5): p. 576-81.

Kriz, J. and M. Lalancette-Hebert, *Inflammation, plasticity and real-time imaging after cerebral ischemia.* Acta Neuropathol, 2009. 117(5): p. 497-509.

Kurebayashi, S., et al., *Characterization of mechanisms of interleukin-6 gene repression by estrogen receptor.* J Steroid Biochem Mol Biol, 1997. 60(1-2): p. 11-7.

Lalancette-Hebert, M., et al., *Live imaging of Toll-like receptor 2 response in cerebral ischaemia reveals a role of olfactory bulb microglia as modulators of inflammation.* Brain, 2009. 132(Pt 4): p. 940-54.

Lalancette-Hebert, M., et al., *Selective ablation of proliferating microglial cells exacerbates ischemic injury in the brain.* J Neurosci, 2007. 27(10): p. 2596-605.

Lalancette-Hebert, M., et al., *Accumulation of dietary docosahexaenoic acid in the brain attenuates acute immune response and development of postischemic neuronal damage.* Stroke, 2011. 42(10): p. 2903-9.

Lalancette-Hebert, M., et al., *Galectin-3 is required for resident microglia activation and proliferation in response to ischemic injury.* J Neurosci, 2012. 32(30): p. 10383-95.

Lehnardt, S., et al., *Toll-like receptor 2 mediates CNS injury in focal cerebral ischemia.* J Neuroimmunol, 2007. 190(1-2): p. 28-33.

Matthews, J., et al., *Estrogen receptor (ER) beta modulates ERalpha-mediated transcriptional activation by altering the recruitment of c-Fos and c-Jun to estrogen-responsive promoters.* Mol Endocrinol, 2006. 20(3): p. 534-43.

Patel, A.R., et al., *Microglia and ischemic stroke: a double-edged sword.* Int J Physiol Pathophysiol Pharmacol, 2013. 5(2): p. 73-90.

Rusa, R., et al., *17beta-estradiol reduces stroke injury in estrogen-deficient female animals.* Stroke, 1999. 30(8): p. 1665-70.

Schreihofer, D.A. and Y. Ma, *Estrogen receptors and ischemic neuroprotection: who, what, where, and when?* Brain Res, 2013. 1514: p. 107-22.

Stein, B. and M.X. Yang, *Repression of the interleukin-6 promoter by estrogen receptor is mediated by NF-kappa B and C/EBP beta.* Mol Cell Biol, 1995. 15(9): p. 4971-9.

Suzuki, S., et al., *Timing of estrogen therapy after ovariectomy dictates the efficacy of its neuroprotective and antiinflammatory actions.* Proc Natl Acad Sci U S A, 2007. 104(14): p. 6013-8.

Suzuki, S., K. Tanaka, and N. Suzuki, *Ambivalent aspects of interleukin-6 in cerebral ischemia: inflammatory versus neurotrophic aspects.* J Cereb Blood Flow Metab, 2009. 29(3): p. 464-79.

Tan, J.C. and R. Rabkin, *Suppressors of cytokine signaling in health and disease.* Pediatr Nephrol, 2005. 20(5): p. 567-75.

Tang, S.C., et al., *Pivotal role for neuronal Toll-like receptors in ischemic brain injury and functional deficits.* Proc Natl Acad Sci U S A, 2007. 104(34): p. 13798-803.

Vegeto, E., et al., *Estrogen receptor-alpha mediates the brain antiinflammatory activity of estradiol.* Proc Natl Acad Sci U S A, 2003. 100(16): p. 9614-9.

Wise, P.M., et al., *Are estrogens protective or risk factors in brain injury and neurodegeneration? Reevaluation after the Women's health initiative.* Endocr Rev, 2005. 26(3): p. 308-12.

Wu, W.F., et al., *Targeting estrogen receptor beta in microglia and T cells to treat experimental autoimmune encephalomyelitis.* Proc Natl Acad Sci U S A, 2013. 110(9): p. 3543-8.

Ziegler, G., et al., *TLR2 has a detrimental role in mouse transient focal cerebral ischemia.* Biochem Biophys Res Commun, 2007. 359(3): p. 574-9.

FIGURE LEGENDS

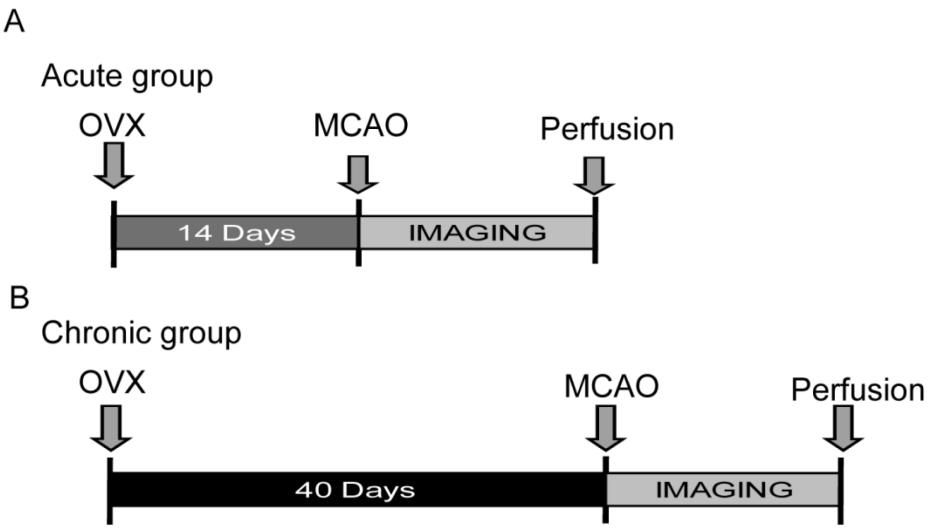

Figure 1: Schematic representation of experimental protocol
(A) Acute and (B) chronic ovariectomy group.

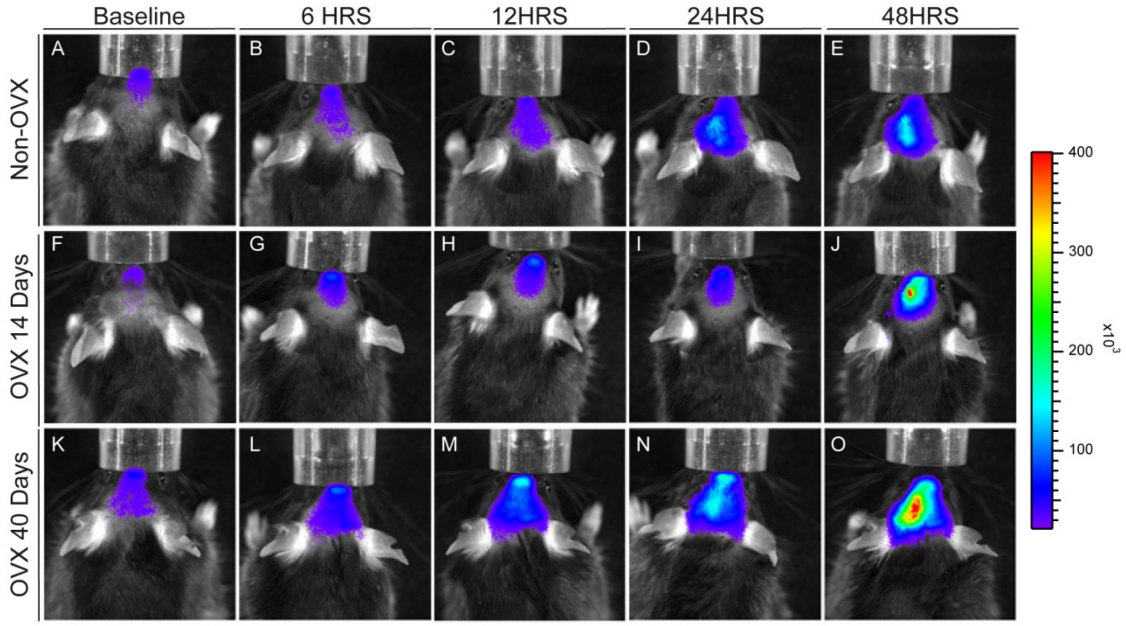
Baseline
6 HRS
12HRS
24HRS
48HRS
Non-OVX
OVX 14 Days
OVX 40 Days
A
B
C
D
E
F
G
H
I
J
K
L
M
N
O
400
300
200
100
x10³

P

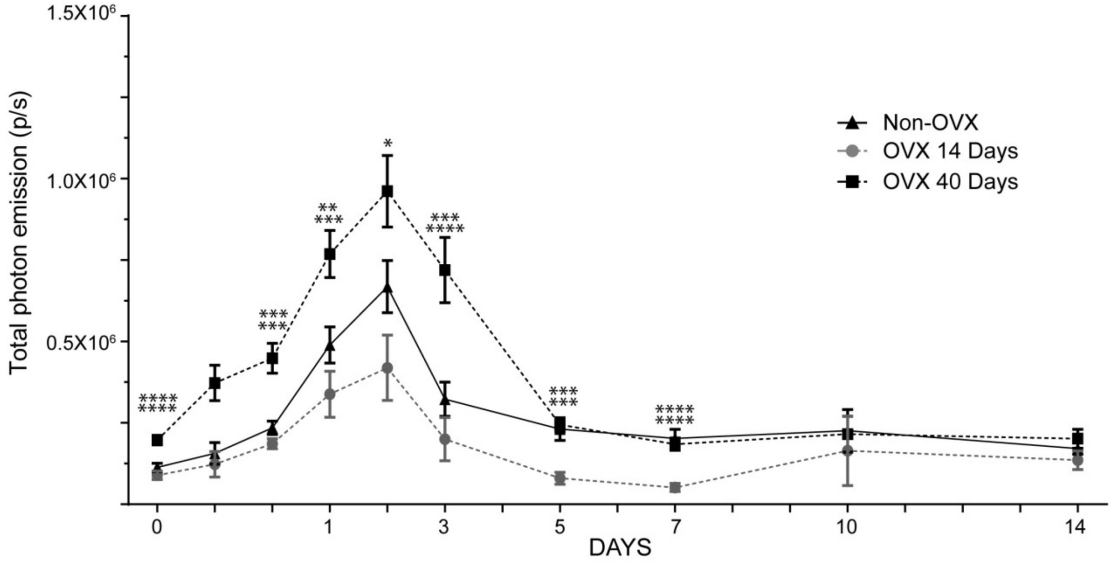
1.5X10⁶
1.0X10⁶
0.5X10⁶
Total photon emission (p/s)
Non-OVX
OVX 14 Days
OVX 40 Days
DAYS
0
1
3
5
7
10
14

Figure 2: Long-term oestrogen deprivation increases microglial activation after stroke in TLR2-luc-GFP mice. Representative images from real-time imaging of bioluminescent TLR2 signal from 6 hours to 48 hours after cerebral ischemia in normal (A-E), 14 days ovariectomized (F-J) and 40 days ovariectomized mice (K-O). Scale on the right is the color map of the photons emission (p/sec/cm^2/sr). (P) Quantification of total photon emission longitudinally in a 2 weeks period reveals strong microglial activation, seen by the induction of TLR2 signalling, in the OVX 40 days group in baseline condition as well as in the first 72 hours after MCAO when compare to the non-OVX or OVX 14 days groups.

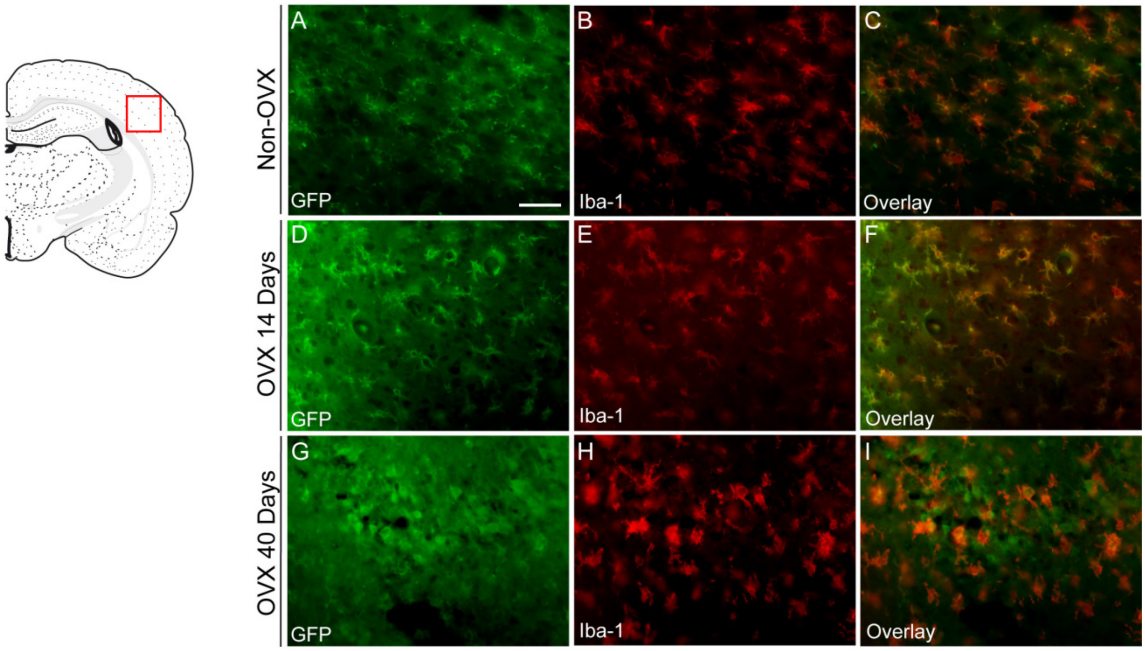

Figure 3: Effect of E2 absence on microglial activation after 48 hours MCAO. Immunofluorescence staining for Iba-1 (red) and GFP (green) was performed in the non-OVX (A-C), OVX 14 days (D-F) and OVX 40 days (G-I) TLR2-luc-GFP mice. Microglial cells display a more activated morphology in the OVX 40 days (G-I) group when compare to controls non-OVX and OVX 14 days group. Clear colocalisation between the Iba-1 and the GFP can be observed in all 3 groups. Scale bar indicate 50 µm.

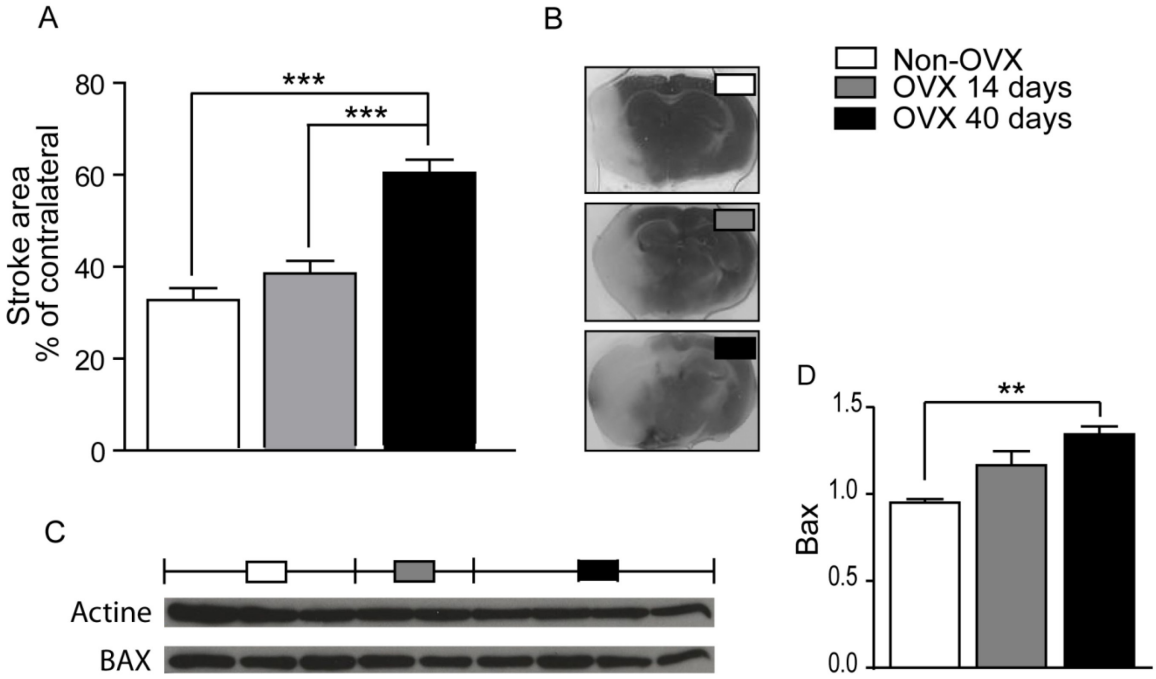

Figure 4: Increase in stroke area can be observed in the OVX 40 days group 48 hours after MCAO. (A, B) No difference in the stroke area region (% of contralateral) is observed between non-OVX and OVX 14 days groups measured by TTC staining. The stroke area region is bigger in OVX 40 days when compared to both groups. (C, D) Assessment by western blotting and quantification of BAX and β-actin protein levels at 48 hours post ischemia of the ipsilateral side of the brains. Values are expressed as mean ± SEM.

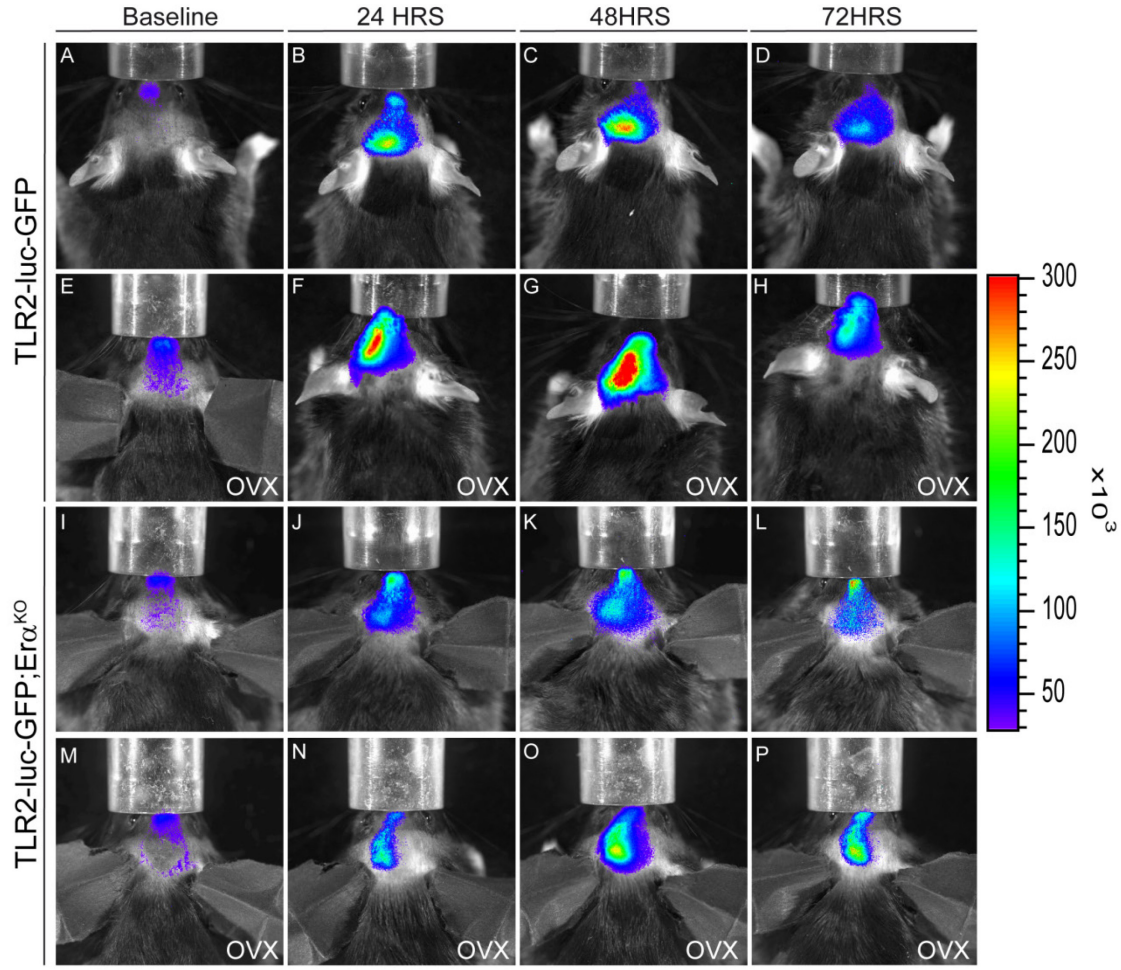
Baseline
24 HRS
48HRS
72HRS
TLR2-luc-GFP
TLR2-luc-GFP;Erα^KO
A
B
C
D
E
F
G
H
I
J
K
L
M
N
O
P
OVX
300
250
200
150
100
50
×10^3

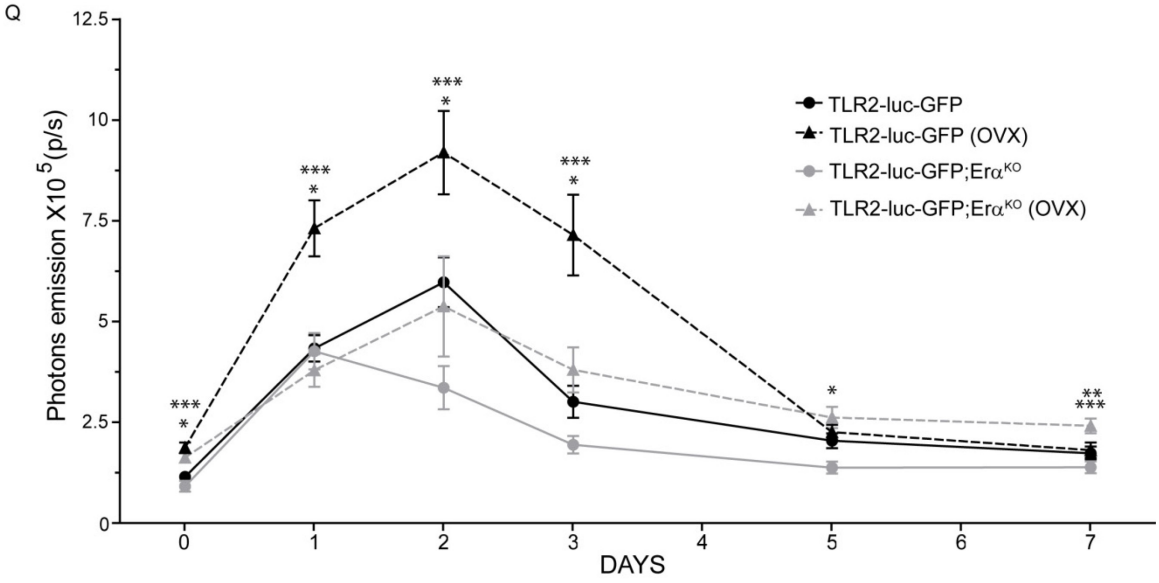
Q
Photons emission X10^5(p/s)
12.5
10
7.5
5
2.5
0
0
1
2
3
4
5
6
7
DAYS
TLR2-luc-GFP
TLR2-luc-GFP (OVX)
TLR2-luc-GFP;Erα^KO
TLR2-luc-GFP;Erα^KO (OVX)

Figure 5: Real-time visualisation of bioluminescence TLR2 signals after cerebral ischemia reveals a decrease in microglial the TLR 2 signals in TLR2-luc-GFP; Erα^{KO} mice after MCAO. TLR2-luc-GFP (A-D), TLR2-luc-GFP (OVX) female (E-H), TLR2-luc-GFP; Erα^{KO} (I-L) and TLR2-luc-GFP; Erα^{KO} (OVX) (M-P) female have been imaged at baseline, 24, 48 and 72 hours after MCAO. The images were recorded from the same experimental animal and reveal the dynamics of the microglia activation throughout the first 7 days in our four groups. Scale on the right is the color map of the photons emission (p/sec/cm^2/sr). (Q) Quantification of luciferase signals with the LivingImage software (Xenogen) revealed a higher TLR2 signal in the TLR2-luc-GFP OVX mice throughout the first days. Values are expressed as mean ± SEM.

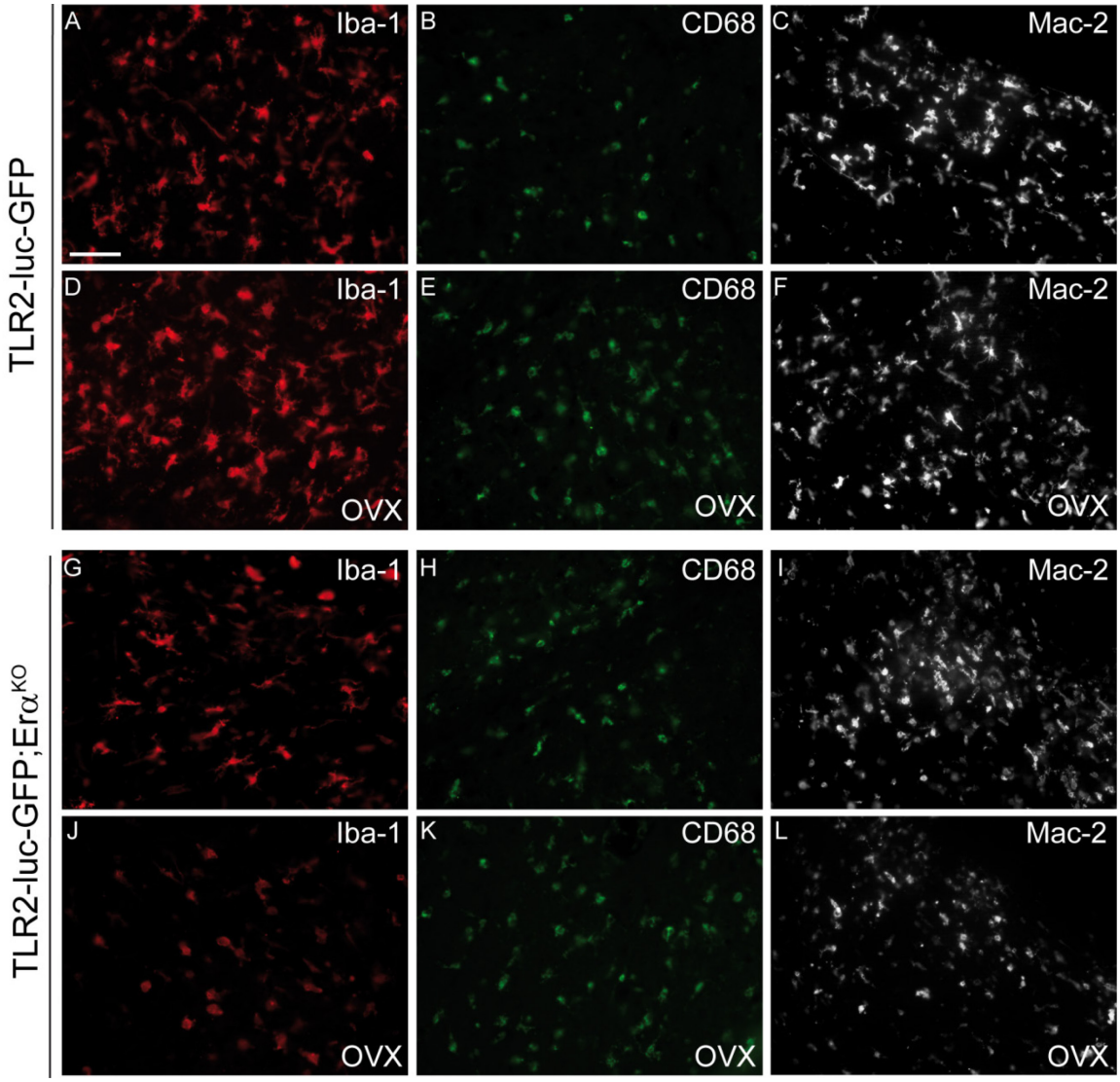

Figure 6: Expression of distinct microglial markers involved in microglia-response 48 hours after stroke. Immunofluorescence markers for Iba1, CD68 and MAC-2 (Gal-3) were performed in all mice groups. A marked increase in microglial marker for Iba1 and CD68 was observed in all experimental groups (Figure 6 A-K). Interestingly, analysis of the Gal-3 (Mac-2) immunoreactivity revealed a decrease in signal intensities in chronically estrogen deprived TLR2-luc-GFP; ERα^{KO} mice (Figure 6C, F, I, L).

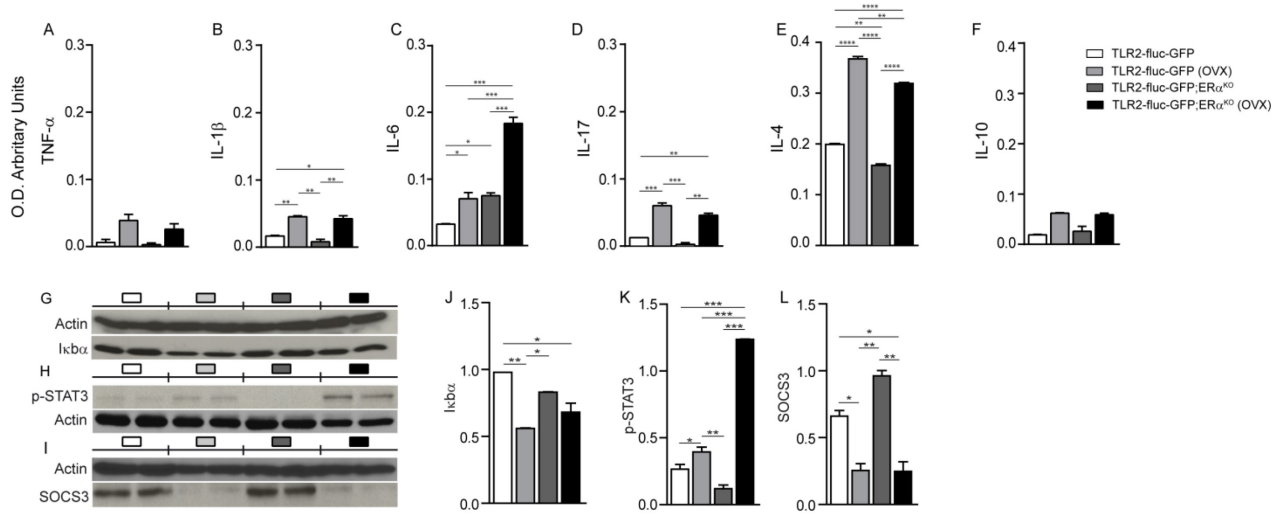

Figure 7: Estrogen deficiency and lack of ERα induces over-activation of IL-6-JAK-STAT pathway implication after MCAO. (A-F) Analysis of the expression of pro-inflammatory cytokines TNF-α, IL-1β, IL-6, IL-17 and anti-inflammatory cytokines IL-4 and IL-10 in the lesion side of the brain shows more cytokines expression in both ovariectomised groups. (G-L) Further assessment by western blotting and quantification of IκBα (G, J), p-STAT3 (H, K), SOCS3 (I, L) and β-actin protein levels at 48 hours post ischemia of the ipsilateral side of the brains reveal a specific activation of the IL-6-JAK-STAT pathway. Values are expressed as mean ± SEM.

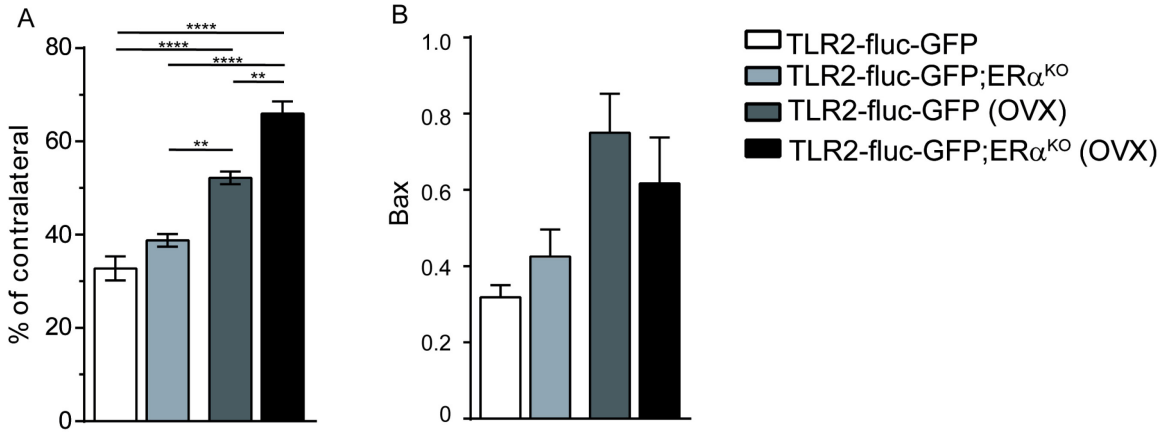

Figure 8: Larger infarct region can be observed in the TLR2-luc-GFP; Erα^{KO} OVX 48 hours after MCAO. (A) No difference in the stroke area region (% of contralateral) is observed between TLR2-luc-GFP and TLR2-luc-GFP; Erα^{KO} groups measured by TTC staining. Both OVX groups show bigger infarct area when compared to their relative controls and the TLR2-luc-GFP; Erα^{KO} OVX has the biggest infarct region of all the groups. Assessment by western blotting and quantification of BAX and β-actin protein levels at 48 hours post ischemia of the ipsilateral side of the brains reveals no significant differences between groups but clearly show tendencies that correlate with the stroke area results. Values are expressed as mean ± SEM.

Chapitre 6. Discussion générale

L'ensemble des travaux exposés dans cette thèse ont pour objectif de mieux comprendre le rôle des microglies ainsi que leur profil d'activation après l'ischémie cérébrale chez le mâle mais aussi chez la femelle. Pour ce faire un chapitre de méthode et trois chapitres expérimentaux sont exposés dans cette thèse.

Dans le chapitre 3, nos résultats démontrent que l'activation microgliale doit être finement régulée pour limiter l'étendue des dommages après l'ischémie cérébrale. L'étude présentée a permis de mettre en évidence la réponse immunitaire inadéquate des souris TLR2KO suite à une ischémie cérébrale. Le but de cette étude était de vérifier l'implication de la voie signalétique du TLR2 ainsi que son effet sur l'activation microgliale au-delà des 72 heures suivant l'ischémie. L'étude a démontré que l'absence du récepteur TLR2 dérégule de façon significative le profil inflammatoire normal en diminuant la capacité de prolifération des microglies résidentes.

Dans le chapitre 4, les souris TLR2-fluc développées par notre équipe ont permis de déterminer si un environnement enrichi pouvait affecter la réponse inflammatoire et ainsi affecter la récupération fonctionnelle des fonctions motrices. Notre modèle nous a donc permis de démontrer que le milieu enrichi atténue de façon significative la réponse microgliale après l'ischémie. De plus, cette diminution générale du niveau d'inflammation se traduit par une meilleure récupération fonctionnelle du membre antérieur atteint.

Pour ce qui est du chapitre 5, les souris générées par notre laboratoire (TLR2-luc-GFP;Erα^{KO}) ont permis de vérifier le rôle de l'estrogène sur le niveau d'inflammation cérébrale. En effet, il est reconnu que le sexe de la souris affecte l'activité microgliale à la suite de l'ischémie cérébrale. Nous avons donc mis en évidence l'importance du récepteur Erα sur la réponse inflammatoire. De plus,

nous avons démontré l'implication de la voie des JAK/STAT lorsque que le récepteur Erα et l'E2 sont absents.

Afin de mieux comprendre l'étendu des résultats obtenus lors de ma thèse, les trois chapitres expérimentaux seront discutés plus en détails.

6.1 L'inflammation et le récepteur TLR2

Dans le chapitre 3, nous avons démontré que pour limiter les dommages neuronaux, l'activation microgliale doit est modulée suite à une ischémie cérébrale. Le récepteur TLR2 initie une réaction pro-inflammatoire ayant des effets opposés à court et à long terme. En effet, nous avons observé des souris, possédant ou non le récepteur TLR2, durant une période de 14 jours après leur avoir induit une ischémie cérébrale transitoire. Peu d'études se concentrent sur les mécanismes pathophysiologiques après une aussi longue période (Lalancette-Hébert, 2009). En effet, la majorité des études se concentrent sur les mécanismes ayant lieu pendant les 24 heures à 7 jours suivant l'accident cérébral (Ziegler, 2007; Ziegler 2010). Notre étude démontre que la grosseur d'une lésion très tôt après l'ischémie cérébrale n'est pas toujours représentative de la grosseur des lésions observées plus tard. Nous avons démontré que l'inactivation du récepteur TLR2 à un effet positif sur la taille de la lésion ischémique durant les premières 72 heures, cependant, à long terme, l'inactivation de ce récepteur nuit au confinement du foyer ischémique. D'ailleurs, après 14 jours, les lésions mesurées chez les souris TLR2KO sont plus grandes que chez les souris contrôles.

Afin de découvrir si un lien existe entre la grosseur de la lésion ischémique et le niveau d'activation des microglies/macrophages, chez les souris TLR2KO, nous avons quantifié par densité optique l'expression d'Iba-1. L'hypothèse de départ étant qu'une lésion cérébrale plus petite à 72 heures serait corrélée avec des niveaux d'activation d'Iba-1 plus faibles. En effet, nous avons démontré un niveau d'activation moindre de cellules Iba-1 chez les souris TLR2KO après 3 et 7 jours. Malgré tout, le volume de la lésion ischémique à 7 jours est plus grand. Le

problème avec la quantification par densité optique est qu'il rend difficile de distinguer s'il y a plus de cellules ou si les cellules sont plus activées. Pour régler ce problème et afin de quantifier et de différencier la population de microglies de la population de macrophages, nous avons fait des FACS. Un marquage qui nous permet de différencier les microglies des macrophages nous a permis de constater que les microglies tout comme les macrophages sont aussi moins présents à 3 et 7 jours après l'ischémie cérébrale chez les souris TLR2KO. Deux théories peuvent expliquer ce phénomène : un recrutement cellulaire plus faible et/ou un taux de prolifération cellulaire plus faible des microglies/macrophages chez les souris TLR2KO.

Afin de savoir si le faible recrutement de monocytes/macrophages venant de la périphérie était en cause, nous avons mesuré la quantité de quelques cytokines chimioattractrices impliquées après l'ischémie cérébrale. Fortement exprimée 24 heures après l'ischémie cérébrale une cytokine ressortie, le MCP-1. Cette cytokine joue un rôle important dans le recrutement de monocytes au site d'inflammation. Le faible taux de recrutement serait donc expliqué en partie par une faible production de MCP-1. Ceci pourrait avoir un impact direct sur le volume de la lésion très tôt après l'ischémie. D'ailleurs, les souris MCP-1^{KO} montrent des lésions cérébrales plus petites deux jours après une ischémie cérébrale (Yan, 2006).

Une prolifération plus faible est le deuxième facteur qui pourrait causer la faible quantité de microglies/macrophages chez les souris TLR2KO. Nous avons donc mesuré le taux de prolifération microgliale en injectant du BrdU aux souris avant et après l'ischémie. La bromodéoxyuridine (BrdU) est un nucléoside synthétique qui s'incorpore dans l'ADN des cellules en cours de réplication. Parce que le BrdU marque toutes les cellules en prolifération, nous avons voulu isoler les microglies faisaient partie de ce groupe. Nous avons donc réutilisé la cytométrie de flux pour mettre en évidence le faible taux de prolifération des microglies chez les souris TLR2KO, 72 heures après l'ischémie cérébrale, le moment où la prolifération a atteint un sommet. Ce faible taux de prolifération microgliale a comme effet de faire

diminuer la quantité d'IGF-1 produit. L'IGF-1 est un facteur neurotrophique et anti-apoptotique très important à la suite d'une ischémie (Lalancette-Hébert, 2007).

En conclusion, l'absence du récepteur TLR2 bouleverse la réponse immunitaire chez la souris. Certes, la faible production de MCP-1 recrute moins de macrophages ce qui réduit la phagocytose des débris cellulaires. Par conte cela diminue aussi le recrutement des leucocytes et cela est bénéfique. D'ailleurs une étude mentionne que surexprimé le MCP-1 augmentent les dommages suite à une ischémie cérébrale (Chen, 2003). Pour ce qui est de la faible quantité d'IGF-1, produit par les cellules résidentes 3 jours après l'ischémie cérébrale, elle causerait une zone de lésion significativement plus grande chez les souris TLR2KO après 14 jours. Grâce à ces résultats on peut affirmer que diminuer l'inflammation initiale serait bénéfique. Par contre, diminuer la phagocytose en plus de diminuer la sécrétion de facteurs neurotrophiques à long terme serait néfaste.

6.2 L'environnement enrichi et la récupération fonctionnelle

Le chapitre 4 porte sur l'effet de l'environnement enrichi (EE) sur la réponse inflammatoire suite à une ischémie cérébrale. Le modèle préconisé pour cette étude fut l'ischémie par photothrombose. Pour ce faire, du rose Bengal est injecté dans la souris i.p. pour être par la suite stimulé à l'aide d'un faisceau lumineux très intense sur le crâne de la souris. Le rose Bengal est un colorant cellulaire qui diffuse facilement dans l'organisme, en plus d'être photosensible. Une fois illuminé, il va générer de l'oxygène activé qui va endommager les cellules endothéliales créant avec le temps la formation d'une thrombose (Labat-gest, 2013). Cette technique est peu invasive et très reproductible. En changeant la grosseur du faisceau et à l'aide de la stéréotaxie on peut choisir l'endroit et la grosseur exacte de la lésion que l'on veut créer. Par contre, cette technique comporte quelques irritants qui sont à considérer lorsqu'on veut l'utiliser comme modèle d'ischémie cérébrale. Le premier point négatif, non négligeable, est que cette technique ne génère aucune région de pénombre. Cette zone potentiellement récupérable ciblée par les agents thérapeutiques. Le deuxième point à considérer est que la

thrombose à lieu indépendamment des plaquettes ainsi que des mécanismes normaux de coagulation. En résumé, cette technique ne reflète pas les mécanismes impliqués lors d'un MCAO (Braeuninger, 2009).

Par contre, cette technique non-invasive nous permet tout de même de créer une petite lésion dans un endroit spécifique du cerveau nous permettant ainsi d'étudier la plasticité cérébrale. Dans le cadre de nos expériences, l'aire sensori-motrice du cortex fut choisie afin de quantifier le remodelage cellulaire de cette région en fonction de deux paradigmes de stimulation: un environnement étant enrichi (EE); l'autre pas. L'EE va favoriser l'utilisation des fonctions cognitives, motrices, sensorielles et sociales. Pour enrichir l'environnement, il suffit de placer les souris dans une cage plus grande et y ajouter des tunnels, des roues et des objets pour se cacher. De plus, la modification de l'emplacement des jouets à tous les deux jours introduit de la nouveauté. L'EE est un facteur de remodelage cérébral très puissant, par contre les mécanismes sous-jacents demeurent incompris. Une théorie a proposé que l'EE puisse agir en modulant le niveau d'inflammation cérébrale grâce à la diminution du niveau de cytokines et de chemokines (Rusher, 2013).

La première étape de l'étude était de démontrer qu'il était possible d'utiliser le modèle d'ischémie par photothrombose avec notre modèle de souris TLR2-luc-GFP. De plus, parce que la chirurgie requiert de couper la peau pour exposer le crâne pour ensuite l'exposer à un faisceau lumineux, nous avons dû démontrer que cette procédure chirurgicale ainsi que la lumière seule ne pouvait pas causer l'activation du récepteur TLR2. Après la photothrombose une forte activation de TLR2 est observée, il s'ensuit d'une baisse graduelle, plus importante chez les souris hébergée dans l'EE. De plus, cette baisse du niveau d'activation du promoteur TLR2 est accompagnée d'une meilleure récupération fonctionnelle, majoritairement de la patte avant, dans le groupe enrichi. Il est important de mentionner que même si la récupération des animaux est plus importante lorsqu'ils sont dans un milieu enrichi, cela n'affecte en rien la grosseur de la lésion. En effet,

la lésion est semblable à celle retrouvée dans le milieu contrôle. L'EE favorise la plasticité cérébrale et non la sauvegarde des neurones dans la zone lésée.

Notre étude démontre aussi qu'il y a beaucoup moins de microglie de type M2 (YM1 positive) dans la zone de lésion des souris venant du milieu enrichi. Une microglie ou macrophage de type M2 fait référence à son profil d'activation. Deux profils sont définis: M1 et M2. L'activation dite classique (M1) est associée à un profil d'activation inflammatoire, mais toutefois nécessaire. C'est la réponse des microglies/macrophages face à un pathogène qui vont alors produire des cytokines pro-inflammatoires comme le TNF-α et le IL-6 pour défendre l'organisme (Boche, 2013). L'activation alternative (M2) est plus anti-inflammatoire, elle favorise la réparation des tissus. Les microglies libèrent alors des cytokines comme l'IL-4, IL-10 et le TGFβ. Il est important de mentionner qu'une microglie a le potentiel d'adopter un statut M1 ou M2 en fonction des stimuli perçus dans son entourage (Boche, 2013). Dans le cas de notre étude, le nombre important de microglies de type M2 retrouvées 14 jours plus tard chez les souris hébergées dans les cages standards serait dû à des niveaux d'activation microgliales plus élevées au départ ce qui nécessiterait une action anti-inflammatoire plus soutenue. La plus faible activation observée chez les souris venant du milieu enrichi pourrait être causée par un niveau de stress plus élevé chez les souris hébergées dans le milieu enrichi. En effet, le stress causé par l'exercice augmente le niveau de corticostérone diminuant ainsi la réponse immunitaire. Cette augmentation de corticostérone n'a pas pour objectif de protéger contre l'élément stresseur mais bien de protéger l'organisme contre ses propres réactions envers l'élément stresseur (Zhang, 2013).

L'effet bénéfique de l'exercice a d'ailleurs aussi été démontré dans le modèle d'ischémie cérébrale transitoire. En effet, il est reconnu que la prescription d'exercice et la stimulation sensorielle est un bon moyen de favoriser la récupération tout en diminuant l'inflammation. Une diminution de l'expression de caspase-3 et une augmentation de Bcl-2 serait observée dans la zone de

pénombre. De plus, l'exercice augmente l'angiogenèse ce qui favoriserais l'apport de sang au cerveau ainsi que la formation de nouveaux vaisseaux (Zhang, 2013).

6.3 L'inflammation et l'oestrogène.

Le chapitre 5 porte sur la caractérisation de la réponse inflammatoire après une ischémie cérébrale dans un modèle différent de souris transgénique. En effet, afin de mieux comprendre le rôle des estrogènes nous avons étudié la réponse inflammatoire chez des souris ovariectomisées et ayant le récepteur Erα supprimé génétiquement. Une grande proportion des études publiées dans le domaine des neurosciences utilise de jeunes mâles. En réalité, rare sont les cas d'ischémie cérébrale qui surviennent chez de jeunes hommes en santé. Ces divergences entre le modèle murin utilisé et le sujet humain expliquerait, en partie, pourquoi les thérapies pharmacologiques développées à l'aide de modèles murins sont inefficaces, voire parfois délétères chez l'homme. Nous avons donc choisi d'utiliser des souris en hypoestrogénie chronique afin de mieux comprendre les mécanismes inflammatoires ayant lieu chez les femmes ménopausées. Le but étant d'expliquer pourquoi les femmes sont plus vulnérables aux ischémies cérébrales après la ménopause. Les premières observations dans notre modèle murin, ont démontré qu'une longue période d'hypoestrogénie génère une activation microgliale basale plus importante chez celle-ci. Cette activation ne sera qu'amplifiée à la suite d'une ischémie cérébrale et va générer 48 heures plus tard des lésions cérébrales significativement plus grandes chez les souris ovariectomisées. Des résultats semblables avaient été démontrés dans une étude antérieure utilisant un modèle différent de souris, la souris GFAP-luc, sans toutefois approfondir les mécanismes inflammatoires sous-jacents (Cordeau, 2008). Cette fois-ci nous avons donc utilisé l'absence du récepteur Erα pour mettre en évidence son implication dans l'activation microgliale suite à une ischémie cérébrale. Le récepteur Erα fut choisi, car il serait le plus impliquée parmi les récepteurs oestrogéniques dans les mécanismes de neuroprotection suite à une ischémie cérébrale. Nous avons aussi démontré la propension vers la voie des JAK/STAT lorsqu'une absence du récepteur Erα est combinée avec une OVX. La

surproduction d'IL-6, une cytokine considérée comme inflammatoire dans les phases aigues de l'ischémie cérébrale, serait en partie responsable des lésions plus volumineuses chez les souris TLR2-luc-GFP; ERα^{KO} OVX après 48 heures.

L'œstrogène est impliquée dans les systèmes nerveux, cardiovasculaire, immunitaire et adipeux. Son absence a donc des effets sur l'organisme en entier (Brown, 2010). De plus, l'œstrogène est aussi impliquée dans le maintien du métabolisme du glucose et des fonctions mitochondriales (Scott, 2014). L'absence d'œstrogène force les neurones à utiliser les corps cétoniques plutôt que le glucose. Ce mécanisme causerait à long terme l'utilisation des corps gras des axones myélinisés comme source de carburant détruisant ainsi la matière blanche (Scott, 2014). Les récepteurs oestrogéniques sont présents sur les microglies, les astrocytes et les neurones, en plus d'être présents sur les cellules du système immunitaire comme les monocytes/macrophages, les cellules T, les cellules B, les cellules dendritiques ainsi que sur les cellules NK (Brown, 2010). La diminution d'œstrogène va accentuer l'inflammation périphérique et centrale observées lors du vieillissement normal. En effet, lors du vieillissement, l'un des changements les plus remarquables dans le cerveau est une augmentation ou une perte de la régulation des facteurs pro-inflammatoires menant à un phénomène connu sous le nom «d'inflamm-aging». La ménopause causée par une perte progressive des hormones comporte des risques et des effets secondaires. Plus la ménopause débute tôt, plus la probabilité de subir des effets négatifs augmente. En effet, le risque de subir une ischémie cérébrale augmente, l'apparition possible de démences double et les chances de mourir de troubles neurologiques sont multipliées par 5 (Scott, 2014). Il a été démontré à maintes reprises, dans les modèles animaux, que l'administration d'œstrogène réduit le niveau inflammatoire cérébral suite à la ménopause ou une ischémie. Par contre, le moment, la durée ainsi que les quantités d'œstrogène à administrer sont des facteurs importants lorsque vient le temps de débuter un traitement hormonal (Suzuki, 2009 et Strom, 2010).

Une catégorie de drogue, les SERMs (selective estrogen receptor modulators) montrent une certaine efficacité pour freiner les effets non désirables discutés ci-dessus. En effet, ce qui les distingue du remplacement hormonal habituel (estrogène seul ou combiné avec la progestérone) sont leurs capacités d'être à la fois des agonistes pour les ERs pour certains tissus et des antagonistes d'ERs pour d'autres tissus. Les SERMs sont des composés synthétiques non-stéroïdiens qui agissent en modifiant la conformation du complexe formé avec les récepteurs oestrogéniques. Ce changement va agir comme catalyseur pour activer plusieurs coactivateurs (CoA) ou corépresseurs (CoR) impliqués dans la régulation de gènes. L'équilibre entre les CoA et les CoR dicterait la réponse génique (Pinkerton, 2014). Ce double effet, en fonction du tissu ciblé, est très important lors d'un usage à long terme de ces composés, car l'activation constante des récepteurs oestrogéniques dans l'endomètre ainsi que dans les tissus mammaires serait néfaste (Pinkerton, 2014). Par contre, des effets positifs des composés SERMs dans les tissus comme les os, le cerveau et le système cardiovasculaire seraient observés chez les femmes ménopausées. Le défi est donc de trouver un composé qui active les voies qui ont des effets positifs essentielles tout en réprimant les voies potentiellement néfastes. À ce jour, aucun composé ne possède toutes ces caractéristiques, c'est pourquoi la combinaison et la recherche de nouvelles drogues sont des domaines actifs. D'ailleurs un SERM (bazedoxifène) combiné à de l'œstrogène équin vient d'être approuvé par la FDA comme traitement hormonal. Il réduirait l'atrophie vaginale, les bouffés de chaleur et préviendrait la perte de la masse osseuse sans toutefois stimuler l'utérus et les tissus mammaires (Pinkerton, 2014). L'administration de SERMs a le potentiel d'être bénéfique chez les femmes et serait une excellente substitution à la thérapie de remplacement hormonal dont les résultats sont plus ou moins convaincants.

6.4 Conclusion et perspectives futures

Il fut question lors de cette thèse de la microglie et de son important rôle dans le système nerveux central. De son activation au centre de la réaction immunitaire, à la récupération fonctionnelle, la microglie remplit plusieurs rôles. Malgré tout,

certaines fonctions restent à approfondir. Afin d'étudier les mécanismes cellulaires inconnus, la bioluminescence est une bonne technique qui permet de mesurer en temps réel l'activation de gènes cibles *in vivo*. Dans le futur, la mise au point et le développement de cette technique aura un impact important dans la découverte de mécanismes pathophysiologiques. C'est pourquoi nous devons continuer de développer des modèles murins avec des marqueurs encore plus efficaces et spécifiques. Le but ultime de toutes recherches étant de pouvoir transposer les acquis chez la souris pour élaborer des thérapies efficaces et personnalisées chez l'humain. La prochaine section abordera donc quelques éléments importants afin de poursuivre mes projets pour s'approcher un peu plus de ce but.

Premièrement, afin de mieux comprendre le rôle des récepteurs oestrogéniques sur l'activation microgliale, il serait important d'étudier la réponse inflammatoire chez des souris TLR2-luc-GFP; ErβKO. En effet, même si le récepteur Erα est réputé avoir le plus d'impact sur la réponse inflammatoire des études ont démontré que le récepteur Erβ modulerait aussi cette réponse. Dans une étude récente des rats ayant subi une ischémie cérébrale par photothrombose on voit leurs fonctions locomotrices s'améliorer à la suite de l'administration d'un agoniste des récepteurs Erβ (Madinier, 2014). Il serait donc intéressant de vérifier le rôle de ce récepteur à la suite d'une ischémie cérébrale transitoire. De plus, afin de maximiser les transferts de connaissances de notre modèle à la femme ménopausée, il serait pertinent de déterminer le rôle de chacun des récepteurs oestrogéniques chez de vieilles souris ovariectomisées. D'ailleurs, une seconde étude récente remet en question l'effet neuroprotecteur de l'E2 chez de vielles souris (22 mois). Contre toute attente chez ces souris, l'administration d'E2 tôt après l'OVX n'a eu aucun effet neuroprotecteur 24 heures après le MCAO (Cai, 2014). Ceci serait causé par une baisse marquée du nombre de récepteur Erα et Erβ chez les vieilles souris et chez les souris adultes ovariectomisées. D'ailleurs, vérifier si l'absence de neuroprotection persiste lors d'une reperfusion plus longue serait à évaluer, car comme il fut observé dans mon troisième chapitre, les tendances observées tôt ne reflètent pas toujours les dommages mesurés tardivement. Cette étude remet

quand même en question l'usage de souris en bas âge pour modéliser des maladies survenant chez des personnes âgées, car même si la baisse d'expression des récepteurs Erα et Erβ est semblable chez les souris adultes OVX et chez les vieilles souris, la zone de lésion ainsi que les déficits neurologiques sont supérieurs chez les vieilles souris.

Deuxièmement, le récepteur TLR2 est impliqué dans de nombreuses maladies infectieuses et non infectieuses il serait donc un excellent candidat thérapeutique. Utiliser un composé pharmacologique pour l'inhiber de façon transitoire à la suite d'un traumatisme serait intéressant. Dans le cadre de mon projet, il suffirait d'induire une ischémie cérébrale chez des souris mâles et/ou femelles et de leur administrer le composé inhibiteur durant les 3 premiers jours. Seulement trois jours, car en se basant sur mon troisième chapitre une inhibition précoce de TLR2 serait bénéfique. De plus, cette étude devrait être couplée à des tests comportementaux. Certes l'étude de la zone de lésion est importante, mais ce qui importe le plus est l'amélioration des capacités motrices et mentales. Cette étude pourrait mettre en lumière l'impact de l'inhibition transitoire du récepteur TLR2 à la suite d'une ischémie cérébrale après une longue période de reperfusion.

Finalement, poursuivre les recherches discutées dans cette thèse est important car il semble évident que le récepteur TLR2 est une bonne cible thérapeutique. Chez l'homme comme chez la femme, son implication dans les processus inflammatoires est indéniable. De plus, l'utilisation d'une drogue inhibitrice efficace pourrait être testée dans une multitude de maladies ou d'infections possédant une composante inflammatoire où le récepteur TLR2 est impliqué.

D'ailleurs, il serait intéressant d'approfondir les différences liées au sexe à l'aide de modèles murins afin d'expliquer la prépondérance de maladies neurodégénératives comme la maladie d'Alzheimer chez les femmes. Plusieurs modifications biologiques surviennent avec l'âge et les cellules du cerveau n'y font pas acception. Chez un individu âgé sain, les microglies vont adopter un

phénotype plus inflammatoire que chez l'adulte. Une fois stimulées, elles vont le rester pour une plus longue période de temps et cette réponse sera amplifiée (Norden, 2013). Les maladies cérébrovasculaires et la maladie d'Alzheimer (AD) augmentent avec l'âge. De plus, les facteurs de risques liés au développement de maladies cérébrovasculaires augmentent aussi les risques de développer l'Alzheimer. Il existe donc des liens non négligeables entre ces deux maladies. En effet, 60 à 90 % des patients atteints de l'AD démontrent à l'autopsie une pathologie vasculaire cérébrale. De plus, une ischémie cérébrale aurait trois fois plus de chance d'accélérer l'apparition des signes distinctifs de l'Alzheimer chez les personnes âgées (Koistinaho, 2005). Créer de petites ischémies aléatoires et répétées en injectant des microbilles dans le système vasculaires cérébrales chez des souris serait une bonne façon de tester cette hypothèse.

Les deux facteurs de risques les plus importants dans le développement de l'AD sont l'âge et le sexe. Deux fois plus de femmes que d'hommes vont souffrir de cette maladie et l'incidence plus élevée chez les femmes de développer l'AD ne peut être attribué seulement au fait que les femmes vivent plus longtemps que les hommes (Vina, 2010). Une des causes de cette divergence serait un polymorphisme dans le gène codant pour apolipoprotéine E (allèle ε4). Chez les femmes, la présence de l'allèle ε4 augmente les risques de développer l'AD de façon plus importante que chez les hommes qui ont pourtant le même allèle. De plus, il est important de noter que son expression dans le cerveau est influencée par le niveau d'oestrogènes (Henderson, 2013). L'autre hypothèse qui expliquerait la probabilité plus élevée chez les femmes de développer l'AD serait aussi liée aux oestrogènes, plus précisément à l'absence d'oestrogène. D'ailleurs chez les souris souffrant d'Alzheimer, le manque d'œstrogène cause aussi des déficits énergétiques. En effet, l'ovariectomie bouleverse la mitochondrie en diminuant l'activité enzymatique et en augmentant le stress oxydatif ce qui perturbe le métabolisme cérébral général et aggrave l'accumulation de l'Aβ dans la mitochondrie (Yao, 2012).

En raison des éléments qui viennent d'être discutés, cette thèse soulève certains points importants qui devront être pris en considération lors de la création d'un nouveau projet de recherche. De plus, l'âge, le sexe et le modèle murin choisis seront à tenir en compte afin de maximiser la personnalisation de la thérapie administrée chez l'homme.

FIN

Bibliographie

Abbas AK, Lichtman AH. Cellular and molecular Immunology. Fifth Edition, Updated Edition, pp 16-32. Elsevier Saunders.

Altin JG, Sloan EK. The role of CD45 and CD45-associated molecules in T cell activation. Immunol Cell Biol. 1997 Oct;75(5):430-45.

Arumugam TV, Okun E, Tang SC, Thundyil J, Taylor SM, Woodruff TM. Toll-like receptors in ischemia-reperfusion injury. Shock. 2009 Jul;32(1):4-16.

Arundine M, Tymianski M. Molecular mechanisms of calcium-dependent neurodegeneration in excitotoxicity. Cell Calcium. 2003 Oct-Nov;34(4-5):325-37.

Benarroch EE. Brain glucose transporters: Implications for neurologic disease. Neurology. 2014 Mar 19.

Boche D, Perry VH, Nicoll JA. Review: activation patterns of microglia and their identification in the human brain. Neuropathol Appl Neurobiol. 2013 Feb;39(1):3-18.

Bohacek I, Cordeau P, Lalancette-Hébert M, Gorup D, Weng YC, Gajovic S, Kriz J. Toll-like receptor 2 deficiency leads to delayed exacerbation of ischemic injury. J Neuroinflammation. 2012 Aug 8;9:191.

Braeuninger S, Kleinschnitz C. Rodent models of focal cerebral ischemia: procedural pitfalls and translational problems. Exp Transl Stroke Med. 2009 Nov 25;1:8.

Broughton BR, Reutens DC, Sobey CG. Apoptotic mechanisms after cerebral ischemia. Stroke. 2009 May;40(5):331-9.

Brown AM, Ransom BR. Astrocyte glycogen and brain energy metabolism. Glia. 2007;55:1263-1271.

Brown CM, Mulcahey TA, Filipek NC, Wise PM. Production of proinflammatory cytokines and chemokines during neuroinflammation: novel roles for estrogen receptors alpha and beta. Endocrinology. 2010 Oct;151(10):4916-25.

Chen Y, Hallenbeck JM, Ruetzler C, Bol D, Thomas K, Berman NE, Vogel SN. Overexpression of monocyte chemoattractant protein 1 in the brain exacerbates ischemic brain injury and is associated with recruitment of inflammatory cells. J Cereb Blood Flow Metab. 2003 Jun;23(6):748-55.

Contag CH, Bachmann MH. Advances in In Vivo Bioluminescence Imaging of Gene Expression. Annu.Rev.Biomed.Eng. 2002; 4: 235-260.

Cui J, Shen Y, Li R. Estrogen synthesis and signaling pathways during aging: from periphery to brain. Trends Mol Med. 2013 Mar;19(3):197-209.

Culmsee C, Vedder H, Ravati A, Junker V, Otto D, Ahlemeyer B, Krieg JC, Krieglstein J. Neuroprotection by estrogens in a mouse model of focal cerebral ischemia and in cultured neurons:evidence for a receptor-independent antioxidative mechanism. J Cereb Blood Flow Metab. 1999;19(11): 1263-1269.

Danton GH, Dietrich WD. Inflammatory Mechanisms after Ischemia and Stroke. J Neuro Exp Neuro. 2003; 62:127-136.

del Zoppo GJ, Sharp FR, Heiss WD, Albers GW. Heterogeneity in the penumbra. J Cereb Blood Flow Metab. 2011 Sep;31(9):1836-51.

Denes A, Thornton P, Rothwell NJ, Allan SM. Inflammation and brain injury: acute cerebral ischaemia, peripheral and central inflammation. Brain Behav Immun. 2010 Jul;24(5):708-23.

Dirnagl U, Iadecola C, Moskowitz MA. Pathobiology of ischaemic stroke: An integrated view. Trends Neurosci.1999;22:391-397.

Dreier JP. The role of spreading depression, spreading depolarization and spreading ischemia in neurological disease. Nat Med. 2011 Apr;17(4):439-47.

Dubal DB, Wise PM. Neuroprotective effects of estradiol in middle-aged female rats. Endocrinology.2001;142:43-48.

Durukan A, Tatlisumak T. Acute ischemic stroke: overview of major experimental rodent models, pathophysiology, and therapy of focal cerebral ischemia. Pharmacol Biochem Behav. 2007;87:179-197.

Eng LF, Ghirnikar RS, Lee YL. Glial fibrillary acidic protein: Gfap-thirty-one years (1969-2000). Neurochem Res.2000;25:1439-1451.

Eyo UB, Wu LJ. Bidirectional microglia-neuron communication in the healthy brain. Neural Plast. 2013;2013:456857.

Gibson CL, Coomber B, Rathbone J. Is progesterone a candidate neuroprotective factor for treatment following ischemic stroke? Neuroscientist. 2009 Aug;15(4):324-32.

Gibson CL, Gray LJ, Murphy SP, Bath PMW. Estrogens and experimental ischemic stroke: a systemic review. J Cereb Blood Flow Matab. 2006;26:1103-1113.

Heart and Stroke Foundation Statistics. 2012. http://www.heartandstroke.com/site/c.ikIQLcMWJtE/b.3483991/k.34A8/Statistics.htm#stroke.

Hoffman GE[1], Merchenthaler I, Zup SL. Neuroprotection by ovarian hormones in animal models of neurological disease. Endocrine. 2006 Apr;29(2):217-31.

Huang Z, Huang PL, Panahian N, Dalkara T, Fishman MC, Moskowitz MA. Effects of cerebral ischemia in mice deficient in neuronal nitric oxide synthase. Science. 1994 Sep 23;265(5180):1883-5.

Iadecola C, Anrather J. Stroke research at a crossroad: asking the brain for directions. Nat Neurosci. 2011 Oct 26;14(11):1363-8.

Iijima T, Mies G, Hossmann KA. Repeated negative DC deflections in rat cortex following middle cerebral artery occlusion are abolished by MK-801: effect on volume of ischemic injury. J Cereb Blood Flow Metab. 1992; 12(5) :727-733.

Jin R, Yang G, Li G. Inflammatory mechanisms in ischemic stroke: role of inflammatory cells. J Leukoc Biol. 2010 May;87(5):779-89.

Johann S, Beyer C. Neuroprotection by gonadal steroid hormones in acute brain damage requires cooperation with astroglia and microglia. J Steroid Biochem Mol Biol. 2013 Sep;137:71-81.

Kong Y, Le Y. Toll-like receptors in inflammation of the central nervous system. Int Immunopharmacol. 2011 Oct;11(10):1407-14.

Labat-gest V, Tomasi S. Photothrombotic ischemia: a minimally invasive and reproducible photochemical cortical lesion model for mouse stroke studies. J Vis Exp. 2013 Jun 9;(76).

Lalancette-Hebert M, Gowing G, Simard A, Weng YC, Kriz J. Selective ablation of proliferating microglial cells exacerbates ischemic injury in the brain. J Neurosci.2007;27:2596-2605.

Lalancette-Hébert M, Phaneuf D, Soucy G, Weng YC, Kriz J. Live imaging of Toll-like receptor 2 response in cerebral ischaemia reveals a role of olfactory bulb microglia as modulators of inflammation. Brain. 2009 Apr;132(Pt 4):940-54.

Liesz A, Suri-Payer E, Veltkamp C, Doerr H, Sommer C, Rivest S, Giese T, Veltkamp R. Regulatory T cells are key cerebroprotective immunomodulators in acute experimental stroke. Nat Med. 2009 Feb;15(2):192-9.

Liew FY, Xu D, Brint EK, O'Neill LA. Negative regulation of toll-like receptor-mediated immune responses. Nat Rev Immunol. 2005 Jun;5(6):446-58.

Liu F, McCullough LD. Interactions between age, sex, and hormones in experimental ischemic stroke. Neurochem Int. 2012 Dec;61(8):1255-65.

Liu F, McCullough LD. Middle cerebral artery occlusion model in rodents: methods and potential pitfalls. J Biomed Biotechnol. 2011;2011:464701.

Macrez R, Ali C, Toutirais O, Le Mauff B, Defer G, Dirnagl U, Vivien D. Stroke and the immune system: from pathophysiology to new therapeutic strategies. Lancet Neurol. 2011 May;10(5):471-80.

McCullough LD, Hurn PD. Estrogen and ischemic neuroprotection: An integrated view. Trends Endocrinol Metab.2003;14:228-235.

Nedergaard M, Dirnagl U. Role of glial cells in cerebral ischemia. Glia. 2005 Jun;50(4):281-6.

Norden DM, Godbout JP. Review: microglia of the aged brain: primed to be activated and resistant to regulation. Neuropathol Appl Neurobiol. 2013 Feb;39(1):19-34.

O'Donnell MJ, Xavier D, Liu L, Zhang H, Chin SL, Rao-Melacini P, Rangarajan S, Islam S, Pais P, McQueen MJ, Mondo C, Damasceno A, Lopez-Jaramillo P, Hankey GJ, Dans AL, Yusoff K, Truelsen T, Diener HC, Sacco RL, Ryglewicz D, Czlonkowska A, Weimar C, Wang X, Yusuf S; INTERSTROKE investigators. Risk factors for ischaemic and intracerebral haemorrhagic stroke in 22 countries (the INTERSTROKE study): a case-control study. Lancet. 2010 Jul 10;376(9735):112-23.

Olmez I, Ozyurt H. Reactive oxygen species and ischemic cerebrovascular disease. Neurochem Int. 2012 Jan;60(2):208-12.

Panickar KS, Norenberg MD. Astrocytes in cerebral ischemic injury: Morphological and general considerations. Glia. 2005; 50:287-298.

Pekny M, Nilsson M. Astrocyte activation and reactive gliosis. Glia. 2005;50:427-434.

Pineau I, Lacroix S. Endogenous signals initiating inflammation in the injured nervous system. Glia. 2009 Mar;57(4):351-61.

Pinkerton JV, Thomas S. Use of SERMs for treatment in postmenopausal women. J Steroid Biochem Mol Biol. 2013 Dec 25.

Ruscher K, Kuric E, Liu Y, Walter HL, Issazadeh-Navikas S, Englund E, Wieloch T. Inhibition of CXCL12 signaling attenuates the postischemic immune response and improves functional recovery after stroke. J Cereb Blood Flow Metab. 2013 Aug;33(8):1225-34.

Saijo K, Glass CK. Microglial cell origin and phenotypes in health and disease. Nat Rev Immunol. 2011 Oct 25;11(11):775-87.

Sampei K, Goto S, Alkayed NJ, Crain BJ, Korach KS, Traystman RJ, Demas GE, Nelson RJ, Hurn PD. Stroke in estrogen receptor-α-Deficient Mice. Stroke. 2000;31 :738-744.

Sasai M, Yamamoto M. Pathogen recognition receptors: ligands and signaling pathways by Toll-like receptors. Int Rev Immunol. 2013 Apr;32(2):116-33.

Saver JL. Time is brain--quantified. Stroke. 2006 Jan;37(1):263-6.

Sawada M, Alkayed NJ, Goto S, Crain BJ, Traystman RJ, Shaivitz A, Nelson RJ, Hurn PD. Estrogen receptor antagonist ici182,780 exacerbates ischemic injury in female mouse. J Cereb Blood Flow Metab.2000;20:112-118.

Schreihofer DA, Ma Y. Estrogen receptors and ischemic neuroprotection: who, what, where, and when? Brain Res. 2013 Jun 13;1514:107-22.

Scott EL, Zhang QG, Vadlamudi RK, Brann DW. Premature menopause and risk of neurological disease: Basic mechanisms and clinical implications. Mol Cell Endocrinol. 2014 Jan 22.

Shichita T, Sugiyama Y, Ooboshi H, Sugimori H, Nakagawa R, Takada I, Iwaki T, Okada Y, Iida M, Cua DJ, Iwakura Y, Yoshimura A. Pivotal role of cerebral interleukin-17-producing gammadeltaT cells in the delayed phase of ischemic brain injury. Nat Med. 2009 Aug;15(8):946-50.

Shin JA, Yang SJ, Jeong SI, Park HJ, Choi YH, Park EM. Activation of estrogen receptor β reduces blood-brain barrier breakdown following ischemic injury. Neuroscience. 2013 Apr 3;235:165-73.

Stoll G, Jander S, Schroeter M. Inflammation and glial responses in ischemic brain lesions. Prog Neurobiol.1998;56:149-171.

Strom JO, Theodorsson E, Holm L, Theodorsson A. Different methods for administering 17beta-estradiol to ovariectomized rats result in opposite effects on ischemic brain damage. BMC Neurosci. 2010 Mar 17;11:39.

Stubbe T, Ebner F, Richter D, Engel O, Klehmet J, Royl G, Meisel A, Nitsch R, Meisel C, Brandt C. Regulatory T cells accumulate and proliferate in the ischemic hemisphere for up to 30 days after MCAO. J Cereb Blood Flow Metab. 2013 Jan;33(1):37-47.

Suzuki S, Brown CM, Dela Cruz CD, Yang E, Bridwell DA, Wise PM. Timing of estrogen therapy after ovariectomy dictates the efficacy of its neuroprotective and antiinflammatory actions. Proc Natl Acad Sci U S A. 2007 Apr 3;104(14):6013-8.

Suzuki S, Brown CM, Wise PM. Neuroprotective effects of estrogens following ischemic stroke. Front Neuroendocrinol. 2009 Jul;30(2):201-11.

Toran-Allerand CD. Estrogen and the brain: beyond ER-α and ER-β. Exp Geronto. 2004;34:1579-1586.

Tremblay MÈ, Stevens B, Sierra A, Wake H, Bessis A, Nimmerjahn A. The role of microglia in the healthy brain. J Neurosci. 2011 Nov 9;31(45):16064-9.

van Praag H, Kempermann G, Gage FH. Neural consequences of environmental enrichment. Nat Rev Neurosci. 2000 Dec;1(3):191-8.

Wang YC, Lin S, Yang QW. Toll-like receptors in cerebral ischemic inflammatory injury. J Neuroinflammation. 2011 Oct 8;8:134.

Werling D, Jungi TW. Toll-like receptors linking innate and adaptative immune response. Vet Immunol Immunopathol. 2003 Jan 10;91(1): 1-12.

Xenogen, Discovery in the living orgasnism, Living Image Software Version 2.50, Californie: Xenogen Corporation, 2004. 129p.

Xing C, Arai K, Lo EH, Hommel M. Pathophysiologic cascades in ischemic stroke. Int J Stroke. 2012 Jul;7(5):378-85.

Yan YP, Sailor KA, Lang BT, Park SW, Vemuganti R, Dempsey RJ. Monocyte chemoattractant protein-1 plays a critical role in neuroblast migration after focal cerebral ischemia. J Cereb Blood Flow Metab. 2007 Jun;27(6):1213-24.

Yamaguchi N, Yuri K. Estrogen-dependent changes in estrogen receptor-β mRNA expression in middle-aged female rat brain. Brain Res. 2014 Jan 16;1543:49-57.

Zhang P, Zhang Y, Zhang J. Early Exercise Protects against Cerebral Ischemic Injury through Inhibiting Neuron Apoptosis in Cortex in Rats. Int J Mol Sci. 2013 Mar 15;14(3):6074-89.

Ziegler G, Freyer D, Harhausen D, Khojasteh U, Nietfeld W, Trendelenburg G. Blocking TLR2 in vivo protects against accumulation of inflammatory cells and neuronal injury in experimental stroke. J Cereb Blood Flow Metab. 2011 Feb;31(2):757-66.

Ziegler G, Harhausen D, Schepers C, Hoffmann O, Röhr C, Prinz V, König J, Lehrach H, Nietfeld W, Trendelenburg G. TLR2 has a detrimental role in mouse transient focal cerebral ischemia. Biochem Biophys Res Commun. 2007 Aug 3;359(3):574-9.